Research on Drought Physiology and Molecular Responses, and Development of Biotechnology Tools for the Drought-Tolerant Wild Watermelon (*Citrullus lanatus* acc. 101117-1)

乾燥耐性の野生種スイカ（*Citrullus lanatus* acc. 101117-1）における乾燥下の生理および分子応答と、生物工学的技術の開発に関する研究

Goitseone Malambane
ホイツィオネ　マランバニ

2018

Research on Drought Physiology and Molecular Responses, and Development of Biotechnology Tools for the Drought-Tolerant Wild Watermelon (*Citrullus lanatus* acc. 101117-1)

A Dissertation

By

Goitseone Malambane

Submitted to The United Graduate School of Agricultural Sciences, Tottori University, Japan
In Partial Fulfillment of the Requirements for the Degree of

DOCTOR OF PHILOSOPHY
Global Arid Land Science (Molecular Breeding)
September 2018

Supervisory Committee:

1. Professor Kinya Akashi, Faculty of Agriculture, Tottori University
2. Professor Hisashi Tsujimoto, Arid Land Research Centre, Tottori University
3. Professor Tsuyoshi Nakagawa, Faculty of Life and Environmental Science, Shimane University

Acknowledgements

In the most sincere way, I would like to express my deepest gratitude to Prof. Dr. Kinya AKASHI, for the valuable time, guidance, support and most importantly the valuable knowledge I have accumulated under his supervision. All this attributes made this work possible and made my life in his laboratory the most pleasant I could ever have imagined.

I would also like to express my deepest gratitude to Prof. Dr. Hisashi TSUJIMOTO and Prof. Dr. Tsuyoshi NAKAGAWA, who continuously interacted and provided valuable guidance on ways to improve my research and achieve better results.

I would also like to extend my sincere gratitude to the Tsukuba University Profs. Dr Satoko NONAKA, Dr. Hiroshi SHIBA and Dr. Hiroshi EZURA for the sharing with me their research idea and significantly contributing to one of the chapters of my study.

My sincere appreciation also goes to the current and former technicians and staff in Prof. Akashi's laboratory for all the assistance they always provided to help me settle in the lab and in Tottori. My sincere regards to Nishio EMIKO who was always willing to help whenever I needed some assistance.

To all the former and present lab members especially Atushi KATO and Tadano SHOTA I cannot thank you enough for the unwavering support you accorded me during my stay in Tottori and Akashi Lab. I will always be thankful.

It would be a grave mistake to forget to show my sincere appreciation to the Ministry of Education, Culture, Sports, Science and Technology of Japan (MEXT) for giving me a once in a lifetime opportunity to pursue my Ph.D at the United Graduate School of Agricultural Sciences and most importantly for the financial support to complete the studies.

I would also like to show my deepest appreciation to the Arid Land Centre and the International Platform for Dryland Research and Education (IPDRE) for the continued support with equipment and financially, this really helped me achieve the goals of my study and to complete my studies.

To the Botswana University of Agriculture and Natural resources, I would like to say my thanks for allowing me to pursue further studies and for all the financial support.

I would also like to appreciate the support from my friends both in Botswana and in Japan for the continued encouragement, especially Tebogo who has been a daily support throughout the studies.

A special gratitude to my family who have been a pillar of strength and helped me see me through the studies with their continued support and encouragement. I would like to mention my mother Kelebile who always makes me see the light when I think its dark. Also would like to express my gratitude to my uncle Mokgweetsi who has been an academic mentor to me.

Most importantly there is no way this work could have been complete without the guidance of the Almight God.

TABLE OF CONTENTS

LIST OF TABLES

LIST OF FIGURES

ABBREVIATIONS

A_N , P_N	Photosynthesis rate
A/Ci	Photosynthesis rate by internal CO_2
ACC	1-aminocyclopropane-carboxylic acid
acdS	ACC deaminase
ACS	ACC synthase
ACO	ACC oxidase
$AgNO_3$	Silver nitrate
APX	Ascorbate peroxidase
AsA	Ascorbate
ATP	Adenosine triphosphate
AVG	Aminoethoxyvinylglycine
BLAST	Basic local alignment search tool
BM	Basal medium
BSA	Bovine serum albumin
CO_2	Carbon dioxide
C_2H_4	Ethylene
$CaCL_2$	Calcium chloride
cAPX	cytosolic ascorbate peroxidase
CAT	Catalase
CBB	Coomassie brilliant blue
CDS	International board for plant genetic resources
CLAPX	*Citrullas lanatus* ascorbate peroxidase
CLMT	*Citrullas lanatus metallothionein*
Cm	Centimeter
CRISPR/Cas9	Cluster regularly interspaced short palindromic repeats/ CRISPR associated proteins
Cv	Cultivar
DM	Dry mass
DNA	Deoxyribonucleic acid
DNase	Deoxribonuclease

dNTPs	Deoxnucleotide triphosphates
DRIP	Drought induced polypeptide
DSBs	Double strand breaks
DW	Dry weight
EDTA	Ethylenediaminetetraacetic acid
ETR	Electron transport rate
FID	Flame ionization detector
Fv/Fm	Quantum yield of PSII
FW	Fresh weight
GAPDH	Glyceraldehyde-3-phosphate dehydrogenase
GC	Gas chromatography
gFW	Grams of fresh weight
GFP	Green fluorescence protein
gRNA	Guide ribonucleic acid
GUS	*uidA* gene
H_2O	Water
H_2O_2	Hydrogen peroxide
HEPES	4-(2-hydroxyethyl)-1-piperazineethanesulfonic acid
HDR	Homology directed repair
HR	Homologous repair
INDELs	Insertions deletions
IPTG	Isopropyl-β-D-thiogalactoside
KCl	Potasium chloride
LB	Luria-bertani
LED	Light emitting diode
LRWC	Leaf relative water content
mAPX	Microbody ascorbate peroxidase
MES	2-morpholinoethanesulfonic acid
$MgCl_2$	Magnesium chloride
mRNA	Messenger ribonucleic acid
MS	Murashige and skoog
NaCl	Sodium chloride
NADPH	Nicotinamide adenine dinucleotide phosphate

NAGK	N-Acetylglucosamine kinase
NHEJ	Non homologous end joining
NPQ	Non photochemical quenching
$^1O_2$	Singlet oxygen
O_2	Oxygen
$^{\cdot}OH$	Hydroxyl radical
PAM	Photospacer adjacent motif
PCR	Polymerase chain reaction
PGPB	Plant growth promoting bacteria
PMSF	Phenylmethane sulfonyl fluoride
*P*NPG	Para nitrophenyl β-D-glucopyranoside
PSII	Photosystem II
PVPP	Polyvinylpolypyrrolidone
qP	Photochemical quenching
qN	Non photochemical quenching
RACE	Deoxyribonucleotide triphosphate
RNA	Ribonucleic acid
ROS	Reactive oxygen species
RT-qPCR	Reverse transcription quantitative polymerase chain reaction
SAM	S-adenosylmethionine
sAPX	Stromal ascorbate peroxidase
sgRNA	Single guide ribonucleic acid
SMC	Soil moisture content
SOD	Superoxide dismutase
SPAD	Chlorophyll meter (Soil-plant analyses development)
T-DNA	Transfer deoxyribonucleic acid
TALENs	Transcription activator-like effector nucleases
TDZ	Thidiazuron
TW	Turgid weight
WM	Wet mass
WW	Wild watermelon

xGLUC	5-bromo-4-chloro-3-indoyl glucuronide
ZFNs	Zinc finger nucleases

CHAPTER 1

INTRODUCTION

1.1 Drought stress

The advent of climate change has brought with itself various environmental problems to the agricultural production. It has lead to erratic and uneven rainfall pattern leading to an increase in desert margins, and the traditional cropping agricultural land slowly turning into arid areas. Year in and year our lower rainfalls amounts are recorded coupled with yearly increase in temperatures, and this has caused alarming concern in the world over. Drought, which can be defined as a period when evapotranspiration exceeds the amount of precipitation received during the growing period of the crop, has been documented as the most critical factor affecting crop growth and production, and has been referred to as the most single threat to food security in the world. With the world population showing a steady increase and calling for more food production to feed the increasing population, this would further aggravate the effects of drought (Chaves 1990; Flexas and Medrano 2002; Farooq et al. 2012).

1.1.1 Effects of drought on crops

The effects of drought on crops vary vastly from the easily visible effects (morphological) and the non-visible (physiological and molecular), and can be experienced by plants at any growth stage. Cell growth is one of the most drought-sensitive physiological processes due to the reduction in turgor pressure. It directly affects plant growth and yield (Taiz and Zeiger 2010), with severe water deficit leading to inhibition of cell elongation leading to stunted growth or necrosis in severe cases (Farooq et al. 2009).

The root system of the plant is the most important part of the plant, as it provides physical stand, store nutrients, and initiates the water and nutrient uptake from the soil to the above ground parts of the plant. Most importantly, the roots act as drought sensor and signaling tool that then send signals to the upper part of plant to activate the tolerance mechanisms (Janiak et al. 2016; Schachtman and Goodger 2008). Faced with moisture deficit, plants usually fails or produces low yields as the photosynthesis mechanisms is highly affected by environmental stresses (Mathobo et al. 2016; Mohsen et al. 2017).

1.1.2 Effect of moistures stress on photosynthetic mechanism

The ability of the plant to utilize the light energy to complete the photosynthesis is also highly influenced by the moisture availability. Photosynthesis is a process that is very essential in both plant growth and productivity. This process has shown to be highly affected by drought stress (Li et al. 2006). The primary limiting factor for photosynthesis has either been attributed to stomatal closure, a tolerance mechanisms of many plants when faced with moistures deficit (Chaves 1990; Prasch and Sonnewald 2015) or metabolic impairment, or both contributing equally as limiting factor (Flexas et al. 2004). As one of the last resort of survival mechanism in extreme moisture stress, the plant will respond by triggering the acceleration of growth stages and move from development stage to reproductive phase. This is a process that needs more energy to complete, thus leading to lower yield than expected because the photosynthesis system is functioning at a minimal (Desclaux and Roumet 1996). Moreover, plant cannot utilize the light energy to its full capacity, as part of the light energy is deflected or dissipated as heat in an attempt to protect the internal mechanism.

1.1.3 The use of chlorophyll fluorescence to study drought effects of plants

Since its discovery, chlorophyll fluorescence (Kautsky et al. 1960; Buttler 1966) has become an important physiological tool. Its importance has been fully utilized to study plant responses to various environmental stresses (Maxwell and Johnson 2000; Schreiber 2000) and on understanding the photosynthetic process (Genty et al. 1989; Krause and Weis 1991; Strasser et al. 2000; Zakhidov et al. 2016). Since then various tools have been developed to make its measurements easier and rapid. During drought stress, excess light energy absorbed in the chlorophyll is safely dissipated (quenched) rather than being transferred to the photosystem II (PSII), thereby acting as a protective process that prevents the formation and accumulation of damaging free radicals (Demmig-Adams and Adams III 2006; Zivcak et al. 2014). The heat dissipation process significantly diverts a larger part of the light energy (Murchie and Lawson 2013), thus resulting in significant reduction of the photosynthetic rate, less energy is photochemical quenched and available to the PSII systems for photosynthesis (Faraloni et al. 2011).

1.2.0 Wild species

The exact definition of wild species has been difficult to finalize, as they have been defined in various ways because of the varying degree of relatedness to the cultivated species. A much closer and universally used definition of wild species is that, they are wild plant species that are more or less similar with the cultivated or domesticated crop species, but has not yet been domesticated and their genetic makeup not yet tampered with (Heywood et al. 2007). Different wild species can be found in different areas around the world, and the area where wild species of a crop are found in abundance gives an idea of the center of origin for the domesticated crop.

Domesticated plant species are a result of evolutionary process of wild species with the aid of plant breeding to meet human's needs, like fast growth and high yield (Pickersgill 2007). Thus wild species can be referred to as the wild ancestors or relatives to the cultivated/domesticated crops, that have evolved with time through plant breeding or adaptation to environmental conditions. The domestication process has resulted in new species having a reduced diversity among them, while high levels of genetic diversity can still be found in the wild species. The rapid domestication of crops also brought about problems of genetic diversity in the wild species, and leading to a highly genetically similar/uniform crop species (Hopkins and Maxted 2011).

The use of wild species gene pool in breeding has been well documented since the early 20th century (Plucknett et al. 1987), and since then the use has rapidly and meaningfully increased over the years. Disease and pest resistance, drought tolerance, salinity tolerance, lodging tolerance are some of the improvement that has been incorporated into cultivated species using the wild species as a donor for genetic breeding material. This makes the wild species a very important genetic resource for studies, as it offers many possibilities of improving existing cultivated species (Pickersgill 2007).

1.2.1 Wild watermelon

Wild watermelon referred to as the wild cousin or the ancestor of cultivated watermelon, and inhabits the Kalahari Desert found in the western part of Botswana. The plant grows very well in the desert under unsuitable growing conditions for the cultivated watermelon and other domesticated crops, where temperature sore up to 45°C and rainfall amounts can be as low as 100 mm for the entire growing season of

the plant. The soils are mostly sandy with poor water holding capacity and have low amounts of nutrient required for plant growth.

Wild watermelon, unlike its widely consumed cultivar watermelon, is not sweet, less palatable and the internal color is mostly white to cream white or yellowish. The mature fruit has a similar size as the cultivated watermelon, and surprisingly contain relatively the same volume of water even when it grows in harsh conditions. Thus it has become an important crop of the desert as it is a valuable source of water for the Kalahari inhabitants, and also useful as feed for the domesticated and wild animals inhabiting the desert.

Several studies have been conducted on the mechanisms that aid the plant to have a superior drought tolerance mechanism. One major mechanism that has been suggested is the sudden closure of the stomata to protect its photosynthesis apparatus and cell components from irreversible damage (Sanda et al. 2011; Nanasato et al. 2010).

Moisture deficit induces expression of various proteins that are involved in cell damage and repair (Riccardi et al. 1998). The rate of defense protein accumulation and subsequent depletion during moisture deficit and plant recovery may be important indicators of stress tolerance, as they may provide insights into drought tolerance and recovery mechanisms. An analysis of proteins on the wild watermelon leaves exposed to moisture eficit for three days showed a higher accumulation of DRIP-1, which was 5 times higher when compared to the domesticated watermelon (Yokota et al. 2000).

In plants, one of the amino acids that accumulate during moisture deficit is the proline as a result of increased flux of glutamate in the proline biosynthesis pathway (Good and Zaplachinski 1994). Moisture deficit effect on accumulation of free amino acid in wild watermelon leaves, showing significant increase in citrulline, arginine and glutamate when exposed to moisture deficit for a short period (Kawasaki et al. 2000). It was suggested that the accumulation of these free amino acids could be related to the decrease in water potential.

An extensive study on the role of accumulated citrulline during moisture deficit was done by Akashi et al. 2001. They found that the citrulline accumulated in watermelon leaves is an effective defense against oxidative stress, as it assists in scavenging hydroxyl radicals and reducing then to non-toxic levels. The accumulated

citrulline assists in keeping vulnerable cellular components active and maintain their cellular function during prolonged drought.

Another tolerance mechanism implied by wild watermelon under moisture deficit is the production of the CLMT2 protein, which has a closer homology with the type-2 metallothionein (MT) (Akashi et al. 2004). The plant MTs are proposed to function as antioxidants, and have been predicted to protect cells against the toxic effects of ROS (Mir et al. 2004). The *in-vitro* studies showed that CLMT2 is a potent scavenger of hydroxyl radicals. This shows that the production of the CLMT2 is another drought tolerance mechanisms in wild watermelon to protect its cellular components like DNA from degradation (Akashi et al. 2004).

The root is the first part of the plant to be exposed to moisture deficits, and they also act as a drought-sensing organ (Janiak et al. 2016). Thus its response mechanism is important to understand total tolerance mechanism of the plant. To explore the molecular mechanisms of the root when exposed to moisture deficits, a comprehensive proteome analysis has carried out to document drought-responsive proteins in the roots (Yoshimura et al. 2008). An increase in the abundance of two types of Ran GTPase was observed on the wild watermelon roots when exposed to moisture deficit. Ran GTPase in plants has been suggested to play a role in regulation of root morphogenesis (Wang et al. 2006). Thus the observed increase of CLRan protein during drought stress was responsible for enhancing primary root growth, as has been shown that overexpression in Arabidopsis increased the growth of primary roots almost 2-fold (Akashi et al. 2016).

1.3.0 Antioxidants

1.3.1 Reactive Oxygen Species (ROS)

The reactive oxygen species (ROS), also known as active oxygen species (AOS) or reactive oxygen intermediates (ROI), are the result of the partial reduction of atmospheric O_2 (Gill & Tuteja 2010; You and Chan 2015). There are basically four forms of cellular ROS, singlet oxygen ($^1O_2$), superoxide radical ($^{\cdot}O_2^-$), hydrogen peroxide (H_2O_2) and the hydroxyl radical ($^{\cdot}OH$), each with a characteristic half-life and an oxidizing potential (Bolwell and Woztaszek 1997). ROS can be extremely reactive, especially for singlet oxygen and the hydroxyl radical and, unlike atmospheric oxygen, they can oxidize multiple cellular components like proteins, lipids, DNA and RNA. Unrestricted oxidation of the cellular components can be very

toxic and ultimately cause cell death (Mittler 2002). These oxidative species are known to accumulate in plant cells in high quantities when the plant is exposed to moisture deficit or other abiotic stress as compared to the period of normal plant growth, where most of the ROS will be kept at minimum levels throughout growth. One of the major cellular sites responsible for ROS production is the chloroplast (Noctor and Foyer 1998).

To cope with the high volumes of produced ROS, the plants have a system in place whereby a series of enzymatic and non-enzymatic antioxidants function in a cooperative manner to quench the ROS to the non-toxic level (Mittler 2004). These are commonly called ROS scavenging antioxidants. Most of the antioxidants scavenge the ROS and convert them from one form to another form of the ROS, like superoxide dismutase (SOD), a front line enzymes which scavenges the superoxide and break it down to oxygen and H_2O_2. The accumulated H_2O_2 needs to be totally converted to non-toxic compounds like H_2O, as H_2O_2 also known to be toxic to cellular proteins (Bowler et al. 1992).

1.3.2 Ascorbate peroxidase (APX)

Ascorbate peroxide (APX) is one of the antioxidant enzymes that scavenge toxic H_2O_2. Therefore, this enzyme is important defense protein during plant tolerance to moisture deficit or other abiotic stress to clean up H_2O_2 after the SOD anti-oxidative enzyme. APX is capable of scavenging the H_2O_2 even at its lowest amounts (Sofo et al. 2015). During the scavenging reaction, one important element that comes into play is the ascorbate (AsA), which is utilized as an electron donor during the neutralization of the H_2O_2. In the absence of AsA, the scavenging of the H_2O_2 becomes impossible, leading to toxicity levels of increasing ROS in plants cells (Shigeoka et al. 2002).

Studies on APX activities on different crops have shown a decrease in chloroplast enzyme activity when exposed to high light stress (Yoshimura et al 1998). Wild watermelon, previous study (Nanasato et al 2010) has shown that the enzyme activity of chloroplast APX increased when the plant is exposed to drought stress (Nanasato et al. 2010).

Research has shown that multigenic families encode APX genes in higher plants. Different plant species have shown varying number of the APX genes. *Arabidopsis* has been reported to contain nine APX genes (Chew et al. 2003), cotton

with highest number recorded so far at 11 genes (Tao et al. 2017), rice has eight (Teixeira et al. 2004), maize with seven (Sytykiewicz 2016; Liu et al. 2012). The different isogenes of the APX are classified into sub-families based on their subcellular localization, thus classified into chloroplastics (stromal and thylakoid), cytosolic and microbody APX families.

1.4.0 *Agrobacterium* transformation

Agrobacterium tumefaciens fall under the genus of Gram-negative bacterium. It inhabits in the soil (Riva et al. 1998), and has been found to cause crown galls in the plants (Nester et al. 1984). Its importance came into light when it was observed that it has the ability to introduce foreign genetic material into plant cell through its Transfer DNA (T-DNA) located in the tumer-inducing (Ti) plasmid. Ti plasmid can be found in many bacteria, as they are known to have a circular DNA structure (Horsch et al. 1986). The process of foreign gene transfer via *Agrobacterium* can be broken down to five important stages: (1) induction of the bacterial virulence system, (2) generation of T-DNA complex, (3) transfer of T-DNA from *Agrobacterium* to the host cell nucleus, (4) integration of T-DNA into the plant genome, and (5) expression of T-DNA genes (Tzfira and Citovsky 2006).

The recombinant gene technology took into use these important factors of the *Agrobacterium* to establish an important vector to be used for introducing foreign genes in plant for genetic and cellular studies. Since then *Agrobacterium* has become the mostly used tool in plant transformation and genetic engineering, as it has proved to be highly efficient. This technique has the ability to integrate a single copy of gene on an individual plant cell as compared to other tools/methods used for gene integration (Gelvin 2003). Initially it was thought to be only suitable for dicotyledons, but later it was then improved to be effective in wide range of plant species (Herrera-Estrella et al. 2005), it is currently been used to introduce foreign genes across various species of plants.

Even though it has become an important tool in genetic recombination, it has had its own limitations when it comes to efficiency. This limitations can be influenced by both external and internal factors, like explant type, vector plasmid or bacterial strain, culture medium, time, temperature, pH, chemicals, antibiotics of the cultivation medium (Ziemienowicz 2014; Koetle et al. 2015).

Various studies have been done to improve the transformation of watermelon. These studies focused on various aspects such as explant source (Tabei et al. 1993), pre-culture of the explant prior to *Agrobacterium* infection (Choi et al. 1994), *Agrobacterium* strain and antibiotics (Akashi et al. 2005), inoculation time (Park et al. 2005), acetosyringone concentrations (Suratman et al. 2010) and inoculation time (Li et al. 2012), to improve the efficiency of *Agrobacterium*-mediated transformation of watermelon.

1.4.1 Ethylene

A phytohormone ethylene is synthesized in plants at specific stages of their life cycle, and is involved in the regulation of many developmental processes, such as fruit ripening, flower fading, leaf abscission, growth in aquatic plants and initiation of flowering in bromeliads (Boller and Kende 1980). Ethylene is also produced as a defense mechanism when plants are subjected to various abiotic and biotic stresses such as pest attack, diseases, wounding, noxious chemicals, drought and waterlogging. However, depending on the extent of stresses and plant species, the role of ethylene can be dramatically different. Plants deficient in ethylene signaling may show either increased susceptibility or increased resistance (Wang et al. 2002).

During transformation, infection of explants with *Agrobacterium* activates the response mechanisms for biotic stress. One of the defense mechanisms is to activate excess production and release of ethylene (Ezura et al. 2000; Nonaka et al. 2008). This attribute plays a major limiting role during the *Agrobacterium*-mediated gene transfer, as emitted ethylene leads to delaying the development of inoculated plants (Glick et al. 1998), and retardation and senescence (Kim et al. 2015). Ethylene is therefore classified as potential plant regeneration inhibitor by Kong and Yeung (1994).

1.5.0 Techniques in functional genomics in plants

Altering of gene sequences in plant cell in a controlled manner has gradually become an important technology in functional characterization of genes (Alberts et al. 2015). One way to achieve these alterations at gene level is through the altering the copy number of a gene (Agrotis and Ketteler 2015). The availability of complete genome sequences and recent development of rapid techniques has made it easier to study cells in a systematic manner (Bunnik and le Roch 2013). These studies on

functional genomics continue to provide major insights in global regulation and integration of biological process both in eukaryotes and prokaryotes.

In recent years, several techniques have been developed to accelerate the functional genomics studies. These technologies include genome editing, which shows a potential to revolutionize crop improvement by making it possible to perturb cells in a systematical manner and create new varieties in a fast, efficient and technically simple way (Zhang et al. 2017). Several genome editing techniques have become extremely valuable tools for functional genomics research, as they have shown to introduce targeted modifications on genomes in a highly efficient manner. and alter the existing DNA pattern with precision (Chira et al. 2017).

1.5.1 Genome editing tools

This technology uses engineered nucleases that are composed of sequence-specific DNA-binding domains fused to a nonspecific DNA cleavage module, enabling an efficient and precise genetic modifications by inducing targeting DNA double strand breaks (DSBs). This results in deletion, addition or replacement of specifics sites on the genome sequences (Zhang 2014; Gaj et al. 2013). Thereafter, the internal repairs of the DSBs are completed by the non-homologous end joining (NHEJ) or the homology directed repair (HDR), with the later more reliable and less erroneous in comparison to the former repair method.

One of the commonly used technologies in site-specific genome editing is the zinc finger nuclease (ZFNs), a fusion proteins comprising an array of site-specific DNA-binding domains adapted from zinc finger containing transcription factors attached to the endonuclease domain of the bacterial FokI restriction enzyme. Each zinc finger domain recognizes a short strand of DNA sequence with a potential to bind to an extended nucleotide sequence that is unique within a genome. For efficient cleavage, the ZFNs are designed in pairs to target the flanking sequences resulting in a cleavage that causes DSBs (Durai et al. 2005; Urnov et al. 2010). Other common technologies includes the transcription activator-like effector nuclease (TALENs), a system comprising of a series of transcriptions activator-like (TALs) proteins that have a high recognition of site specific sequences, and a FokI nuclease that functions like a cleaving scissor inducing a DSBs on the specific sequence with the ability to activate or cause some INDELS (Cermak et al. 2011). Just like any other technologies,

these two genome-editing tools have their own limitations, thus a latest new technology has been developed to gap the limitations of the previous tools.

1.5.2 Clustered regularly Interspace short palindromic repeats (CRISPR)/Cas 9

The latest genome editing tool that have proved to be low cost, simple to use, most versatile and having more precision in genetic manipulation is the CRISPR/Cas9. This new system has been exploited from a bacterial host defense system, which detects and destroys foreign sequences from invading bacteriophages (Sorek et al. 2013). The CRISPR/Cas9 system is composed of: (1) single guide RNA (sgRNA) that aids to direct the system to a specific site on the target sequence, (2) guide RNA (gRNA); a 20 nucleotide sequence that is usually designed resembling a small segment on the targeted genome sequence, and is used to determine the specific site to be edited through a Watson-Crick base pairing. To aid cleavage, the gRNA homologous sequence must be adjacent to the conserved photospacer-adjacent motif (PAM): (3) The Cas 9 nuclease, which causes a DSB on the target site (Lowder et al. 2015; Ma et al. 2015). After the generation of DSBs, the genome is repaired by the NHEJ, which is known to be highly error-prone and likely to cause INDELS of the sequences during repair (Zhao et al. 2016).

The advantages of the CRISPR technology as compared to the previous two tools (ZFNs and TALENs) is (1) it is very easy to construct and set up the Cas9 nuclease and the RNAs, (2) it can be designed so that it targets multiple sites on the same genome at once using multiple set of guide RNAs simultaneously, and (3) the efficiency has been noted to be higher than the previous techniques.

1.6 Aims of the study

The goals of this thesis were to provide further information on the tolerance mechanisms of the wild watermelon by studying the physiological responses, molecular responses of ROS scavenging enzyme during the drought stress. . The final part of the thesis was to develop and improve the biotechnology tools for the use in studying drought tolerance mechanisms of the wild watermelon. These studies will shed further light on the tolerance mechanism of the plant at both physiological and molecular level.

The specific aims were as follows:

1. To evaluate stress effects, plant biologists have often depended on the use of growth chambers that are postulated to mimic the natural environment. This has led to questions been asked of about the effectiveness of these artificial environments, in giving closely related to the natural drought conditions. Therefore, in this study I aimed at evaluating whether they are any physiological differences or similarities when the wild watermelon is grown in natural environment as compared to the artificial environment.

2. When exposed to drought stress, various plants have shown down regulation of the APX activity. But wild watermelon has shown a different trend, with the APX showing an increase in activity. Understanding if this increase happens at transcriptional level will come in handy in exploring and transferring important traits to other plants to improve drought tolerance. It is important to profile and characterize the wild watermelon APX gene families. Thus, in this study I undertook to evaluate the accumulation pattern of mRNA of the gene encoding the wild watermelon APX, and profile them for future researches.

3. The *Agrobacterium*-mediated technique has become one of the most important tools for genetic transformations of crops. The tool has been used to transfer several genes of importance in various model plants. Its efficiency on non-model crop has not reached its full potential because of several factors like plant defense mechanisms in response to *Agrobacterium* as abiotic stress. One of the responses is the release of ethylene, which interferes greatly with transformation. Thus, it is important to evaluate various factors that can reduce the ethylene interference. In this study I aimed to evaluate and document ethylene inhibitors that can improve *Agrobacterim*-mediated gene transfer in wild watermelon.

4. When exposed to drought stress, wild watermelon has shown to accumulate various compounds, which are believed to aid the plant's tolerance to drought. It is important to understand how these compounds contribute to the tolerance mechanisms. The disruption of the gene coding for biosynthetic enzymes of compounds has been suggested as an easy and effective way. One tool that has

shown high effectiveness in other crops is the latest CRISPR/Cas9 editing tool. Thus, developing the tools to cause directed mutation on wild watermelon will come in handy in studying the role of various genes, enzymes and compounds in drought tolerance mechanism. Therefore in this study I undertook to develop and evaluate the CRISPR/Cas9 tool to perform directed disruptions on genes of interest on wild watermelon.

This studies aims to further understand drought tolerance mechanisms of wild watermelon, and also provide important information for plant breeders to improve drought susceptible species.

Chapter 2

Evaluating physiological differences and similarities between watermelon plants growing in controlled and natural conditions

2.1 Introduction

The rapidly changing climatic conditions have brought along them the undesirable conditions that are not suitable for plant growth and production. High temperatures and unreliable rainfall have led frequent drought and increase in desert margin. These margins are now creeping into most of the agricultural production areas, rendering them unsuitable for crop production. This undesirable conditions has made commonly-known field crops struggling to maintain the growth and productivity, thus reducing yield significantly.

The need to maintain food production to feed the ever-increasing population has led to developing technologies to counter the problem. One of the technologies is the design of structures that can be manually or automated to mimic either the suitable growing conditions, or can be altered to suit the requirements for the specific study. Therefore, leading to controlled environment agriculture (CEA), referred to as the use of structures that can modify the internal environment to achieve optimum plant growth. Crop models that are able to estimate the plant responses to various climatic conditions and other factors have been used for the CEA. All aspects of the natural environment may be modified for maximum plant growth and economic return. Controls may be imposed on air and root temperatures, light, water, humidity, carbon dioxide, and even plant nutrition (Jensen and Collins 1985; Wittler and Castilla 1995; Marsh and Albright 1991).

Initially these artificial climate structures were designed to facilitate research on plant responses to different environmental conditions (Tsitsimpelis et al. 2016: Harvey 1922). With the problem of shortage of productive land and advancement of technology, these structures have grown in size with the capacity to be used for mass production.

The continued used of the controlled environment structures for researches that aims to evaluate natural environment effects of plants has been under constant spotlight among the research fields. One argument has been that the use of the structures might leads to a cultural ‘glass wall’ between lab and field scientists (Kohler 2002), leading to differences in interpreting results because of variation on concepts, protocols and terminology used by each community for growing plants and evaluating genotypic or environmental effects (Blum 2014).

Plant biologists often depend on the controlled environment structures to understanding the physiological and molecular responses, with the ultimate aim to improve plant performance in the field. What is often overlooked is how results from controlled conditions translate back to field situations (Poorter et al. 2016). Therefore it is important to regularly cross check these concepts to avoid a situation whereby research that aims to address similar issue might have different interpretation of results. In this study we undertook to evaluate the performance of the two watermelon species under the natural (open field) and the controlled (growth chamber) conditions.

2.2 Materials and methods

2.2.1 Plant materials

Two species of watermelon were used in this study; (1) a highly drought tolerant wild watermelon (*Citrullus lanatus* acc. No. 101117-1) (Kawasaki et al. 2000) which is a natural inhabitant of the Kalahari Desert in Botswana and has been self-pollinated for at least three times, and (2) a commercially-sold cultivar watermelon (*Citrullus lanatus* cv. Matsuribayashi-777, Hagihara Farm, Nara, Japan).

2.2.2 Growth conditions

2.2.2.1 Natural (open field) and controlled environment (growth chamber) conditions

The two species were grown in the open field at the Botswana University of Agriculture and Natural Resources (BUAN). BUAN is located at Sebele, Gaborone, Botswana, at Latitude 240 33' S, Longitude 250 54' E, 994 m above sea level. The research site is located in the South Eastern part of Botswana, which is characterized semi-arid climatic zone with a mean annual temperature of 26.4°C and mean annual precipitation of 538 mm. The study was conducted from late February until March in 2017. The environmental conditions for the growing period are provided in Fig. 2.1.

The second growing conditions was in the growth chamber with controlled conditions set at light intensity of 800-1,000 μmol photons m^{-2} s^{-1} under a 16 h light and 8 h dark photoperiod, with temperatures set at 30°C, and relative humidity of 50% for the entire growth and monitoring period of the experiments.

2.2.2.2 Pre-planting treatment and planting

The seeds were soaked overnight in water and kept at 30°C in the dark. The next morning, the seeds were planted in the field for field study, or in pots filled with a horticulture soil for pot experiments in the growth chamber.

The field conditions were basally dressed by commercially-bought fertilizer (NPK ratio of 3:2:3) at 90kg/ha. After germination, the plants were maintained by watering every 2 days until they reached a stage where five true leaves were fully grown. Supplementation with 1,000x Hyponex solution was done for the potted plants in the growth chamber. When the leaves were fully grown, moisture deficit stress was introduced by stopping watering to plants.

2.2 Data collection

Data was collected at different time points from the onset of stress induction, with 0 days being the last watering day before the stress induction, and then 3, 5, 7, 9 and 11 days after stress induction (DAI). Physiological measurements were done on the third true leaf and replicated four times then later averaged to get final recording.

2.2.3 Measurement of available water content of the soils

For the potted plants in the growth chamber, gravimetric soil moisture content was determined essentially as described previously (Reynolds 1970). Briefly, after harvesting leaf samples, entire aboveground plant tissues were cut out, then the moist soil together with the planting pot were weighed and recorded as the wet mass. Then the soil was oven dried at 105°C for 72 h, and it was weighed and the mass recorded as the dry mass. The available water content (AWC) was determined by the following formula (Reynolds 1970);

$$\text{AWC} = \frac{\text{wet weight} - \text{dry weight}}{\text{dry weight}} \text{ X } 100$$

2.2.4 Measurements of photosynthetic and chlorophyll parameters

Leaf chlorophyll content was measured 3-4 h after sunrise for the field conditions, and for the growth chamber plants the data was collected after the onset of light regime using SPAD-502plus meter (Konica Minolta, Tokyo, Japan). The CO_2 assimilation and chlorophyll fluorescence were measured in the third true leaves using an open gas exchange system LI6400XT photosynthesis meter (LI-COR Biosciences, Nebraska, USA). A 2 cm radius IRGA gas chamber was used for all the measurements, with a setting of chamber temperature at 25°C, CO_2 flow rate at 400 μmol mol^{-1}, PPFD at 1,000 μmol photons m^{-2} s^{-1}, and relative humidity at 50%. The CO_2 assimilation was measured 4 h after the sunrise or onset of light regime, while the chlorophyll fluorescence parameters of dark-adapted leaves were measured early morning before sunrise or before the onset of light regime when the plants were dark adapter for more than 5 h at least.

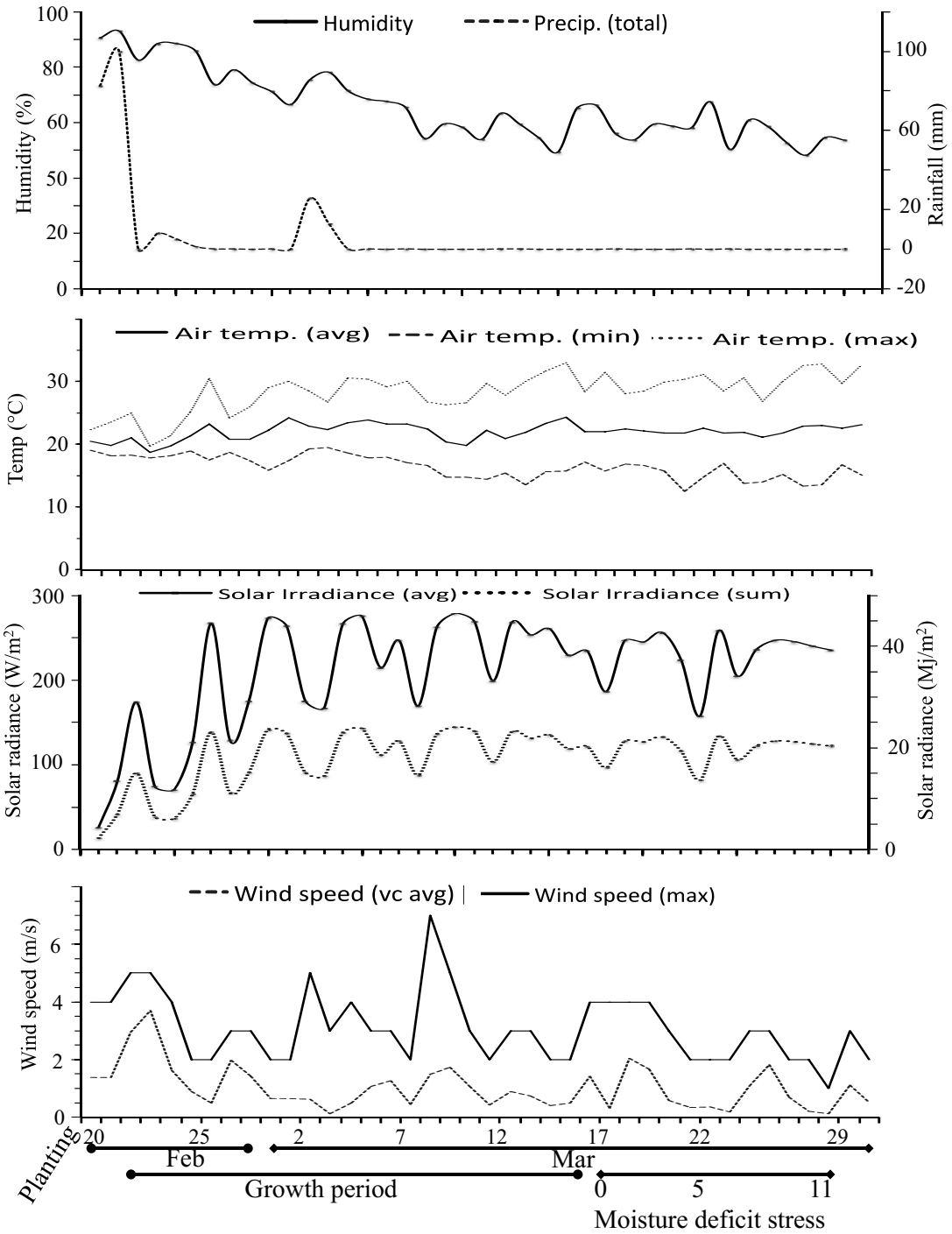

Fig 2.1. The climatic weather data during planting, monitoring and data collection in the natural open field in Gaborone, Botswana. The data is presented for (a) daily precipitation (mm) and humidity (%), (b) minimum, maximum and average day temperatures (°C), (c) solar radiation in W/m^2 and Mj/m^2 and (d) average and maximum wind speed (m/s). The x-axis shows the period of the study in date of the month format.

2.3 Results and Discussion

2.3.1 Weather conditions of the two growing conditions

The weather conditions of the open field during the data collection period showed average air temperature of 21.9 ± 0.36°C (Fig. 2.1). The average temp in the open field was lower than to the set temperatures in the growth chamber (30°C) for the entire plant and monitoring period. The two figures were contrastingly different, as the open field had a high variation in temperatures recorded, with the minimum air temperatures recorded at 15.4 ± 1.44 °C and maximum recorded at 29.5 ± 1.38°C. These high variations cannot be ignored, as it has been suggested variations in environmental conditions can influence variation of the results (Limpens et al. 2012). Notable is the precipitation recorded for the data period was very minimal, at an average value of 0.1 ± 0.08 mm per day. These minimal rainfall values were an advantage when imposing moisture deficit stress to evaluate the plants response to limited moisture. The average humidity was recorded at 59.5 ± 5.0%, a value closer to one set in the growth chamber experiments.

2.3.2 Changes in soil moisture content and morphological growth of crops

The plants morphological appearance is usually the first indicator of drought stress on plants, as drought stress usually results in plants wilting, yellowing of leaves followed by necrosis and falling off. These symptoms appear differently on different plants even when exposed to the same environmental stress, thus can be used as an initial monitoring tool for drought tolerance. When exposed to the same drought stress in the growth chamber conditions, the wild watermelon showed mild symptoms in terms of drought effect as compared to the cultivated species (Fig. 2.2), as the cultivated species showed severe wilting and yellowing of leaves while exposed to moisture limitations for a period of 11 days. This gives an initial indication that the wild watermelon has a higher tolerance to moisture deficit stress as compared to its cultivated relative. Observations in the field conditions on morphology of the plants under moisture deficit showed that the cultivar watermelon was more susceptible to drought stress. At the end of the study in the open field, the leaves were wilting and falling off in the cultivar watermelon (data not shown). These symptoms were not

observed for the wild watermelon plants, as their leaves were still intact at the end of the study.

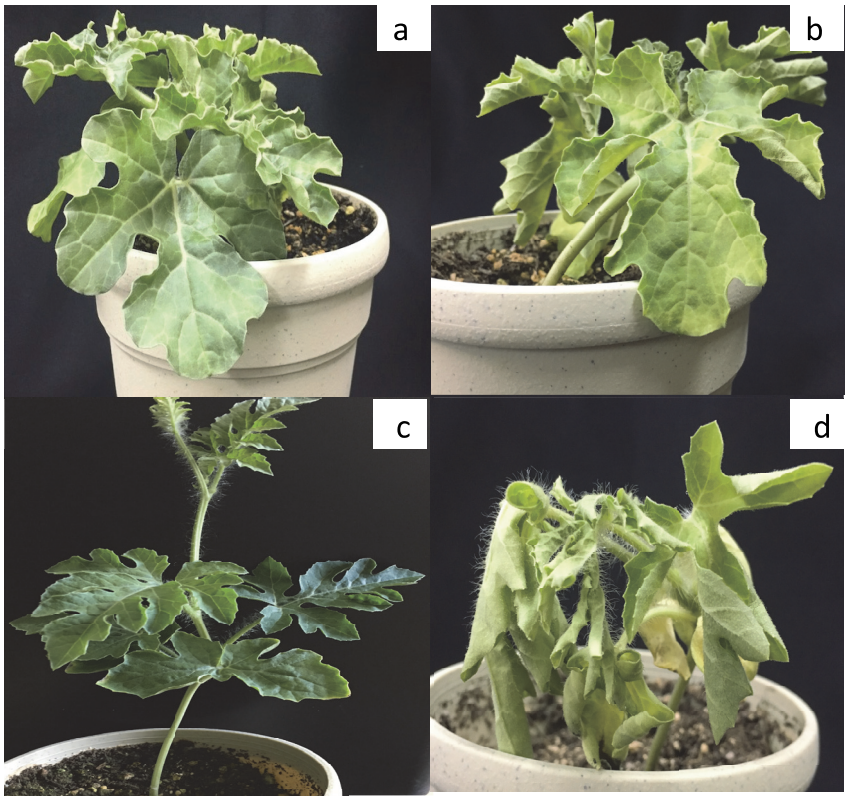

Fig 2.2. The morphological appearance of the two watermelon species grown in the controlled environment, before and after exposure to moisture deficit, pre-moisture deficit photos were taken on the last day of watering (0 DAI) while moisture deficit photos were taken at 11 DAI. Wild watermelon at 0 DAI (a); wild watermelon at 11 DAI (b); cultivar watermelon at 0 DAI (c); and cultivar watermelon at 11 DAI (d).

Monitoring the soil moisture status for growing plants is important as a requirement for the formulation and testing of any rigorous mechanistic hypotheses, such as those relating to the mechanisms of drought tolerance or adaptive responses in any plant when exposed to moisture deficit (Jones 2007). In this study, soil moisture was analyzed to determine the extent of stress exerted on the plant root as a consequence also on the whole plant. The roots are the initial parts that are affected or exposed to moisture deficit. Roots are known as the initiator of the signal transduction as they usually send chemical signals to initiate several stress response mechanisms or processes in the plant. Thus, soil water measurements were done in order to confirm limitation of available water content (AWC). The results show a rapid decline of AWC on the soils used in the growth chamber (Fig. 2.3). The initial soil moisture

content for both crops was recorded at near 80% or field capacity (FC) in this study, and the decline was observed as early as 3 DAI reaching the permanent wilting point (PWP) after 9 DAI. PWP is defined as a point where the soil only contains 10% or less of the water available to the roots (Grewal et al. 1990). Varying AWC was observed at every DAI point, thus signifying the difference in degree of stress exposure at every time point in the growth chamber condition. Available soil moisture content was not determined in the open field experiments.

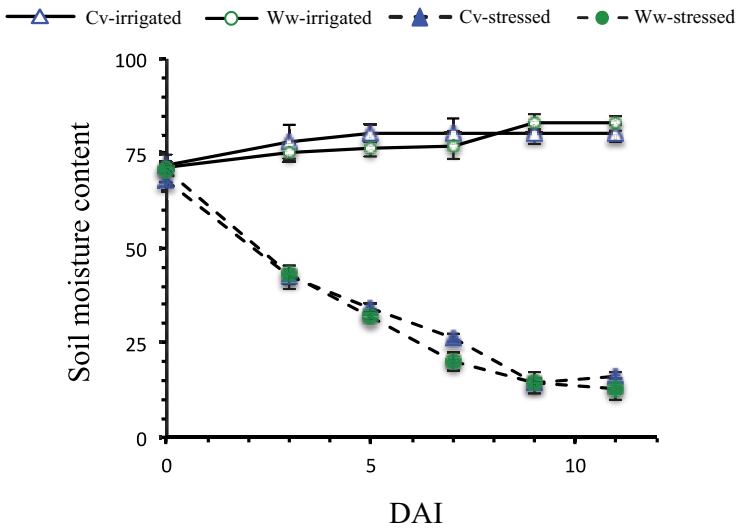

Figure 2.3. The available water content (AWC) in the soils was determined based on the gravimetric method. The figure shows the measurement taken for the controlled environment plant. The open blue triangle represents irrigated cultivar watermelon, the closed blue triangle represents the cultivar watermelon under moisture deficit, the open green circles represents irrigated wild watermelon and the closed green circle represents the wild watermelon under moisture deficit.

2.3.3 Photosynthesis and leaf physiological parameters

Photosynthesis, an important process in plant growth, has shown to be highly affected by drought. Effects of drought on photosynthesis has also shown to be varied among crop species. Drought exposure leads to decrease in gaseous diffusion, and results in metabolic constraints in plants (Pinheiro and Chaves 2011). In this study, high variation among the watermelon species was observed in response to moisture deficit (Fig 2.4a). The response showed a similar trend, even though varying in degree, for both controlled and open field environments.

The average assimilation recorded in irrigated plants were recorded at 27.63 ± 1.46 µmol CO_2 m^{-2} s^{-1} and 22.22 ± 0.46 µmol CO_2 m^{-2} s^{-1} for the wild and cultivated

species, respectively, under the open field management. For the growth chamber plants, the averages values were 24.35 ± 1.51 μmol CO_2 m^{-2} s^{-1} and 20.62 ± 1.08 μmol CO_2 m^{-2} s^{-1} for the wild and cultivated species, respectively. The wild watermelon response to moisture deficit was slightly sharper in the open field with a drop to 4.76 ± 1.39 μmol CO_2 m^{-2} s^{-1} at 5 DAI, as compared to 8.24 ± 1.28 μmol CO_2 m^{-2} s^{-1} recorded at the same time point under controlled environment. The values recorded at 11 DAI for the wild watermelon was 0.71 ± 0.21 μmol CO_2 m^{-2} s^{-1} and 0.64 ± 0.14 μmol CO_2 m^{-2} s^{-1} for the open field and growth chamber conditions, respectively. A delayed response was observed for cultivated watermelon in both growth conditions. Observation made at 5 DAI showed that the reduction of assimilation was recorded at 10.44 ± 1.71 μmol CO_2 m^{-2} s^{-1} and 12.25 ± 1.40 for the open field and growth chamber plants, respectively. These observations show that the wild watermelon has a better response mechanism than cultivar watermelon when exposed to moisture deficit stress.

One of the survival mechanisms that are attributed to drought-tolerant crops is their ability to restrict its stomatal opening during moisture deficit in order to minimize water loss from the leaves. This process does also limit the gaseous exchange that is essential for the photosynthetic process. An observation of the two watermelon species in this study showed two different responses of stomatal conductance when exposed to moisture deficit. The wild watermelon showed a similar trend with the CO_2 assimilation. A rapid decline in conductance was observed with 3-fold decline for plants grown in the open field, and 2-fold in the growth chamber plants at 3 DAI (Fig 2.4b). The cultivated watermelon did not show any significant decrease at 3 DAI. This could suggest a slow response of the cultivated watermelon to moisture deficit. The decline was significant for the wild species as compared to cultivated species for the entire monitoring period in both growing conditions. For the wild watermelon, the down-regulation was more intense in the open field. At the end of the moisture deficit treatment, the values for the two species in both growth conditions were not significantly different in terms of stomatal conductance.

The sudden closure of stomata in response to moisture deficit stress should have a direct influence on the intercellular CO_2 concentration. When the stomata close, they limit the gaseous exchange into the leaf cells. The closure will result in reduction

of carbon dioxide present in leaf mesophyll, thus reducing the photosynthesis process. This then brings a change in the CO_2 to O_2 ratio, leading to a rise in photorespiration rate during water stress. Athar and Ashraf (2005) observed that the stomatal closed completely during severe drought, resulting in both photosynthesis and photorespiration rates to lower. For the two species of watermelon, the internal CO_2 varied greatly on both the control conditions and the moisture deficit conditions, with the wild species recording higher values of intercellular CO_2 (Fig 2.4c).

Wild watermelon irrigated plants grown in the growth chamber recorded an average internal CO_2 of 362.62 ± 13.39 μmol CO_2 mol^{-1}, while that of the cultivated species was recorded at 306.91 ± 10.18 μmol CO_2 m^{-1}. A non significant decline was observed for the wild species with 341.27 ± 14.84 μmol CO_2 mol^{-1} recorded at 3 DAI, and the cultivated species also showed a non significant change under moisture deficit as compared to the irrigated plants recording at 320.94 ± 11.41 μmol CO_2 mol^{-1} at 3 DAI. Thereafter, the recordings in cultivar watermelon showed a decline reaching 268.33 ± 16.12 μmol CO_2 mol^{-1} at 11 DAI, while the wild species intercellular CO_2 was slightly higher for the same period recorded at 321.16 ± 11.47 μmol CO_2 mol^{-1}. The changes of internal CO_2 was more pronounced when plants were grown in the field conditions, where at 3 DAI a significant decline was observed for both plants. The decline was observed until the end of study at 11 DAI, where the recording stood at 298 ± 13.13 μmol CO_2 mol^{-1} for the wild and 288 ± 9.12 μmol CO_2 $mol^{-1}$for the cultivated species. The internal CO_2 values at 11 DAI were not significantly different between two species in both growth conditions.

In previous studies, the reduction of photosynthesis has been attributed to several factors like damage to any of the photosynthesis mechanism like photosynthetic pigments and photosystems, electron transport chain, and carbon dioxide reduction pathways. Damage at any level reduces overall synthetic capacity of plants (Ashraf and Harris, 2013), thus it is important to determine if the decline in the photosynthetic process is not a result of the damaged mechanisms. Measurements of the chlorophyll content provide gives an important insight into the physiological status of the plant, and offer an idea on the damage of the photosynthetic pigments (Gitelson and Metzlyak 2003).

In this study, observations on irrigated plants showed that no significant difference was observed for the SPAD reading between the two species recorded in

the open field. A slight significant difference was observed in the growth chamber grown control plants (Fig 2.4d).

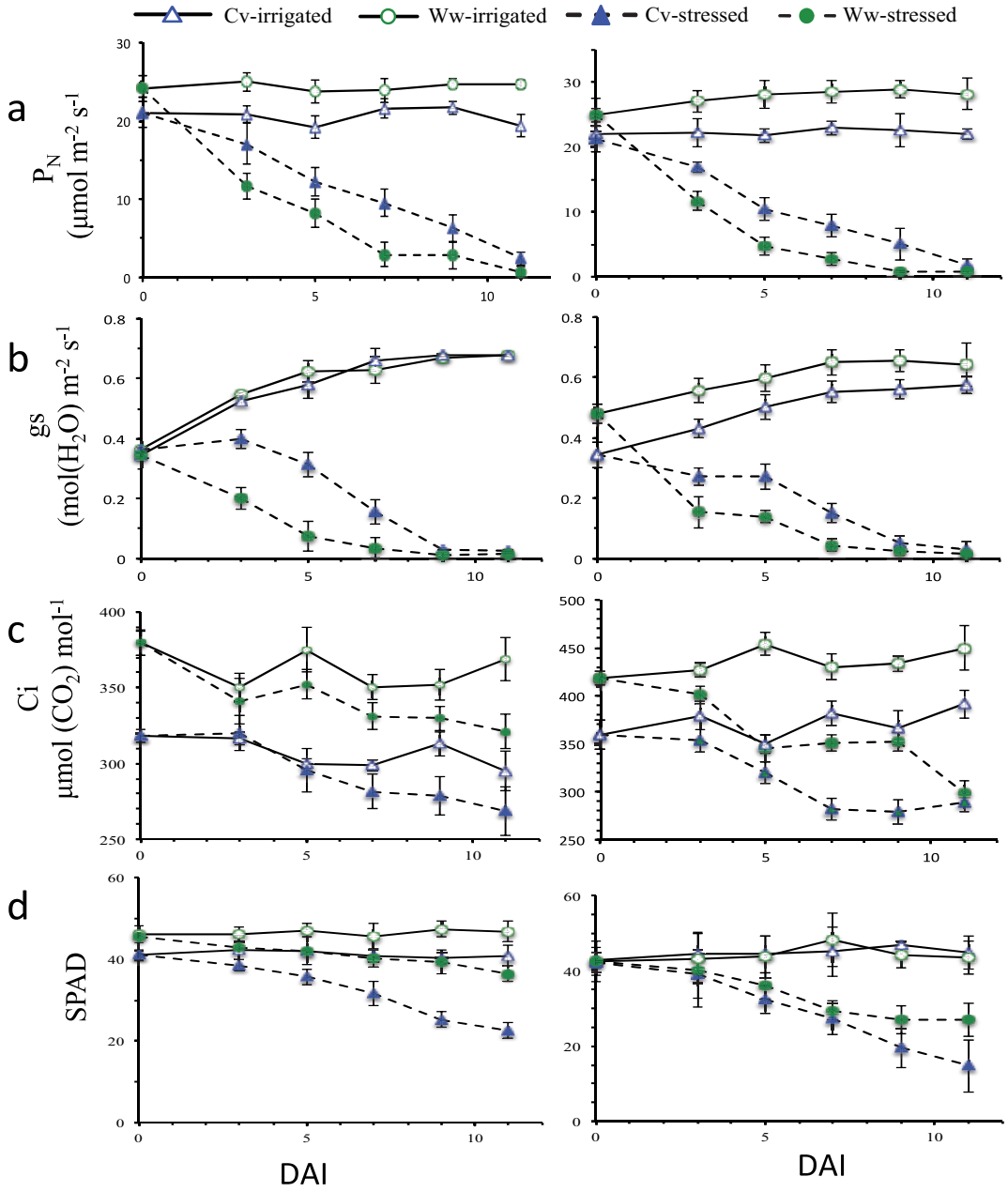

Figure 2.4. Effects of moisture deficit coupled with high light on the (a) photosynthetic rate (P_N), (b) stomatal conductance (g_s), (c) intercellular CO_2 concentration (C_i) and (d) photosynthetic pigmentation/chlorophyll content (SPAD). The open blue triangle represents irrigated cultivar watermelon, the closed blue triangle represents the cultivar watermelon under moisture deficit, the open green circles represents irrigated wild watermelon and the closed green circle represents the wild watermelon under moisture deficit. The left panel represents the data collected in plants grown under the controlled environment, while the right panel is the presentation of data collected from plants grown in open field. DAI indicates the stress time point in days after withdrawal of watering the plants. Means are for n=3, with bars showing the standards deviations of means.

Under moisture deficit stress, open field plants recorded a sharper decline in chlorophyll level, when compared to the counterparts grown in the growth chamber. At 11DAI, the recordings for the open field grown plants for the two species was 26.93±4.37 and 14.73±5.95 for wild and cultivated species, respectively, while for the growth chamber grown plants the SPAD reading were 36.43 ± 2.98 and 22.56 ± 1.49 for the wild and cultivated species, respectively, at 11 DAI.

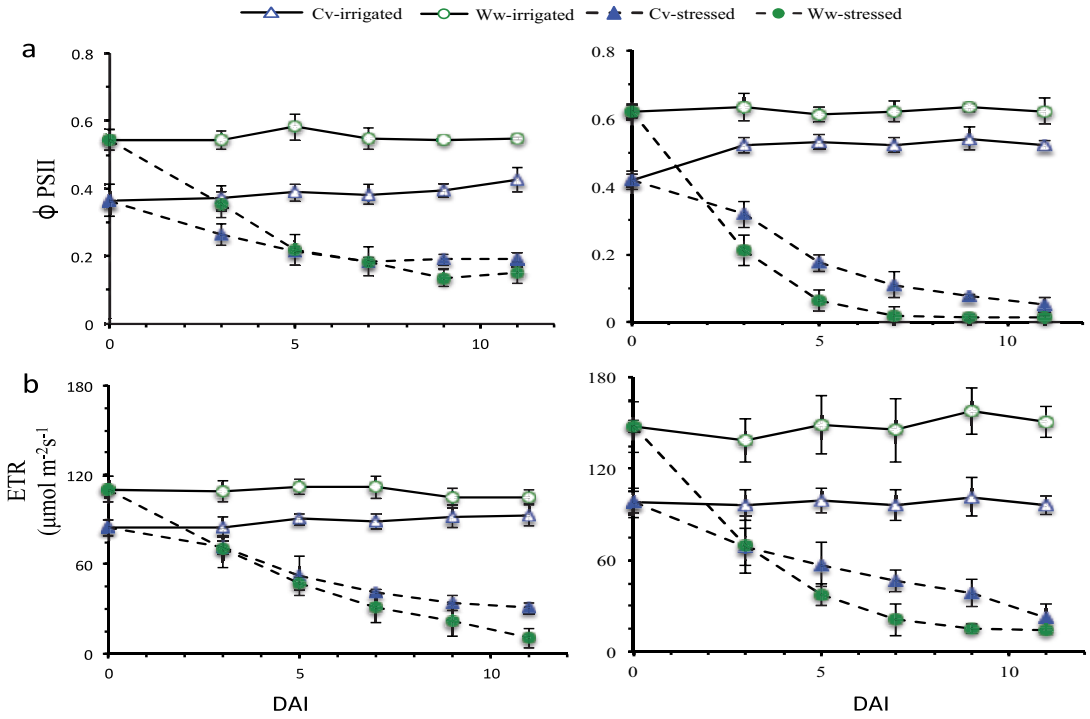

Figure 2.5. The effects of moisture deficit and excess light on the two watermelon species as monitored by photosystem II activity (ϕPSII) and electron exchange rate of the PSII (ETR). The open blue triangle represents irrigated cultivar watermelon, the closed blue triangle represents the cultivar watermelon under moisture deficit, the open green circles represents irrigated wild watermelon and the closed green circle represents the wild watermelon under moisture deficit. The left panel represents the data collected in plants grown under the controlled environment, while the right panel is the presentation of data collected from plants grown in open field. DAI indicates the stress time point in days after withdrawal of watering the plants. Means are for n=3, with bars showing the standards deviations of means.

2.3.4 Analysis of PSII and electron transport

The average ϕPSII values for the two plant species grown in open field under irrigation were higher when compared to their counterparts grown in the growth chamber. Upon imposition of moisture stress, a rapid decline was observed in both

plants under both growth conditions (Fig 2.5a). The wild plants grown in the field showed a much extensive decline compared to the cultivated plants or the wild plants grown in the growth chamber. From 5 to 11 DAI under the growth chamber condition, the PSII efficiency for the wild and the cultivated species were not significantly different each other. A highly pronounced difference was observed in the open field, where at 5 DAI the recordings stood at 0.064 ± 0.026 and 0.17 ± 0.024 for the wild and cultivated species respectively. The same trend was observed until the end of moisture deficit study at 11 DAI. The rapid decline suggests that at very low moisture availability the PSII are inactivated rendering them non functional. An exposure to excess light during drought stress usually triggers photorespiration, a process where the plant manages the excess light energy as a means protecting the PSII. The excess excitation energy will be immediately diverted toward driving the photorespiration pathway, thereby providing an efficient means for photo-protection at the expense of oxidation of previously assimilated carbon (Eisenhut et al. 2017), therefore it can be suggested that the photorespiration plays an important part in the protection of the PSII.

The electron transport rate (ETR) is a function of the PSII mechanisms thus it is highly correlated with the PSII activity. A similar pattern of response of the ETR to PSII activity was observed for both plants under the two conditions (Fig. 2.5b). The average recordings for the irrigated plants in the growth chamber condition was observed at 108.89 ± 7.33 and 88.96 ± 5.96 for the wild and cultivated species, respectively, while those of crops grown in the open were at 148.05 ± 16.34 for the wild and 97.82 ± for the cultivated plants. The final values observed at 11 DAI were not significantly different for each plant species grown either in the field or under controlled environment. The ETR reflects the efficiency of transformation of light energy in PSII, which indicates the efficiency of primary light capture when the PSII reaction center were partially shut down. Thus it correlates with the activities of PSII and can evaluate the transfer rate of photosynthesis electrons between PSI and PSII (Krall and Edward 1992; Martínez-Carrasco et al. 2002).

The maximal quantum yield of PSII photochemistry (Fv/Fm) showed varying tendencies. For plants grown in the growth chamber under irrigated conditions the Fv/Fm for the 2 species varied in the early stages of data collection, but at the end they showed no significant difference (Fig 2.6a).

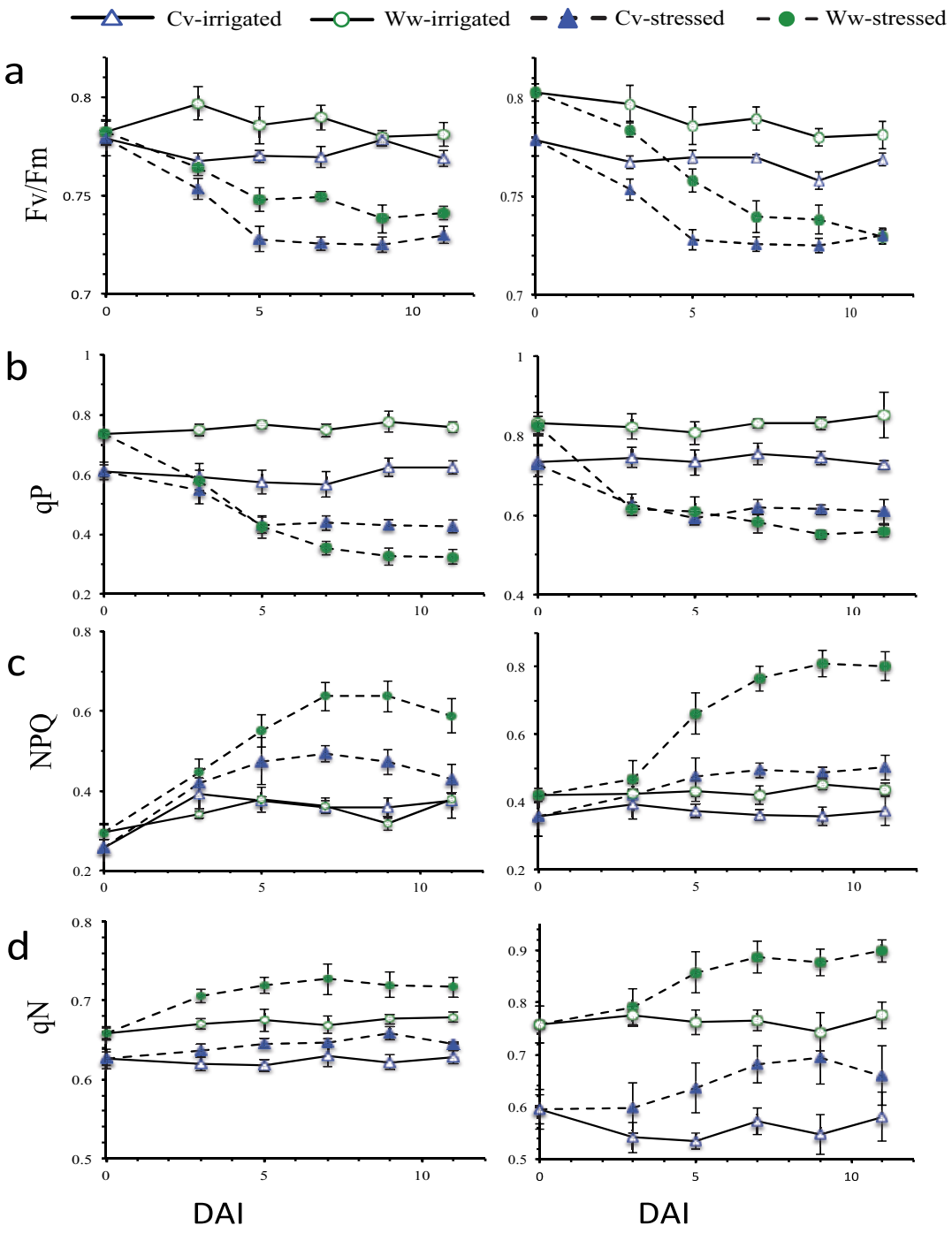

Figure 2.6. The effect of moisture deficit and excess light stress on the two watermelon species as monitored by the; (a) quantum yield of the PSII (Fv/Fm); (b) photochemical quenching (qP); (c) non-photochemical quenching (NPQ) and (d) qN. The open blue triangle represents irrigated cultivar watermelon, the closed blue triangle represents the cultivar watermelon under moisture deficit, the open green circles represents irrigated wild watermelon and the closed green circle represents the wild watermelon under moisture deficit. The left panel represents the data collected in plants grown under the controlled environment while the right panel is the presentation of data collected from plants grown in open field. DAI indicates the stress time point in days after withdrawal of watering the plants. Means are for n=3, with bars showing the standards deviations of means.

Observations made in the open field for irrigated plants showed a distinct difference between the two species throughout the study. The rate of decline for both plants in either of the growth conditions showed a similar trend. No significant difference was observed at 11 DAI between the plants in the open field, with Fv/Fm values dropping to 0.72 for both the crops. Under the growth chamber a slight difference was observed at 11 DAI, as wild plants Fv/Fm values were 0.74 ± 0.003 and the cultivated was at 0.73 ± 0.004.

The photochemical quenching (qP) has been widely used to determine the amount of light energy converted to chemical energy to be used in the photosynthesis process. The qP gives an indication of the proportion of PSII reaction centers that are open or functional. The effectiveness of the qP also acts as a protective mechanism as it maximize the production of O_2 in the PSII antenna (Muller et al. 2001). Under irrigated conditions the qP of both plants was steady but significantly different from one another, with the wild species showing a higher proportion of PSII reactions centers (Fig. 2.6b).

Exposure to moisture deficit showed a decline in the qP for both plants in a significantly different manner in both growth conditions. At 3 and 5 DAIs, the values for both crops in the separate growing conditions showed no significant difference. After the 5 DAI, qP values of the cultivated species did not change much as they stayed relatively the same until the end of the study. On the other hand, the values for the wild species continued to decline until they reached 0.32 ± 0.023 and 0.56 ± 0.016 for plants grown in the growth chamber and open field, respectively.

Under moisture deficit and high light stress, plants are known to dissipate light energy as heat, and this process protects the delicate PSII system (Masahiro et al. 2016). The major dissipation method is through the non-photochemical quenching (NPQ). NPQ is usually determined in plants through dark adaptation kinetics, as it has been noted that high energy state quenching relaxes within minutes when the leaf is placed in darkness (Maxwell and Johnson 2000). It is therefore important to determine the heat dissipation of different species under moisture deficit in trying to understand their tolerance mechanisms. It has been suggested that the species that can dissipate more heat will have the ability to protect its photosynthetic mechanisms, thus avoid any damage that can result in cell death.

Under irrigated treatments for both growing conditions, the two watermelon species showed closely related heat dissipation tendencies recording non-significantly different values over the entire growing period (Fig 2.6c). Exposure to moisture deficit activated a sudden increase in heat dissipation on the wild species grown in both field and in growth chamber. In the growth chamber condition, the increase seemed to be stabilized at 9 DAI, while in the open field the increase was observed until 11 DAI. The final NPQ values recorded for the wild species was at 0.58 ± 0.042 for plants in the growth chamber and 0.80 ± 0.036 for plants grown in the open field. The increase was also observed in cultivated watermelon, but the magnitude was lower than for the wild species. A highest peak of 0.49 was observed at 7 DAI in either of the growth conditions.

The observed trend suggests that the wild species tends to minimize the activities in the photosynthetic system as a protection measure, and maximize the dissipation of excess light energy as heat. Also the results shows that in the open field the dissipation is much stronger, suggesting that the field conditions could have been more harsh as compared to the growth chamber conditions.

2.3.5 A/Ci curves analysis

The A/Ci curve (net CO_2 assimilation rate, or P_N, versus calculated internal CO_2 concentrations, or Ci) analysis has become an important tool in determining the extent of damage to the photosynthetic parameters caused by drought stress (Manter et al. 2000). The A/Ci curve works on the inherent assumption that Ci is influenced by the active catalytic site of Rubisco. However, limitations to mesophyll CO_2 conductance, which are not incorporated in A/Ci measurements, may result in a difference between Ci (Manter and Kerrigan 2004).

The response of net photosynthesis to internal leaf CO_2 concentration (A/Ci curve) was determined at 1,000 μmol m^{-2} s^{-1} of PPFD. The measurements started at 400 μmol mol^{-1} of CO_2. Once the steady state was reached, the CO_2 concentration was gradually lowered to 50 μmol mol^{-1} and then increased stepwise up to 1000 μmol mol^{-1}. Net photosynthesis values were plotted against the respective internal leaf CO_2 concentrations (Ci) to produce an A/Ci response curve at different time points of moisture deficit (Fig 2.7). The maximum CO_2 assimilation with elevated CO_2 concentration was recorded at 32.67 ± 2.89 and 21.62 ± 1.78μmol m^{-2} s^{-1} for wild and

cultivated species respectively for the plants at 0 DAI grown in the open field.

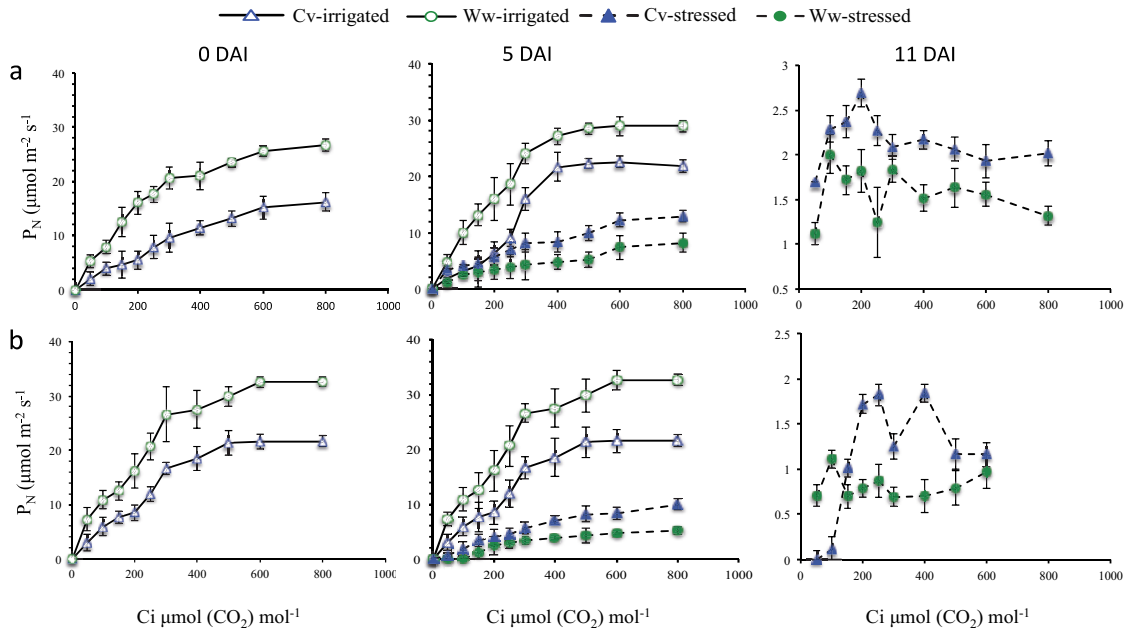

Figure 2.7. A/Ci curves showing the effect of different CO_2 internal concentration on watermelon plants exposed to drought stress. The open blue triangle represents irrigated cultivar watermelon, the closed blue triangle represents the cultivar watermelon under moisture deficit, the open green circles represents irrigated wild watermelon and the closed green circle represents the wild watermelon under moisture deficit. The top panel (a) represents the data collected in plants grown under the controlled environment, while the lower panel (b) is the presentation of data collected from plants grown in open field. DAI indicates the stress time point in days after withdrawal of watering the plants. Means are for n=3, with bars showing the standards deviations of means.

When the plants were exposed to drought stress, the A/Ci curve showed a sudden drop in the values of CO_2 assimilation. The decline was more rapid in plants grown in the open field as compared to growth chamber. At 11 DAI, the values were higher for the cultivated plants in both growing conditions when compared to the wild plants. The cultivated plants still showed the response to elevation of CO_2 even at the extreme moisture deficit, as it showed slight increases in CO_2 assimilation. The lower values of net photosynthesis rates in the A/Ci curves at 11 DAI could be associated stomatal conductance observed in the plants when the moisture stress intensified. This trend of dramatic decrease in CO_2 can be generally interpreted as an indication that the photosynthetic capacity of water-stressed plants was strongly impaired by biochemical damage (Centritto et al. 2009).

In conclusion, observations on plants in the open field showed several variations when compared to the plants in the growth chamber. Even though the variations were observed, the trend in the physiological changes was relatively similar in both conditions. The study of plant physiology in the open field conditions cannot be ignored, because it can vary from one extreme to another during the growing period, and it offers better understanding on the responses of plants under natural conditions, that is not provided in the controlled climate conditions.

Chapter 3

The cDNA structures and expression profile of ascorbate peroxidase gene family during high light and water deficit stress in wild watermelon

3.1 Introduction

Ascorbate peroxidase (APX) is reported to be an efficient scavenger of ROS, as it contributes to the hydrogen peroxide detoxification. It is present across a wide spectrum of plant kingdom, and they exist within different organelle in the cells, and play a significant role in stress tolerance (Saxena et al. 2011). APX differs from other peroxidases in its dependency on ascorbate as the source of reducing power, and becomes unstable in its absence (Shigeoka et al. 2002). Multigenic families of APX have been reported in various plants that are commonly referred to as isozymes, and mainly classified on the basis of their sub-cellualr localization. Even though they are closely related, they have shown different structural and kinetic properties, possessing specific conserved domains and signal peptides for each isozymes (Pandey et al. 2017).

Based on the structural and amino acid composition, five main isoforms of APX have been documented in plants, namely; the cytosolic (cAPX), mitochondrial (mitAPX), chloroplastic (chlAPX), stromal-APX and thylakoidal-APX), and microsomal (mAPX) (Caverzan et al. 2012; Yoshimura et al. 1999).

These enzymes are believed to collectively maintain the redox balance under stress, and this close coordination helps the protection from oxidative stress (Liu et al. 2012; Yin et al. 2014).

One of the characteristics of the APX is the susceptibility to the H_2O_2 in the absence of ascorbate (Hiner et al. 2000; Kitajima et al. 2006; Kitajima et al. 2007). The susceptibility varies among the isoforms, with chAPX showing highest degree of sensitivity and its half-life time under hydrogen peroxide has been recorded at 15 sec (Yoshimura et al 1998). The cytosolic APX has been found to be more stable under the ascorbate-depleted conditions (Ohya et al. 1997). These properties of the APX have made it easier to separately quantify their activities.

Assaying of the APX enzyme activity on wild watermelon exposed to drought stress conditions has shown an increase in the chAPX (Nanasato et al. 2010). The expression of the cAPX has been found to have no significant change in the wild watermelon leaves when exposed to same conditions. The gene families encoding the APX have been shown to vary in number among various plant

species. To understand further the role of each isoform of APX in wild watermelon, it is important to characterize the gene families expressed during drought stress, and to document the express their expression pattern. To our best knowledge no report has been found on the annotation APX isoforms of the watermelon species. Therefore in this research, I report on the cDNA structure, profiles and activity of the APX on the leaves of the drought tolerant wild watermelon leaves. I profiled the changes in mRNA when the plant is exposed to varying days of high light and moisture deficit stress.

3.2. Materials and Method

3.2.1 Plant materials and growth conditions

Wild watermelon (*Citrullus lanatus* acc. No. 101117-1) (Kawasaki et al. 2000), a natural inhabitant of the Kalahari Desert in Botswana, was self-pollinated for at least three times, and their seeds were used in this study. The seeds were soaked overnight in water at 30°C in the dark, then in the next morning the seeds were planted in pots filled with a horticulture soil. The germinated seedlings were grown in a growth chamber under LED lights with light intensity of 800-1,000 μmol photons m^{-2} s^{-1} under a 14 h light and 10 h dark photoperiod, with air temperature at 30°C, and relative humidity of 50% for entire growth and monitoring periods. After germination the plants were watered daily, with supplementation of 1,000-fold diluted Hyponex solution (Hyponex Japan, Osaka, Japan) twice a week until they reached a stage where fifth true leaf has fully expanded. When the leaves were fully grown, water deficit stress was introduced by withholding watering to the plants.

3.2.2 Data and sample collection

Wild watermelon plants were grown until their fifth true leaves have fully expanded, and then withholding watering of the plants imposed water defict stress. Then data was collected at different time points from onset of stress induction, with 0 day being the last watering day before the stress induction, and then 3, 5, 7, 9 and 11 days after stress induction. Physiological measurements were done on the third fully open leaf, replicated four times, and then later averaged to get final values. The three upper leaves were collected for both mRNA extraction and enzyme assay.

3.2.3 Characterization of cDNA clones for APX genes

Watermelon cDNA and genomic sequences for putative APX genes were searched against a genome sequence database of *Citrullus lanatus* subsp. vulgaris cv. 97103 (Guo et al, 2013; www.cucurbitgenomics.org) with known BLAST settings and a threshold of 1e-10. Subcellular locations of these gene products

were predicted by the Wolf PSORT and DeepLoc-1.0 programs (Nakai and Horton 1999; Armenteros 2017). To analyse the intron-exon structure of the studied genes, a Gene Structure Display Server (Hu et al. 2015) was used to produce genome structure of the APX gene based on the CDS and corresponding genome sequences information.

The GenomeNet (Kanehisa et al. 2002; Kanehisa and Goto 2000) tools were used to generate the amino acids alignment. A neighbor joining analysis-based phylogenetic tree was constructed using the wild watermelon, Arabidopsis, Spinach and pumpkin amino acid sequences to examine relatedness of APX genes. Sequences information are shown in Table 3.1.

Leaf samples were quickly snap frozen into liquid nitrogen, and stored at -80°C until RNA isolation. Total RNA was extracted with the application of Spectrum Plant Total RNA Kit (Sigma Aldrich, Missouri, USA) and, subsequently, trace amounts of genomic DNA were degraded using the On-Column DNase I Digestion Set (Sigma Aldrich, Missouri, USA). The cDNA synthesis were performed using ReverTra-Ace-α synthesis kit (Toyobo Co., LtD, Osaka, Japan) using an Oligo(dT) primer (Toyobo Co.LTD, Osaka, Japan).

CDSs of wild watermelon were amplified by PCR using pairs of primers designed to anneal flanking 5'- and 3'-UTR regions (Table 3.2), with wild watermelon cDNA prepared from a leaf of wild watermelon that was exposed to water deficit stress for three days. The PCR products were separated in an agarose gel electrophoresis, and amplicons with expected sizes were purified from the agarose gel using Qaigen MinElute, and Gel Extraction Kit (QIAGEN Hilden, Germany), and then sub-cloned into an Invitrogen TOPO-BLUNT vector (Life technologies, CA, USA). Sequences of the clones were analyzed by BigDye terminator v3.1 Cycle Sequencing Kit (Applied Biosystems, CA, USA). The sequences obtained after sequencing were translated into amino acids and then an alignment of the amino acids was done using the ClustaW online tool.

Table 3.1. Accession numbers for plant APX genes that were used in this study.

Organism	Gene	Accession number [*1]
Arabidopsis thaliana	AtAPX1	AT1G07890.1
	AtAPX2	AT3G09640.1
	AtAPX3	AT4G35000.1
	AtAPX5	AT4G35970.1
	At.sAPX	AT1G77490.1
	At.tAPX	AT4G08390.1
Spinach	So.cAPX	D85864
	So.mAPX	D84104
	So.sAPX	D83669
	So.tAPX	D77997
Pumpkin	Cka.mAPX	AB070626
	Cka.sAPX	D88420
	Cka.tAPX	D83656

[1] For Arabidpsis, AGI locus identifiers were shown. For spinach and pumpkin, NCBI/EMBL/DDBJ accession numbers were shown

Table 3.2. Primer sequences used in this study

Usage	Primer name	Primer sequence
Full length cDNA amplification		
	APX-1F	CTTTTCAAGAGAATCTCAGCC
	APX-1R	CGTTTGAACTTCTGGAGAAG
	APX-2F	CATTTTTTCCAAGTTTCATCACC
	APX-2R	TTTTCCCCCGTTCCAATTGC
	APX-3F	TGCTCTGTAGCCTCCTCCC
	APX-3R	AATCGACCTTGCTACTGTAA
	APX-4F	TCTGCATTCTTATCCAAGATTTCA
	APX-4R	TGGAAGAATATCTTTCTTCTGTATAA
	APX-5F	GAAAACTCAAATTTCAACTAAATCC
	APX-5R	CTCATAAATAGATTAATTTAAACACTCAAA
3'-RACE		
	Apx5-1086F+Kpn	GCGGTACCTGCTGGAGAGAAGTTCG
	3sites-Adaptor	CTGATCTAGAGGTACCGGATCC
	3sites-Poly-dT	CTGATCTAGAGGTACCGGATCCTTTTTTTTTTTTTTTT
RT-qPCR for CLAPX		
	CLAPX1-77F	TTGTTGCTGAGAAGCACTGC
	CLAPX1-195R	TTCCGCTGCGTTCTTCATTG
	CLAPX2-79F	ATCGCTGAGAAGAACTGTGC
	CLAPX2-163R	CACCGGTCTTGGTTTTCTGGTC
	CLAPX3-71F	TCATTGCCAATCGGAACTGC
	CLAPX3-162R	AGGCCCACCAGTTTTTGTAG
	CLAPX4-134F	ACGACGCTGAAACGAAAACC
	CLAPX4-253R	TGGCCTTCACAGTTTCACAG
	CLAPX5_I-1004F	CTGAAGCCCATGCCAAACTC
	CLAPX5_I-144R	CTGATAGCTCTCTCTTTCCATATGAG
	CLAPX5_II-1004F	CTGAAGCCCATGCCAAACTC
	CLAPX5_II-1146R	ACTTGTTTTTTAATCCTTTCCATATGAGTA
RT-qPCR for rerefence genes		
	Actin-F	TGGTCGTACAACAGGTTGTGC
	Actin-R	TTCGGCAGTGGTTGTGAACATG
	Tubulin-F	GGTCAGGAAGTTGGCTGATAAC
	Tubulin-R	CACTGACAAGCGCTCTAACAAC
	GAPDH-F	CCGATGAGGATGTTGTTCTCTAC
	GAPDH-R	CATTGTCGTACCAAGTCACCAG
Sequencing		
	M13-F	GTAAAACGACGGCCAG
	M13-R	CAGGAAACAGCTATGAC

3.2.4 Measurement of water relation

Leaf relative water content was measured essentially as described previously (Smart 1974) with following modification. The leaves were harvested, and fresh weight was quickly measured on Unibloc AUX 120 balance (Shimadzu, Kyoto, Japan) to avoid loss of moisture from the leaves, and recorded as the fresh weight (FW). After the measurements of FW, the leaf samples were placed in zip-lock plastic bags that were filled with distilled water, and kept overnight at room temperature. Next day, excess water was removed by blotting the leaves within the paper towels, then the water-saturated leaves were weighed and recorded as turgid weight (TW). The turgid leaves were then oven dried at 80°C for 3 days, and their weights were recorded as the dry weights (DW). The LRWC (%) was calculated by the following formula (Smart 1974);

$$\frac{FW-DW}{TW-DW}\ x\ 100 \quad (1)$$

Available water content (AWC) was determined essentially as described previously (Reynolds 1970) with following minor modification. After harvesting leaf samples, entire aboveground plant tissues were cut out, then the moist soil together with the planting pot were weighed and recorded as the wet mass, then the soil was oven dried at 105°C for 72 h after which it was weighed and the mass recorded as the dry mass. The available water content (AWC) was determined by the following formula (Reynolds 1970);

$$\text{AWC} = \frac{\text{wetmass-drymass}}{\text{drymass}}\text{Xd} = \frac{wet\ weight-dry\ weight}{dry\ weight}\ X\ 100 \quad (2)$$

3.2.5 Measurements of photosynthetic parameters

Leaf chlorophyll content were measured 3-4 h after the onset of light regime using SPAD-502plus meter (Konica Minolta, Tokyo, Japan). Leaf stomatal conductance was measured by SC-1 leaf porometer (Decagon Devices, Washington, USA) 5 h after the onset of light regime. CO_2 assimilation and chlorophyll fluorescence were measured in the third true leaves using an open gas exchange system LI6400XT photosynthesis meter (LI-COR Biosciences,

Nebraska, USA). A 2-cm radius IRGA gas chamber was used for all the measurements, with a setting of chamber temperature at 25°C, CO_2 flow rate at 400 µmol mol^{-1}, PPFD at 1,000 µmol photons m^{-2} s^{-1}, and relative humidity at 50%. The CO_2 assimilation were measured 3 h after the onset of light regime, while the chlorophyll fluorescence of dark-adapted leaves were measured early morning before the onset of light regime when the plants were kept in darkness for more than 5 h.

3.2.6 APX enzyme assay

Crude leaf extracts was prepared essentially as described previously (Nanasato et al. 2010) with following minor modifications. Approximately 200 mg of leaf tissues were ground to a fine powder using a pestle and mortar, with the aid of liquid nitrogen in a 1 ml of homogenization buffer containing 50 mM potassium phosphate, pH 7.0, 1 mM EDTA, 1 mM sodium ascorbate, 1% (w/v) 3-[(3-chloramidopropyl) dimethyl-ammonio]- 2-hydroxyl-1-propanesulfonate, and 2% polyvinylpolypyrrolidone. The homogenized samples were centrifuged at 12,000 × g for 20 min at 4°C, and then the supernatant was collected into a new tube. The extract was desalted by running through an Amicon ultracel 3K filter (Merck Millipore Ltd, Burlington, MA, USA), and their protein concentration was quantified by the Bradford assay (Bradford 1976) with Protein Assay CBB Solution (Nacalai, Kyoto, Japan) and the Multiscan FC (Thermo Fisher Scientific Inc, Waltham, MA, USA), using various concentrations of bovine serum albumin as the standard.

APX enzyme activity was measured essentially as described previously (Nakano and Asada 1981; Amako et al. 1994) with following modifications. The 1 ml volume of reaction mixture consisted of 50 mM potassium phosphate buffer, pH 7.0, 1 mM sodium ascorbate, 10 µl of the crude leaf extract. The assay was activated by addition of 0.5 mM of H_2O_2 substrate (Wako pure chemical industries, Osaka, Japan), and a sample without the H_2O_2 substrate was used as a reference. The oxidation of ascorbate was continuously monitored at 290 nm on UH5300 spectrophotometer (Hitachi, Tokyo, Japan), and the absorption coefficient of 2.8 x 10^{-3} M cm^{-1} (Nakano and Asada 1981) was used for the

calculation of reaction rates. One of the properties of the APX isoforms is the rapid inactivation when incubated with H_2O_2 in limited ascorbate conditions, with chloroplastics APX being half inactivated in just 15 s while the cytosolic APX being less sensitive to incubation in depleting ascobate (Ishikawa et al. 1998; Yoshimura et al. 2000). This property was used to estimate the chloroplast and cytosolic isoforms following the method of Yoshimura et al. 1998.

3.2.7 Quantification of APX gene expression

The pairs of specific primers used for RT-qPCR analysis of wild watermelon APX genes (Table 3.2) were designed using the Primer3 online tool (Untergasser et al. 2012). The designed primers were then used to quantify the mRNA abundance of wild watermelon APX genes using the Light-Cycler 480 (Roche Diagnostics GmbH, Mannheim, Germany), run using LightCycler 480 SYBR Green I Master Kit (Roche) according to the manufacturer's instruction. Three references genes which showed highly homogeneous expression in a wide range of tissue types, developmental stages and environmental stimuli in watermelon (Kong et al. 2014), i.e. γ-actin (ylsACT), α-tubulin (ylsTUB), and glyceraldehyde-3-phosphate dehydrogenase (ylsGAPDH), were used as reference genes for internal controls, and their normalized value was used to calculate relative abundance of respective APX mRNAs. The profiling of mRNA quantification was run with three biological replications, each consisted of averages of three technical replications.

3.3 Results and Discussion

3.3.1 Genome structure of the identified APX genes

Using the protein sequences deduced from all APX genes in *Arabidopsis thaliana* (Panchuk et al. 2002; Table 3.1) as the queries, I identified five homologous genes in the whole genome sequence of cultivar watermelon (*Citrullus lanatus* subsp. *vulgaris* cv. 97103) in the Cucurbit Genomics Database. Based on the degree of similarity to the Arabidopsis APX sequences, the five genes identified are herein referred to as *CLAPX1, CLAPX2, CLAPX3, CLAPX4* and *CLAPX5*. The genebank reference and identification numbers of these genes can be found in Table 3.3.

To understand better the relatedness of the APX isogens, the gene structures were compared (Fig 3.1) based on the intron-exon arrangements of the five wild watermelon APX genes. The genome structure showed differences in arrangement, length and also number of exons and introns in every APX isogenes, with 9-12 exons predicted in these *CLAPX* genes (Fig. 3.1).

A comparative analysis between the wild watermelon and the cultivar watermelon (Table 3.3) showed high percent of similarities in amino acids sequence even though the sequences themselves amoung the two species were not 100% identical (data not shown). The subcellular location predicted by WoLF PSORT for each isogenes showed that, *CLAPX*1 and *CLAPX5* are localized in the chloroplast, while *CLAPX2*, *CLAPX3* and *CLAPX*4 were predicted as the cytosolic localized APX. Discrepancies were observed when using the other predicting tool DeepLoc 2.0, as it classified *CLAPX1* as the cytosolic APX, and *CLAPX2* and *CLAPX3* as perisomal APX.

Table 3.3. Summary on ascorbate peroxidase genes in watermelon

Isoenzyme name	cultivar watermelon (cv. 97103)				wild watermelon (Acc. No.101117-1)				
	Chr. [*1]	Locus name	Locus position	Unigene ID	Acc. ID [*2]	NT sim. (%) [*3]	Length of AA [*4]	WoLF PSORT [*5]	Deep Loc [*5]
CLAPX1	2	Cla013254	30982510..30986181(-)	wmu39844	MH178405	99.2	250	chl	cyt
CLAPX2	3	Cla008291	2065040..2073452(-)	wmu23766	MH178406	99.2	249	cyt	cyt
CLAPX3	2	Cla015833	3993709..3997744(+)	wmu34919	MH178407	99.2	286	cyt	per
CLAPX4	1	Cla014301	29858539..29862551(-)	wmu57455	MH178408	99.5	296	cyt	per
CLAPX5-I	8	Cla013927	14858020..14864092(-)	wmu44297	MH178409	99.1	427	chl	mit/chl
CLAPX5-II	8	Cla013927	14858020..14864092(-)	wmu05603	MH178410	99.0	378	chl	mit/chl

[*1] Chromosome number in which APX gene was encoded.

[*2] DDBJ/Genbank/EMBL accession numbers of APX sequences for the Acc. No. 101117-1.

[*3] Percent similarity of CDS nucleotide sequences between APXs from cv. 97103 and Acc. No. 101117-1.

[*4] Length of amino acid deduced from the CDSs in Acc. No. 101117-1.

[*5] Subcellular location of the gene product in Acc. No. 101117-1 was predicted by WoLF-PSORT and DeepLoc-1.0 programs, and expressed as chl (chloroplast), cyt (cytosol), per (peroxisome), and mit (mitochondria).

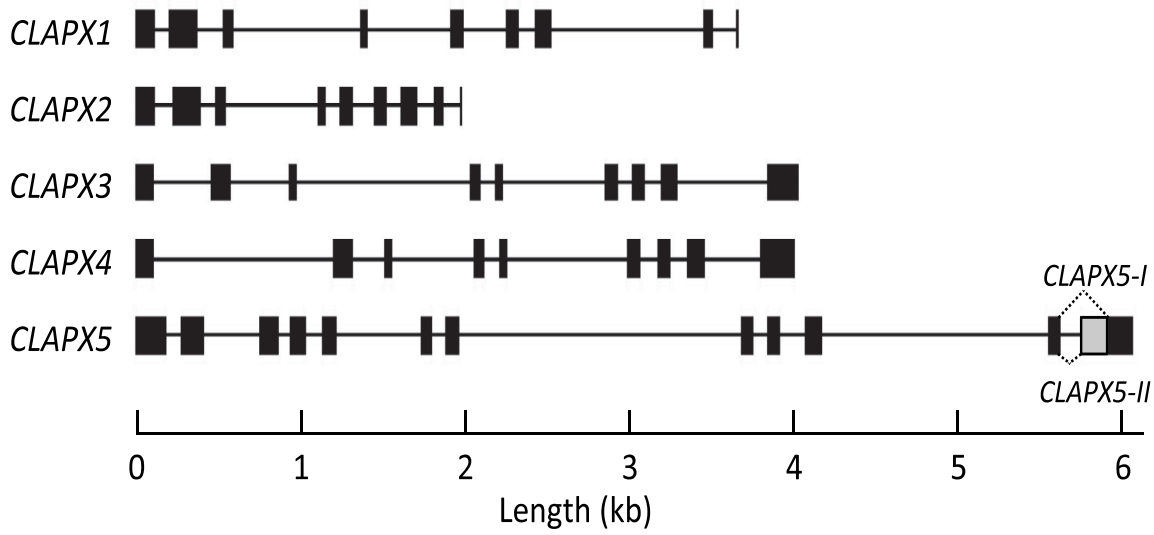

Figure 3.1. Schematic representation of watermelon APX gene structures. Exon regions are shown as black boxes and intron regions are shown as horizontal lines. Patterns of alternative splicing in intron 11 of *CLAPX5* are shown by broken triangular lines, and a region within exon 12 that is absent in one variant of the mature mRNA (*CLAPX5-I*), but present in another variant (*CLAPX5-II*), is shown as a gray box.

3.3.2 The 3'-RACE analysis

The polyadenylation of mRNA has shown to be an important process in gene expression of eukaryotes, with the mature mRNAs possessing a poly(A) tract, that in turn functions to facilitate transport of the mRNA to the cytoplasm and its subsequent stabilization and translation (Wu et al. 2011). The polyadenylation

process requires two major components: the cis-elements or poly(A) signals of the pre-mRNA, and the trans-acting factors that carry out the cleavage and addition of the poly(A) tail at the 3'-end (Li and Hunt 1997). It has been suggested that the multiple forms of plant polyadenylation complex, together with the diversified polyA signals may explain the intensive alternative polyadenylation and its regulatory role in biological functions of higher plants (Hunt et al. 2012). The poly(A) tail contributes regulatory information to the polyadenylation processes through interactions with RNA processing factors and poly(A)-binding proteins, thus making them important in gene expression (Hunt 2012). Therefore, it is important to locate the junction between cleavage site and the poly (A) tails. Beside, the chloroplast APX has been documented to have isogenes derived from the alternative splicing (Jespersen et al. 1997). It is therefore important to identify any splicing effects in this study.

The 3'-RACE experiments using a forward primer in exon 11 detected two different splicing patterns that matched with the C-terminal of the two *CLAPX5* isogenes cDNA sequences. In *CLAPX5-II*, an occurrence of the shorter intron 11 by the alternative splicing generated an in-frame stop codon immediately after exon 11, resulting in the shorter CDS in comparison to the *CLAPX5-I* variant. The 3'-RACE experiments revealed that poly(A) tails began at two different cleavage sites (Loke et al., 2005; Shen et al., 2008), designated proximal and distal cleavage sites, which positioned at 47 and 75 nucleotides downstream, respectively, from the last nucleotide of the terminator codon of *CLAPX5-I* (Fig. 3.2). Both of the proximal and distal cleavage sites occurred for *CLAPX5-I* and *CLAPX5-II* transcripts, implying that the selection of cleavage site for the poly(A) tail attachment may not influence the pattern of alternative splicing, in contrast to the case in spinach (Yoshimura et al. 1999). Putative near upstream elements (NUEs) of the cis-acting poly(A) signals were found at 22-28 nucleotides upstream of the cleavage sitess (Fig. 3.2).

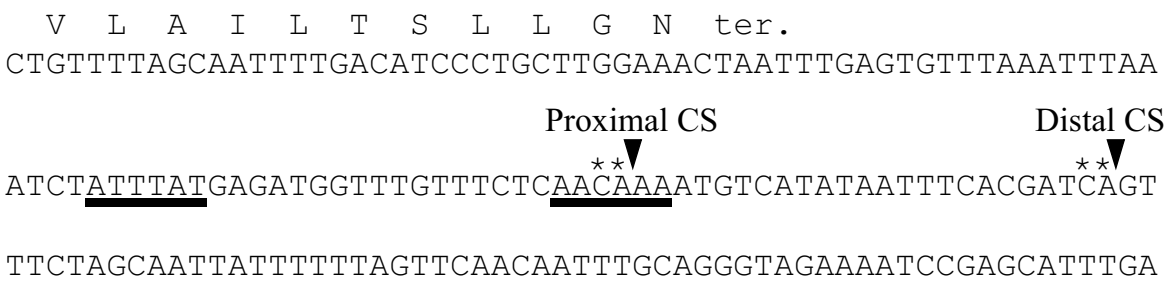

Fig 3.2. The observed cleavage sites for addition of poly(A) tails, and putative cis-acting poly(A) signals in the *CLAPX5* gene. The positions of observed proximal and distal cleavage sites (CSs) for the addition of poly(A) tails were shown by the downward arrows, and the conserved CS motifs were indicated with asterisks on top of the dinucleotides. The hexanucleotides for the putative near upstream elements (NUEs) of the poly(A) signals (Loke et al., 2005) are shown by the underlines.

A further analysis of the C-terminal amino acid sequences of *CLAPX5-I* and *CLAPX5-II* showed a strong sequence similarity with those of tAPX and sAPX from pumpkin. It has been shown that pumpkin tAPX and sAPX were generated from a single gene by alternative splicing, and the C-terminal extension in tAPX contains a putative thylakoid-spanning domain (Mano et al. 1997). Comparison of genomic sequences between *CLAPX5* and pumpkin chloroplast APX (Fig. 3.3 and Fig. 3.4) showed that their C-terminus genomic regions were markedly conserved, including the conserved splicing junction between exon 11 and intron 11, and the alternative junctions between intron 11 and exon 12. These observations suggest that the two mRNA variants from *CLAPX5*, i.e., *CLAPX5-I* and *CLAPX5-II*, may correspond to tAPX and sAPX, respectively, and the two watermelon APX isoenzymes may be generated from a single gene by an alternative splicing mechanism which is similar to that in pumpkin.

As a result of alternative polyadenylation and splicing, four mature mRNA variants were observed, two associated with the tAPX, and the remaining two associated with the sAPX.

a

```
CLAPX5-1   PAGEKFEAAKYSYGKRELSDSMKQKIRAEYEGFGGSPDKPLPTNYFLNIIVVIAVLAI  420
           |||||||+|||||||||||||||||||||||||#|||||||||||||||||||||+|||||||
Cka.tAPX   PAGEKFDAAKYSYGKRELSDSMKQKIRAEYESFGGSPDKPLPTNYFLNIILVIAVLAI  414

CLAPX5-1   LTSLLGN  427
           |||||||
Cka.tAPX   LTSLLGN  421
```

b

```
CLAPX5-II  PAGEKFEAAKYSYGKD  378
           ||||||+||||||||||
Cka.sAPX   PAGEKFDAAKYSYGKD  372
```

Figure 3.3. C-terminus amino acid alignment between *CLAPX5* and pumpkin chloroplast APXs. Amino acid alignments of C-terminal region for a pair of *CLAPX5-I* and pumpkin thylakoid Cka.tAPX (a), and a pair of *CLAPX5-II* and pumpkin stromal Cka.sAPX (b). The region spanning exon 11 and exon 12 is shown for each pair. Identical amino acids are labeled by vertical lines, similar amino acid residues between the pair are labeled as +, and amino acids with different chemical properties are labeled as #.

```
        P  A  G  E  K  F  E  A  A  K  Y  S  Y  G  K                (i)
CLAGK5  CCTGCTGGAGAGAAGTTCGAGGCCGCCAAATACTCATATGGAAAGgtcgtatacattacaaactttcatattt-tcatttcatttctttgcacaattgaa 99
        |||||#|||||||||||#||#|||||||||||||||||#||#|||||||||||#|||||||||||||||#|#|||  #|||||||||#|||||||##||##|#
Cka.APX CCTGCAGGAGAGAAGTTTGATGCCGCCAAATACTCATACGGGAAGgtcgtatncattacaaactttcttntttcccatttcatttatttgcatgataaat 100
        P  A  G  E  K  F  D  A  A  K  Y  S  Y  G  K

                                                                  (ii)  D  *
CLAGK5  gtcttcagaaaatctcatgtcttcgtaaaatgtttatcttctctacttttggctgtctactgcaggattaa---aaaacaagtct-catgttttgttgtg 195
        #||||#|#|||||||  ||||||#|||||||||||||||||||||||||||#|||||||||||||#|   |||||||||#|  |||||||||||||
Cka.APX ttctttaaaaaatctc--gtcttcataaaatgtttatcttctctacttttggttgtctactgcaggattgattaaaaacaagtttccatgttttgttgtg 198
                                                                        D  *

CLAGK5  ccacttgtcttttaataatacaagt--cgaagctttattcaagtccttgacatctgtgatgtc-acgtctaaaaaaaacttggaagtcttaaatgaagga 292
        #| |#|||| |||||| ||||#|||  #||||#|#|||||#|##||#|||||||||||||||| #|||||    ||||||||||||#|||||||||#|
Cka.APX ac-cgtgtc-tttaat-atacgagttgagaagatatattccaaaccctgacatctgtgatgtccgcgtcta----aaacttggaagtctaaaatgaagca 291

                                          (iii) R  E  L  S  D  S  M  K  Q  K  I  R  A  E  Y  E  G  F  G
CLAGK5  gaaatggaataaaattcaatagt--attgcctatttgaattgcagAGAGAGCTATCAGACCCAATGAAGCAGAAGATTCGGGCTGAATACGAAGGTTTTG 390
        | |||||||||||||||||||  ||||||||||||||||||||||||||||||||##|||||||||||||||||||||||#|||||||||#|#||||
Cka.APX g-aatggaataaaattcaatagtgtattgcctatttgaattgcagAGAGAGCTATCAGATTCAATGAAGCAGAAGATTCGGGCGGAATACGAAAGCTTTG 390
                                                  R  E  L  S  D  S  M  K  Q  K  I  R  A  E  Y  E  S  F  G

          G  S  P  D  K  P  L  P  T  N  Y  F  L  N  I  I  V  V  I  A  V  L  A  I  L  T  S  L  L  G  N  *
CLAGK5  GTGGAAGTCCAGATAAGCCTTTACCAACAAACTACTTCCTTAATATCATTGTTGTGATTGCTGTTTTAGCAATTTTGACATCCCTGCTTGGAAACTAA 488
        ||||||||||||||||||||||||||||||||||||||||||||||||||||||||||##|||||||||||||||||#|||||||||||||||#||##|||||||#|
Cka.APX GTGGAAGTCCAGATAAGCCTTTACCAACAAACTACTTCCTTAATATCATACTTGTGATTGCTGTTTTGGCAATTTTGACATCTCTTCTAGGAAACTGA 488
          G  S  P  D  K  P  L  P  T  N  Y  F  L  N  I  I  L  V  I  A  V  L  A  I  L  T  S  L  L  G  N  *
```

Figure 3.4. Comparison of genome sequence between *CLAPX5* and the pumpkin chloroplast APX gene in the region that corresponds to the C-terminus. A nucleotide sequence alignment between *CLAPX5* and the pumpkin chloroplast APX gene in their C-terminal region is shown. The region spanning exon 11 and exon 12 is presented. Identical nucleotides between the two sequences are labeled as vertical lines and different nucleotides are labeled as #. Deduced amino acid sequences for *CLAPX5* and pumpkin chloroplast APX are presented on top of and below the nucleotide sequences, respectively. Terminator codons are indicated by asterisk (*). A conserved "gt" motif at the beginning of intron 11 is boxed and labeled as (i), while the conserved "ag" motif for the termination of intron 11 for *CLAPX5-II* and *CLAPX5-I* are also boxed and labeled as (ii) and (iii), respectively.

An alignment of the amino acids sequences of the six *CLAPX* genes (Fig. 3.5) showed a relatively high degree of homology among the sequencs. This is not suprising because a highly conserved domain among the APX isogenes has been noted before (Yoshimura et al. 1998).

The chloroplastic APX genes can be further characterized into two subgroups based on their localities inside the chloroplast; the stroma and the thylakoid types. The *CLAPX 5–I* and *CLAPX5-II* isogenes have a closer association with the thylakoid and the stroma types, thus it can be said one isogenes belongs to either of the localities in the chloroplast.

Figure 3.5. Amino acid sequence alignment of deduced wild watermelon APX isoenzymes.

Sequence alignment was performed by the ClustalW program. The amino acids with 100% homology are shaded in black among the sequences, while the 80% homology among the sequences is show in gray color.

3.3.3 Phylogenetic analysis

Phylogenetic analysis of *CLAPXs* with *Arabidopsis*, spinach, and pumpkin APX isoenzymes demonstrated that *CLAPX1* and *CLAPX2* were in the clade of cytosolic APXs from other plants, while *CLAPX3* and *CLAPX4* were more closely associated

with microbody-type (Fig. 3.6). *CLAPX5-I* and *CLAPX5-II* were rather distant from the cytosolic and microbody isoenzymes, and strongly associated with chloroplast APXs from other plants. The grouping gave a clear indication of the localization of the *CLAPX*s, as they were grouped in different clades with APXs from other crops.

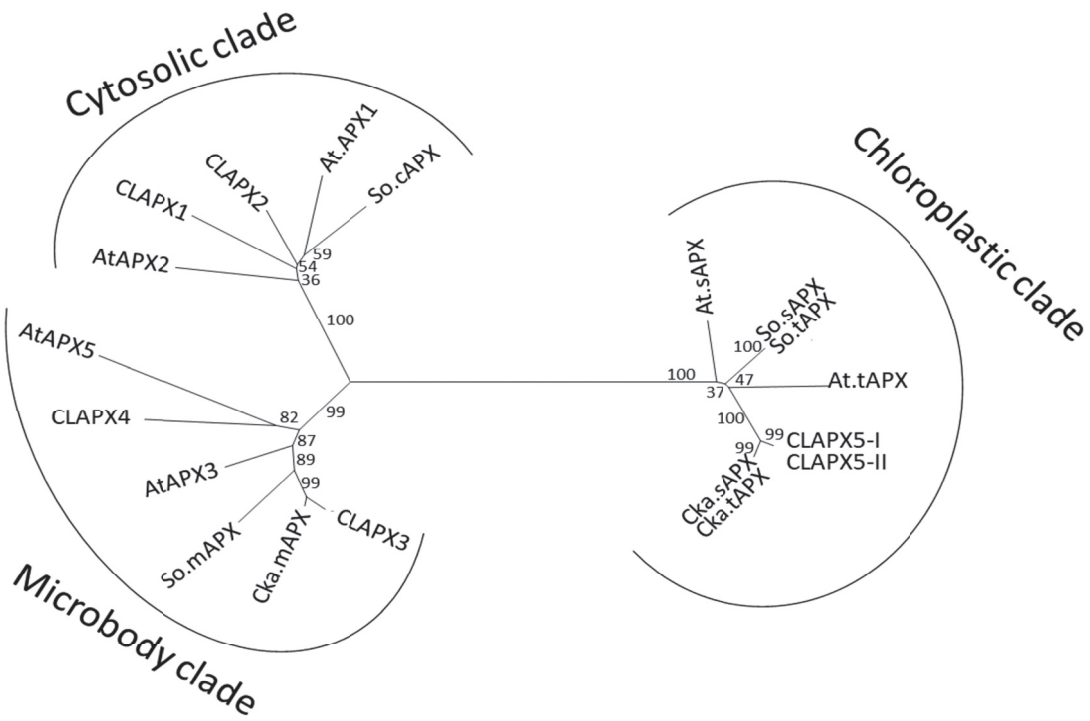

Figure 3.6. Phylogenetic analyses of *CLAPX* isoenzymes. APX protein sequences from wild watermelon, *Arabidopsis*, spinach, and pumpkin were used to construct a phylogenetic tree using a neighbor-joining algorithm in the ClustalW program. Sequence information on the *Arabidopsis* (from AtAPX1 to AtAPX5), spinach (So.sAPX and So.tAPX), and pumpkin APXs (Cka.sAPX, Cka.tAPX, and Cka.mAPX) are described elsewhere (Ishikawa and Shigeoka 2008). Three main APX types with different intracellular localizations (chloroplast, cytosol, and microbody; Ishikawa and Shigeoka 2008) are assigned to each clade.

3.3.4 Soil moisture and leaf relative water content

Soil water measurements were done in order to comfirm limitation of available water content (AWC) to the plants roots. Moisture content has been documented as one of the drought indicators (Rahman 1973; Sheffield and Wood 2007), with roots as responder that send chemical signals to the whole plant to initiate several stress response processes in the plant. The decrease in AWC is shown in Fig 3.7a. The AWC at day 0 was recorded at 154%, and gradually

decreased until 12% recorded at day 11. This result shows varying AWC at every day point, thus signifying the difference in degree of stress level at every time point.

Leaf relative water content (LRWC) was high at all time points during the stress period, showing that the internal moisture was maintained at high level regardless of the stress intensity (Fig. 3.7c). In this study, the level of internal leaf moisture were above 75% even at the 12% soil moisture level, suggesting the prescence of endurance mechanism of wild watermelon during moistures deficit stress, which avoid tissue dehydration by maintaining higher internal leaf moisture. This attribute can be associated with stomatal closure that comes in handy to reduce the moisture loss from the leaves. Mechanical disruptions that often lead to cell death can be avoided in the drought tolerant species (Flower and Ludlow 1986). The rate of RWC in drought tolerant plants has shown to be higher under drought stress as compared to sensitive plants (Pirzad et al. 2011; Hayatu et al. 2014).

3.3.5 Physiology of wild watermelon under water deficit

Measurements of the stomatal conductuctance has been used as a reliable indicator for the rate of internal gaseous exchanges, and also used to estimate the respiration rate in the leaf. The stomatal conductance measured in the wild watermelon showed correlating tendency of the stomata with the progression of drought (Fig. 3.7b), at day 0 the stomata opening was at its highest with recording of 592.7 ± 61.91 mmol m^{-2} s^{-1}, the lowest recording of 53.8 ± 1.68 mmol m^{-2} s^{-1} were observed at day 11. The first notable response of plants to drought stress is to minimize water loss that is facilitated by the stomatal aperture (Flexas and Medrano, 2002). The stomata closure is more influenced by soil moisture than the plant internal water (Niinements et al. 2009), with the root acting as a sensor that sends chemical signals through the xylem to the leaf, resulting in stomata closure (Hamanishi and Cambell 2011;Brunner et al. 2015), as experienced in our research that leaf water content did not change significantly as compared to the soil moisture (Fig. 3.7c).

A change in the chlorophyll content, an important indicator of chloroplast development, leaf nitrogen content, general plant health, and leaf senescence (Noodén et al. 1997; Xiong et al. 2015) was measured as the SPAD value (Uddling et al. 2007) randomly on the fully expanded leaves (Fig. 3.7d). The values shows that initial chlorophyll content before stress induction (day 0) was recorded at 46.43 ± 2.81 and no significant differences were observed at day 3 and 5, while a slight decrease was observed on the leaves for the later days with the lowest of 28.36 ± 1.09 recorded at the day 11. Chlorophyll content is known to provide valuable information about physiological status of plants, and can directly determine photosynthetic potential (Gitelson and Merzlyak, 2003). The chlorophyll measured based on the SPAD values showed a little decline as stress progressed and thus reducing the productivity of the crop.

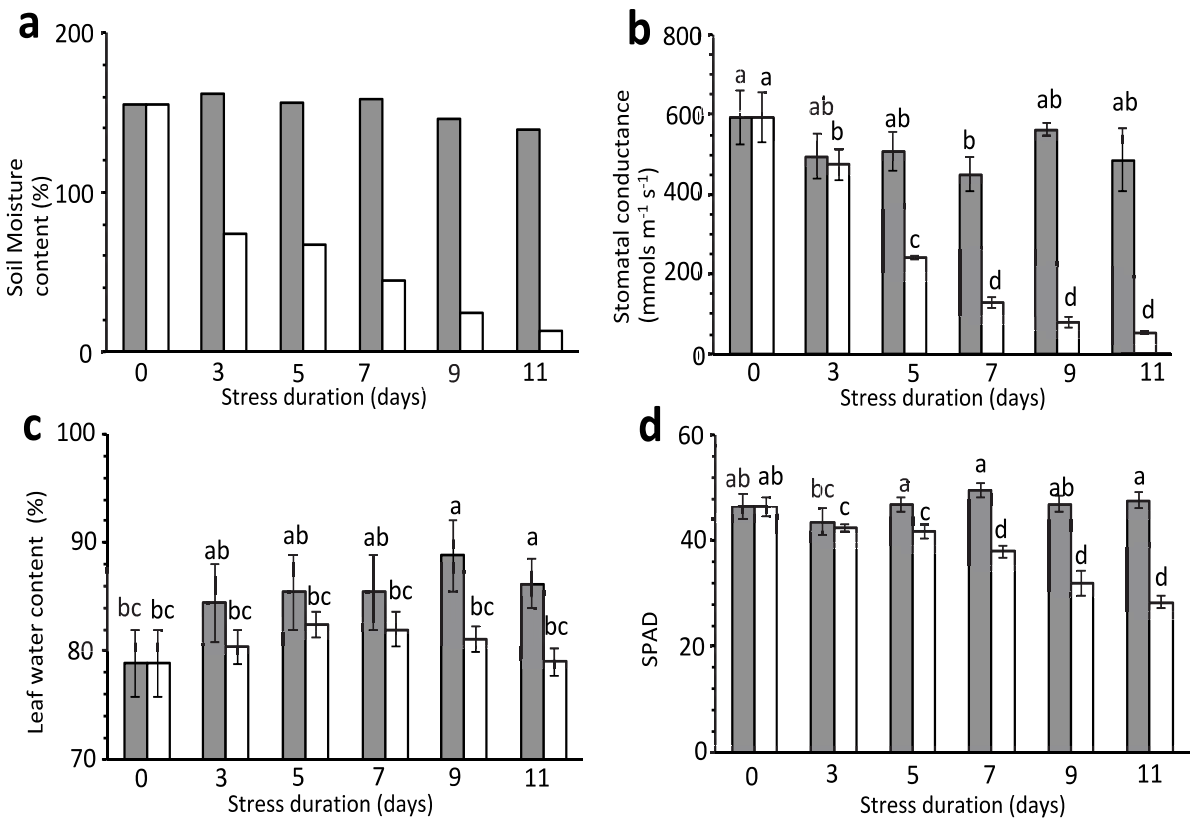

Figure 3.7. Changes in the water relation and foliar chlorophyll levels in wild watermelon under drought. Changes in the (a) soil moisture content, (b) stomatal conductance, (c) leaf water content, and (d) SPAD value during drought are presented. In (a), the values are the result of a single measurement, whereas the values in (b), (c), and (d) are given as mean ± SD (n = 3). Duncan multiple range tests were performed at 95% significance levels, and the significant differences among the values are indicated by the relevant letter(s) on top of each plot.

3.3.6 Analyses of photosynthetic parameters

Photosynthetic CO_2 assimilations were determined on the third true leaves of wild watermelon using the LI6400XT photosynthesis meter. The measurements showed that before the stress imposition (day 0) the CO_2 assimilations was recorded at 25.05 ± 2.20 µmol CO m^{-2} s^{-1} (Fig. 3.8a), then a sudden drop was observed after withholding irrigation on the plants, the measurements recorded the values to 15.88 ± 2.29 and 8.68 ± 4.23 µmol CO m^{-2} s^{-1} at day 3 and 5 after the onset of water deficits, respectively. On the final day of stress treatment (day 11), minimal assimilation rate of 0.69 ± 0.04 µmol CO m^{-2} s^{-1} was recorded. Because chlorophyll content at day 11 was still reasonable high (Fig. 3.8c) and stomatal conductance was nearly completely suppressed at this stage, the reduction of the CO_2 assimilation could be attributed to the the closure of stomata; a known drought avoidance strategy by drought tolerant crop as observed by Skirycz and Inze (2010) in order to save the internal moisture.

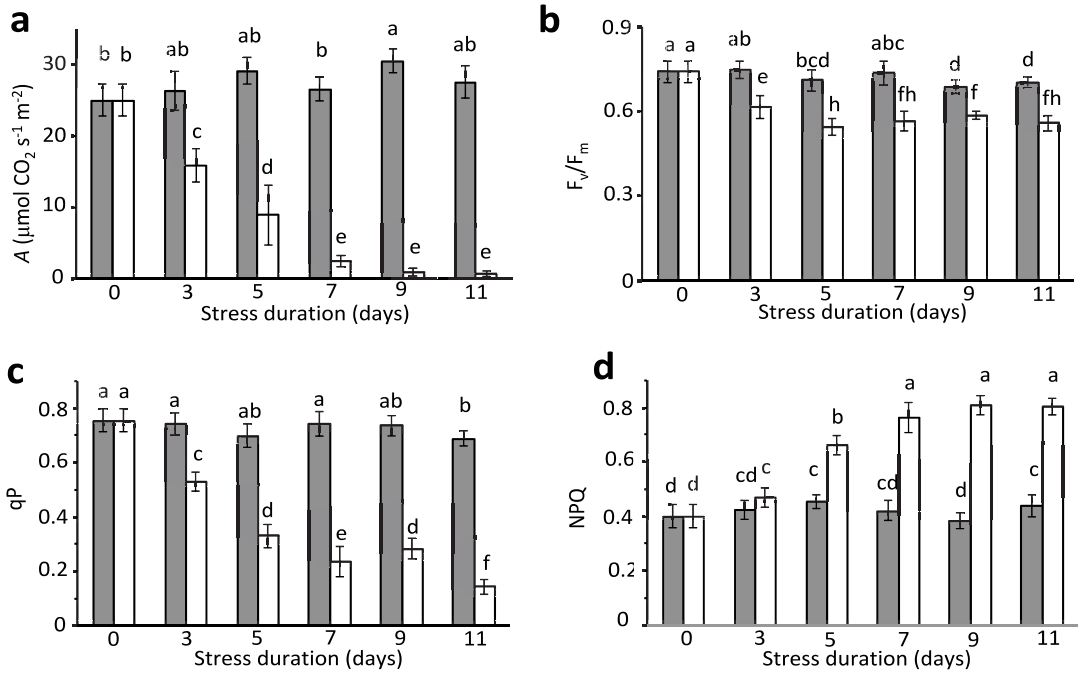

Figure 3.8. Photosynthesis and chlorophyll fluorescence parameters of the wild watermelon under drought. Changes in the (a) CO_2 assimilation, (b) F_v/F_m for maximum PSII activity, (c) qP value for photochemical quenching, and (d) NPQ value for non-photochemical quenching (d) during drought are shown. The values are given as mean ± SD (n = 3). Duncan multiple range tests were performed at 95% significance levels, and the significant differences among the values are indicated by the relevant letter(s) on top of each plot.

Chlorophyll measurements were then performed to get an understanding of the extent of damage on the photosynthetic apparatus. Dark adaptation of leaves or Fv/Fm measurements can be used as an indicator for the photosynthesis performance as it reflects the maximum efficiency of converting the absorbed light into chemical energy to be used in the photosynthesis process (Herppich and Peckmann 2000). A healthy dark adapted plant/leaf will have all its reaction centers closed thus giving a saturating pulse will give maximum value of fluorescence, therefore a saturating pulse can be used to determine the extent of damage to the reaction centers.

In this research, dark adaptation of leaves was measure early morning before the onset of light after the dark/night period. The initial values of Fv/Fm on the healthy leaves were recorded at 0.74 ± 0.039 (Fig. 3.8b), but after day 3 the values showed a small drop to 0.61 ± 0.04 and stabilized at day 5 until the end of the stress treatment. The chlorophyll content results showed that the photosynthetic mechanisms were not significantly affected by moisture deficit stress in wild watermelon (Fig. 3.7d). Therefore the slight reduction of the fluorescence values could be attributed to the minimal damage caused by the drought stress, and induction of sustained quenching as suggested by Demmig-Adams and Adams 2006.

Because Fv/Fm does not give complete information on the use of the excess excited energy, thus two other fluorescence parameters were taken into consideration to determine the effects of moisture stress on the plants. The one being non-photochemical quenching (NPQ), a process where excess energy is dissipated as heat from the reaction centers in order to sustain the centers from any damage that might be caused by excess light energy. The other being photochemical quenching (qP), which is used to estimate the proportion of open PSII reaction centers, and represents a fraction of the light energy translated to photochemical energy for use in the photosynthesis process. Monitoring of these two quenching parameters is important, as a stressed plant will not be able to fully capture and exploit all the absorbed energy.

Observation of the two quenching showed a steady decrease of the qP (Fig. 3.8c), suggesting that a larger portion of the reaction centers closed under stress

condition. The qP values under moisture stress declined significantly from the 0.75 ± 0.04 during the normal condition to 0.53 ± 0.035 at day 3, 0.33 ± 0.044 at day 5 and finally at day 11 the qP values were recorded at 0.14 ± 0.026. In constrast, the quenching of excess light energy as heat showed a more pronounced increase when the plants were exposed to moisture stress. The non-photchemical quenching (NPQ) values under control conditions were steady through the experiment at an average of 0.43 ± 0.031 (Fig. 3.8d), whereas under moisture deficit the NPQ values showed a sudden increase with 0.66 ± 0.036 recorded at day 3, 0.76 ± 0.056 recorded at day 7 and finally at the peak (day 11) of moisture stress NPQ was recorded at 0.80 ± 0.03. These observations suggested a higher ability of the wild watermelon to dissipate more heat through the process of protecting its reaction centers as described in Chapter 2. The ability of the plant to dissipate more of the excess energy plays an important role in the tolerance mechanisms, as excess energy absorbed can damage the photosynthetic apparatus. Therefore, the high ability of the wild watermelon can be consolidated as part of its drought tolerance strategy (Sanda et al. 2011).

3.3.7 APX enzyme activity in leaves under varying stress days

The quantification of the APX enzyme activity was done for the two isoforms of the APX, being the chloroplast APX (chlAPX) and the cytosolic APX (cAPX) as described in the method section. One important trait of the APX isozymes is the inactivation under the incubation with H_2O_2 under limited ascobate. The chlAPX has shown to be highly sensitive with half inactivation time was recordeded at 15s when incubated in H_2O_2 with the limited amounts of ascorbate (AsA) (Yoshimura et al. 1998), while the cAPX being less sensitive to the H_2O_2. The differential sensitivity of the APX to H_2O_2 was used to quantify the chAPX and cAPX separately, by quantifying unincubated crude extracts as total APX, and then quantifying the crude extracts after 5 min incubation in H_2O_2 for the measurement of the cAPX. Subsequently, the values of chAPX were deduced by deducting the value of cAPX from the total APX. The initial activity for the two isoforms was not significantly different, with chlAPX recording 0.67 ± 0.14 mmol

mg protein^{-1} min^{-1}, while cAPX activity was at 0.57 ± 0.08 mmol mg protein^{-1} min^{-1} (Fig. 3.9).

As the drought stress progressed, a rise in the chlAPX was observed, with values reaching its peak at 5.31 ± 0.45 mmol mg protein^{-1} min^{-1}, while those of the cAPX did not show much significant difference with total average values of 0.59 ± 0.072 mmol mg protein^{-1} min^{-1} (Fig. 3.9). The sharp increase observed in the chlAPX from day 3 could be regarded as the ROS burst stage, whereby an increase of ROS is experienced in plants when exposed to moisture deficit stress. This may lead to an increased activation of the APX enzymes (Sofo et al. 2015). The chloroplast APX enzyme activity started to decline after a sharp peak at day 5 to the value of 2.91 ± 0.21 mmol mg protein^{-1} min^{-1} at day 11. For the cAPX activity a slight increase was observed at day 5, where the value of 1.67 ± 0.23 mmol mg protein^{-1} min^{-1}. The rest of the stress days the cAPX activity was not significant different. Similarly, Nanasato et al. (2000) did not observe any significant change of cAPX in their study.

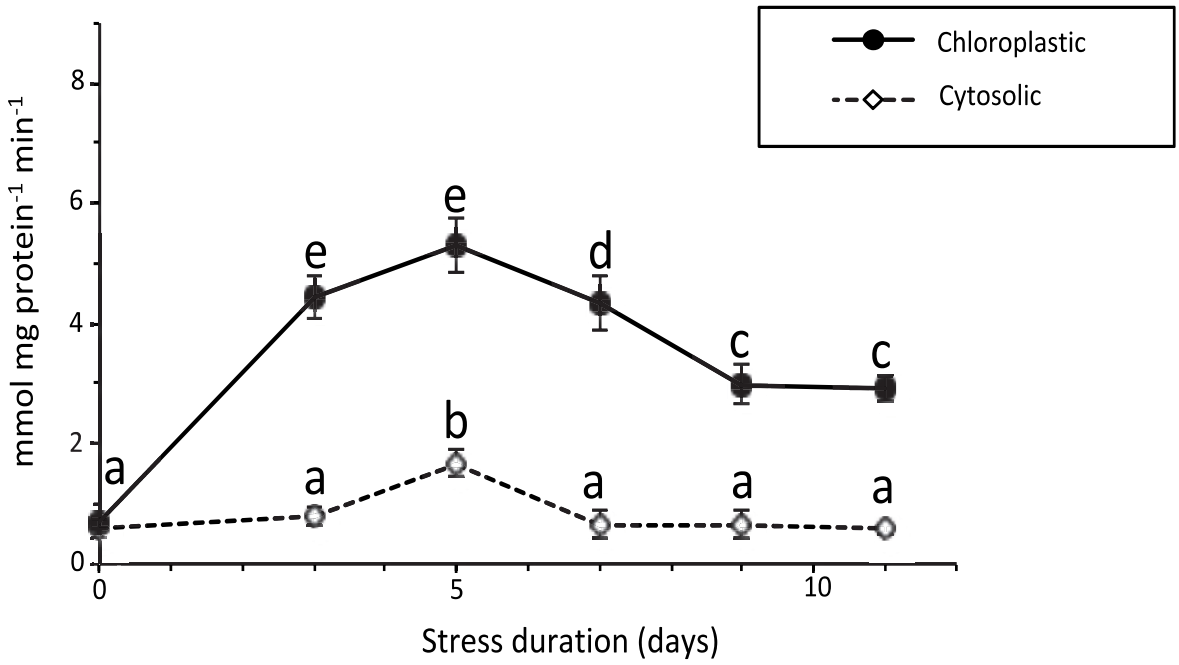

Figure 3.9. Changes in the APX enzyme activity in the leaves of wild watermelon under drought. Solid lines with closed black circles represent the values for chloroplast APX specific activity, while dotted lines with white diamond symbols represent those of cytosolic APX specific activity. The values are given as mean ± SD (n = 3). Duncan multiple range tests were performed at 95% significance levels, and the significant differences among the values are indicated by the relevant letter(s) on top of each symbol.

3.3.8 APX mRNA expressions on leaves during drought stress

Changes in the mRNA abundance for the six APX isoenzymes during drought were examined by RT-qPCR analyses. Concerning the *CLAPX5* mRNAs that had two splicing variants as described above, primers were designed to span the exon-intron junction so as to detect each variant independently. Consequently, a complex and distinct profile of mRNA abundance was observed among the different APX genes (Fig. 3.10). *CLAPX1* showed a sharp increase at day 3 and peaked at day 7 with a 3.3-fold increase in the expression.

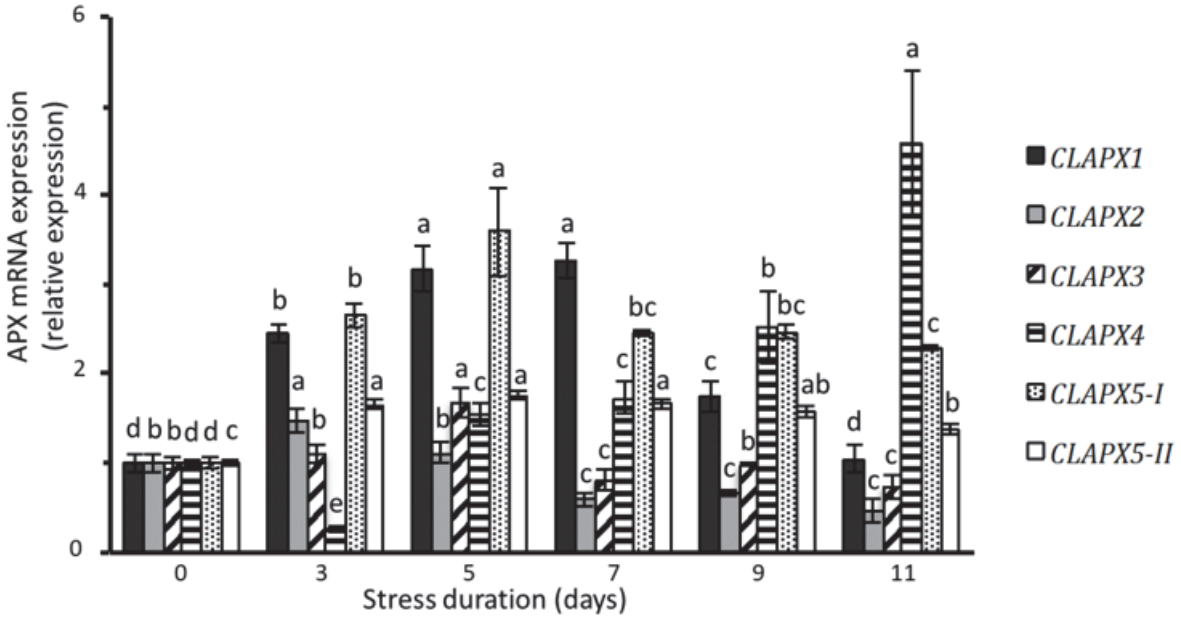

Figure 3.10. The mRNA expression profiles of *CLAPX* genes under drought. Change in the mRNA abundance for *CLAPX* genes were examined by RT-qPCR analyses. Values are normalized by an average of three reference housekeeping genes for γ-actin, α-tubulin, and GAPDH, and expressed as relative values to those of day 0. The values are given as mean ± SD (n = 3). Duncan multiple range tests were performed at 95% significance levels, and the significant differences among the values are indicated by the relevant letter(s) on top of each bar.

After day 7, the expression gradually returned to a level similar to that before stress induction. The expression of *CLAPX2* and *CLAPX3* showed a slight increase during the early days of stress (day 3 and 5), and then a reduction for the remainder of the experiment. The expression pattern of *CLAPX4* was complex

in that a suppressed expression was observed at day 3, and then gradually increased from day 5, reaching its highest value at day 11.

Gene expression of *CLAPX5-I* variant showed an increase in the early phase of the stress at day 3, peaked at day 5, then decreased towards day 11 (Fig. 3.10). The expression of *CLAPX5-II* showed a lower magnitude of increase at day 3, and stayed at the same level until day 9. It is noteworthy that the temporal induction of mRNA abundance for *CLAPX5-I*, which was most related to thylakoid APX in other plants, resembled the temporal induction of chloroplast APX enzyme activity (Fig. 3.9). This observation imply that transcriptional upregulation of *CLAPX5-I* in the early phase of drought stress may result in the fortification of chloroplast APX activity. Overall, these observations indicate the presence of distinct regulation for controlling mRNA abundance of the APX genes, which may reflect different physiological roles among APX isoenzymes in wild watermelon under drought. Future studies on the potential influence of this regulatory mechanism, to the intracellular redox status and physiological behavior in wild watermelon under drought, are anticipated.

In conclusion, the structures of the APX gene family and their cDNAs in drought-tolerant wild watermelon were characterized, together with the alternative-splicing event identified in *CLAPX5*, which potentially generated two different isoenzymes with different C-terminal amino acid sequences. Physiological and biochemical analyses of wild watermelon showed a reduction of stomatal conductance and CO_2 assimilation rate, and an increase of NPQ, which was accompanied with a significant increase in the enzyme activities of both stromal and cytosolic APXs. Temporal patterns of mRNA abundance during drought were markedly different among the APX genes, suggesting that the respective APX isoenzymes may have different physiological roles in the adaptation of this plant to drought stress.

Chapter 4

Comparative effects of ethylene inhibitors during *Agrobacterium*-mediated transformation in wild watermelon

4.1. Introduction

With the threat of climate change leading to more frequent and sporadic droughts in the future, it is important to give focus on plants that show potential in tolerating severe drought stress condition. These plants adapt to the harsh water deficit environments by exhibiting excellent physiological, morphological and/or metabolic adaptations (Bray 2001; Osakabe et al. 2014), which are exerted by unique molecular mechanisms that are essentially different from the commonly known model plants like Arabidopsis, which are not by nature, tolerant to the severe drought stress.

Wild watermelon (*Citrullus lanatus* acc.10117-7), an inhabitant of the Kalahari Desert, can strive and produce fruits in one of the harshest environment characterized by minimal rainfall, high temperatures and strong sunlight (Miyake and Yokota 2000). Unique responses to the drought stress have been reported in this plant, such as the biosynthesis of compatible solute citrulline (Akashi et al. 2001), stimulation of root growth (Yoshimura et al. 2008), and dynamic proteome changes (Akashi et al. 2011). These observations make this plant to be an attractive source of useful genetic traits for *Agrobacterium*-mediated molecular breeding (Akashi et al. 2005). Examining the gene function in wild watermelon will be valuable not only for elucidating the molecular mechanisms underlying the excellent drought resistance, but also mining gene resource for conferring the stress resistance to other crop species.

Agrobacterium transformation has become an important molecular breeding tool because of its unique ability to efficiently transfer and integrate genes into genome of a host plant (Newell 2000; de la Reva et al. 1998). Its capability to transfer a particular segment of the T-DNA of the tumor-inducing (Ti) plasmid in the cell nucleus and be able to stably integrate in the host genome has then been extensively explored and manipulated. The *Agrobacterium* Ti-plasmid has been manipulated to replace the tumor-causing T-DNA with other transgenes being inserted in the T-DNA regions. Because of the complexity of manipulating and introducing transgenes in the Ti-plasmid, alternative strategies have been developed to utilize the *Agrobacterium* by developing T-DNA binary vectors or plasmids which are easy to use even for beginners (Kakkar and Verma 2011). Several successful transgenic plants with traits of importance have been developed through this technique.

The optimization of the *Agrobacterium*-mediated transformation is an important aspect to consider in order to improve its efficiency. Like any other

technique, its efficiency of the technique is influenced by external factors like medium used (Chen et al. 2004), concentration of antibiotics (Raffeiner et al. 2009) optical density of transformation medium and infection time of explants (Sivanandhan et al. 2016), duration and temperature during co-cultivation (Jin et al. 2005), and researchers' skills. It is also influence by internal factors like toxic compounds that inhibit bacterial growth during co-cultivation (Carvallo et al. 2004). *Agrobacterium* transformation has potential to trigger expression of some genes which are components of defense machinery in the host cell (Veena et al. 2003), programmed cell death activated by reactive oxygen intermediates produced during oxidative burst (Parrot et al. 2002), the plant metabolites and phytohormones (Nonaka and Ezura 2014) that inhibit *Agrobacterium* mediated transformation.

Ethylene is a phytohormone and plays an important role in defense mechanism in response to both abiotic and biotic stresses. In stressed plants the initial peak of ethylene initiates the protective response, whereas the successive peaks initiates processes that tends to harm or obstruct plant growth (Glick 2005). This attribute plays a major limiting role during the *Agrobacterium*-mediated gene transfer, as inoculation of explants with *Agrobacterium* has been shown to induce excess release of ethylene, which subsequently lead to either delaying growth and development of inoculated plants (Glick et al. 1998) or growth retardation and senescence (Kim et al. 2014). Therefore ethylene has been classified as potential plant regeneration inhibitor by Kong and Yeung 2014.

Therefore the ethylene released from the explants wound is justifiable one important factor that reduces the efficiency of *Agrobacterium*-mediated gene transfer in plants. In ethylene biosynthetic pathway, methionine is converted to *S*-adenosylmethionine (SAM) by SAM synthetase, then metabolized to 1-aminocylopropane-1carboxylic acid (ACC) by ACC synthase (ACS), a committing enzyme for ethylene biosynthesis. ACC is then converted to ethylene catalyzed by ACC oxidase (ACO) (Adams and Yang 1979; Poel and Straeten 2014). Chemical inhibitors such as $AgNO_3$, a suppressor to ethylene perception (Beyer 1976), and aminoethoxyvinlyglycine (AVG), a specific inhibitor for ACS, have been widely used to alleviate the negative effects of ethylene and improve transformation process in Brassicas plants (deBlock et al. 1989; Wahlroos et al. 2003; Takasaki *et al.* 2004), bottle gourd (Han et al. 2005), *Hevea brasiliensis* (Kala et al. 2012), mustard (Pua and Chi 1993), safflower (Belide et al. 2011), and ryegrass (Qiao et al. 2011).

In contrary, studies showing less positive benefit of chemical inhibitors have been reported in maize (Ishida et al. 2003), orange, grapefruit and citron (Marutani-hert et al. 2012). Studies further showed that a phosphate-dependent enzyme ACC deaminase is known to catalyze the decomposition ACC, thus reducing the formation of ethylene (Minami et al. 1998: McDonnell et al. 2009).

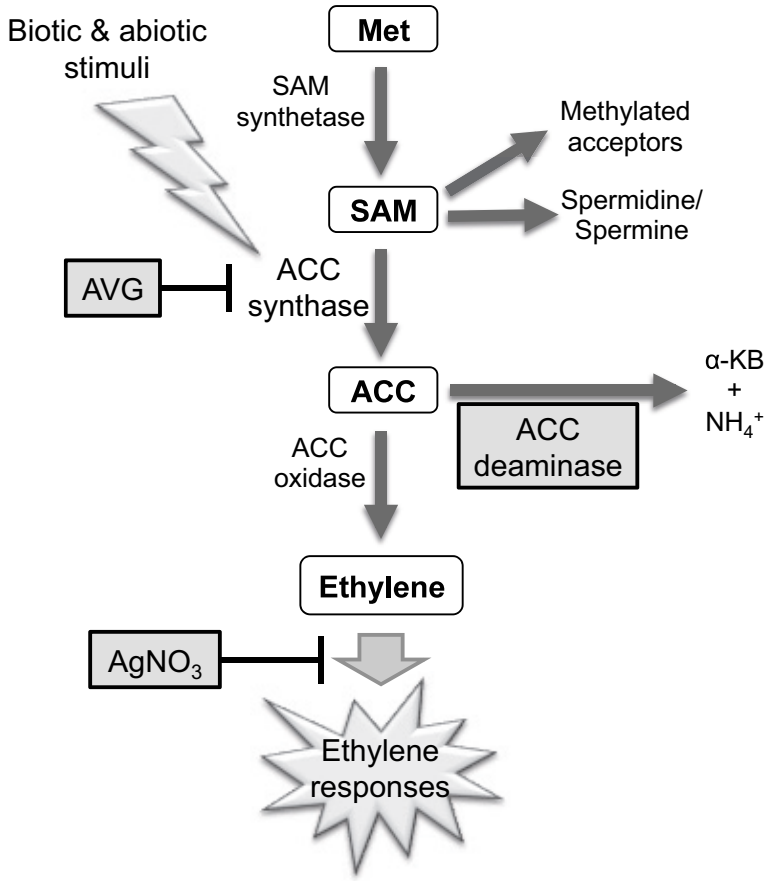

Figure 4.1. Schematic diagram of ethylene biosynthesis with the enzymes that synthesize or oxidase 1-aminocylopropane-1-carboxylic acid (ACC) to produce ethylene. The chemical and biological effectors showing different points of inhibition or decomposition of the ethylene synthesis intermediate are highlighted by gray squares. Met, L-methionine; SAM, *S*-adenosyl-L-methionine, AVG, aminoethoxyvinylglycine; $AgNO_3$, silver nitrate; α-KB, α-ketobutyrate.

The Plant-borne ACC is then converted into ammonia and α-ketobutyrate by the enzyme ACC deaminase (Honma and Shimomura 1978). The success of ACC deaminase in modulating the synthesis of ethylene (Glick 2005; McDonnell et al. 2009; Poel and Straeten 2014), aiding transformation (Nonaka et al. 2008; Nonaka et

al. 2014; Kim et al. 2014) and promoting plant growth (Zahir et al. 2007; Singh et al. 2015) have been widely reported in various crops species.

Reduction or management of evolved ethylene during infection and co-cultivation of transformation material is very crucial in improving the efficiency of gene transfer. It is important to evaluate various methods of reducing the ethylene evolution in several crops to select and document the superior ones.

Therefore in this chapter, I report the efficiency of different ethylene inhibitors during *Agrobacterium*-mediated gene transfer in wild watermelon.

4.2 Materials and methods

4.2.1 Chemicals

All reagents used in here were purchased from Wako chemicals, Osaka, Japan, or otherwise described elsewhere.

4.2.2 Bacterial strain and plasmid culture conditions

An *Agrobacterium* strain EHA105, which was generated from EHA101 through site-directed deletion of the kanamycin resistance gene from the Ti plasmid (Hood et al. 1992), was used in this study. The *Agrobacterium* EHA105 was transformed with a binary vector pIG121-Hm, which contains *uid*A (GUS) gene with an intron sequence from plant (Akama et al. 1992).

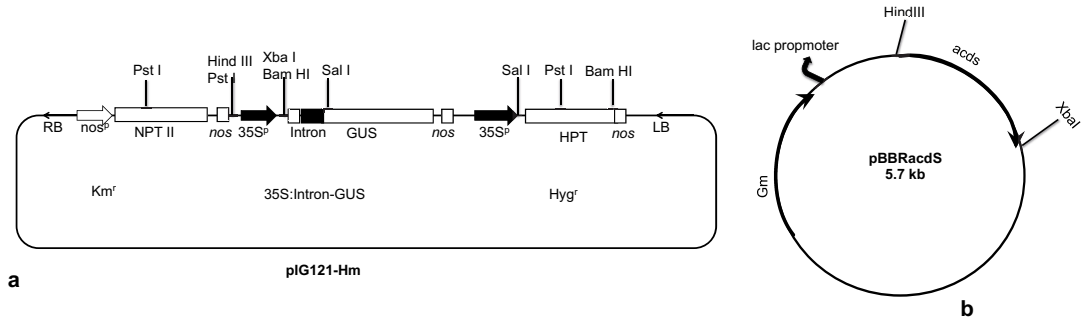

Figure 4.2. The schematic diagrams of the two vectors used in this experiment (a) pIG121-Hm with the Gus intron, and (b) pBBRacds with the acds gene intron. The pBBR-MCS-5 was reconstructed by digesting out the acds genes with XbaI and HindIII restriction enzymes.

The pBBRacds plasmid that carries the ACC deaminase gene was described previously (Nonaka et al. 2008). The pBBRcont plasmid was constructed by digesting out the ACC deaminase gene from the pBBRacds using the *Xba*I and *Hin*dIII restriction enzymes, followed by blunting of the resultant nucleotide overhangs by Klenow fragment of *E. coli* DNA polymerase I (New England Biolabs, Ipswich, MA, USA) in the presence of 2.5 mM dNTPs, then self-ligated by a TOYOBO Ligation high kit (Toyobo, Osaka, Japan).

The pBBRacds or pBBRcont plasmids together with the pIG-121-Hm (Fig. 4.2) were dual introduced in the *Agrobacterium* strain EHA105 by electroporation (Biorad micropulser, Biorad, Hercules, CA, USA) according to the manufacturer's instruction. The transformed cells were selected and cultured in LB medium

supplemented with 50 mg l^{-1} rifampicin and 50 mg l^{-1} hygromycin for *Agrobacteria* containing pIG121-Hm, and 50 mg l^{-1} rifampicin, 50 mg l^{-1} hygromycin, and 50 mg l^{-1} gentamicin for *Agrobacteria* containing both pIG121-Hm and pBBR vector derivatives. *Agrobacterium* suspension cultures at a density of OD600 = 0.5~0.7 were used for the transformation experiments.

4.2.3 Plants materials and genetic transformation

Seeds of wild watermelon, *Citrullus lanatus* acc. No. 101117-1 were prepared as described previously (Akashi et al. 2005) with following minor modifications. A scalpel and forceps were carefully used to de-coat and peel the seeds with minimum damage to the cotyledons. The de-coated seeds were then sterilized in a solution containing 5% sodium hypochlorite and 0.005% Tween20 for 10 min, and then rinsed five times with sterile water. The sterilized seeds were then soaked in sterile water and kept in the dark overnight at 30°C. The next day the seeds were grown on basal medium (BM) containing Murashige and skoog (1962) salts, 10 mg l^{-1} thiamine, 100 mg l^{-1} myo-inositol, 30 g l^{-1} sucrose and 0.8% agar in the dark at 30°C for 4 days.

The expanded cotyledons were sectioned into 5 mm square explants using a sterile blade. Infection was done immediately by soaking the explants in the *Agrobacterium* suspension solution (containing GUS vector or GUS+pBBR vector) for 10 min, and then blotted on sterile filter papers to remove excess liquid. The inoculated explants were then co-cultivated for 7 days on BM agar medium supplemented with 4 mg l^{-1} 6-benzyladenine and 10 mg l^{-1} acetosyringone, and grown at 28°C under a 16 h photoperiod. In the ethylene inhibition experiment, BM medium was supplemented with either commonly used chemical inhibitors i.e. 1 μM aminoethoxyvinlylglycine (AVG) or 40 μM silver nitrate. For shoot formation, the explants after co-cultivating for 7 days were rinsed 5 times with sterile water, 3 times with 100 mg l^{-1} meropenem trihydrate and then cultured for 2 weeks on shoot inducing media containing BM supplemented with 10 g l^{-1} polyvinlypyrrolidone (PVP) (Nacalai tesque, Kyoto, Japan), 1 mg l^{-1} 4-3-indolyl butyric acid, 10 mg l^{-1} acetosyringone, 100 mg l^{-1} thidiazuron (TDZ) (Nacalai tesque, Kyoto, Japan), 100 mg l^{-1} meropenem trihydrate and 50 mg l^{-1} hygromycin. The explants were then maintained at 28°C under a 16 h photoperiod. All the experiments were repeated 3 times and for every repetition the treatments were replicated 3 times.

4.2.4 Ethylene gas quantification

To quantify ethylene gas evolved from agro-infected watermelon explant tissues, the *Agrobacterium*-inoculated explants with different ethylene effectors were cultivated in the BM medium in a 15 ml glass vial (Fig. 4.3) with a rubber cap sealed with Para-film (Bemis laboratories, Clara, Ireland), which allows needles through, and remains intact to eliminate chances of gas leakage. The explants were co-cultivated with *Agrobacteria* for 7 days with 16 h light per day. To measure the evolved ethylene, a 1 ml gas syringe was used to withdraw gas from the vial at 3, 5 and 7 days after inoculation (DAI), and directly injected onto the gas chromatography.

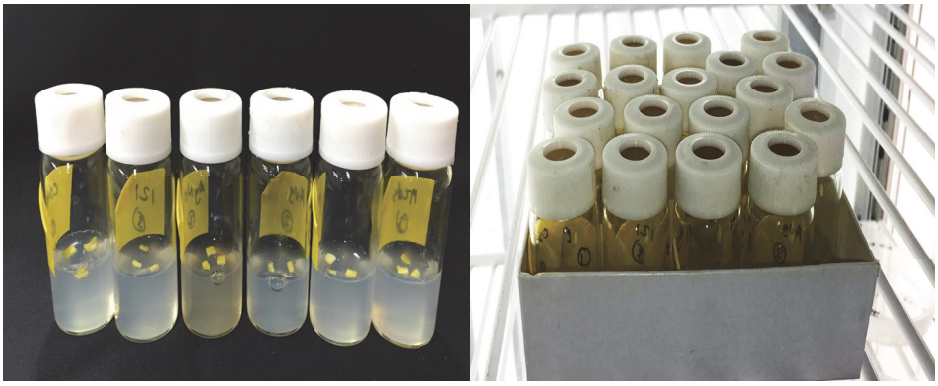

Figure 4.3. Co-cultivation of the transfected wild watermelon explants, incubated in BM medium with AVG, $AgNO_3$ to inhibit ethylene production. The explants were co-cultivated in air-tight vials to minimize the escape of the ethylene gas to near zero so as to be used for the quantification of the accumulated gas in the headspace.

Quantification of ethylene was performed by gas chromatography essentially as described previously (Bassi and Spencer 1985), with following modification; A column chamber of gas chromatography GC 4000 (GL Science, Tokyo, Japan) coupled with flame-ionization detector (FID) equipped with a DB-5 column (30 m x 0.32 mm, 0.25 µm, Agilent Technologies, Santa Clara, MA, USA) was used to quantify the ethylene gas. The oven temperature was set at 60°C and the flow rate of the helium carrier gas was set at 30 cm^3 min^{-1}. Under these conditions, the retention time for ethylene was estimated at 1.9 min. Quantification of ethylene was performed with a standard curve generated from serial dilution of the commercial ethylene gas standard (GL Science, Tokyo, Japan).

4.2.5 Histochemical β-glucuronidase (GUS) assay

Histochemical GUS assay was performed as described previously (Jefferson et al. 1987) with following minor modifications; post agro-infiltration explants selected at different days after incubation were selected and incubated overnight at 37°C in a GUS assay solution containing 100 mM sodium phosphate buffer (pH 7.0), 10 mM EDTA, 0.1% Triton, 0.5 mM potassium ferrocyanide, 0.5 mM potassium ferricyanide and 0.5 mg ml^{-1} 5-bromo-4-chloro-3-indoyl glucuronide (X-gluc). After incubation in the GUS assay solution the explants were then soaked in absolute ethanol overnight to remove chlorophyll coloring and other intrinsic pigments. After discoloration the stained explants were viewed under the microscope and pictures were taken for quantification of the stained areas. Quantification of the GUS-stained area on the leaf disks was performed using ImageJ (Schneider 2012).

4.2.6 Spectrophotometric assay of GUS activity

Spectrophotometric assay for GUS enzymatic activity was performed essentially as described previously in Falciatore et al. (2002). Approximately 1 g of the agro-infiltrated explants post incubation period was homogenized in extraction buffer (50 mM $NaPO_4$ (pH 7.0), 10 mM β-mercaptoethanol, 10 mM EDTA) with a pinch of sea sand in a pre-chilled pestle and mortar on ice. The homogenate was centrifuged at 20,000 x g for 15 min at 4°C, then the supernatant was collected into a new 1.5 ml tube. A small sample of the extract (100 μl) was assayed in 900 μl assay buffer (extraction buffer with 1 mM of *p*-nitrophenyl β-D-glucopyranoside) and incubated at 37°C for 2 h. The assay was terminated by adding 400 μl of 2.5 M 2-amino-2-methylpropandiol. The absorbance was then measured at 415 nm against a substrate blank. Enzyme blanks were also assayed and measured and the values subtracted from assayed samples to eliminate the chlorophyll color effect.

4.2.7 Molecular analysis

Genomic DNA was extracted from the shoots using DNA PLANT MINI KIT (Qiagen, Valencia, CA, USA) following manufacture's protocol. The DNA was first amplified with a pair of actin reference primer (Act-F: 5'CATTCTCCGTTTGGACCTTGCT-3' and Act-R: 5'TCGTAGTTTTCTCAATGGAGGAACTG-3') to check the intactness of the DNA.

The GUS gene was amplified with a pair of primers (GUS-F: 5'-CAACGAACTGAACTGGCAGA-3', and GUS-R: 5'GGCACAGCACATCAAAGAGA-3') which were designed to amplify 989 bp fragment on the GUS gene, while the *npt*II gene was amplified with a pair of primers (Km-F: 5'-GGCTATTCGGCTATGACTGG-3', and Km-R: 5'-AGCCAACGCTATGTCCTGAT-3') which were designed to amplify 620 bp fragment of the nptII gene. The region outside the T-DNA border was amplified with a pair of primers (Bor-F: 5' –CCTGGCAAAGCTCGTAGAAC-3', and Bor-R: 5' –GTATTCGTGCAGGGCAAGAT-3') that were designed to amplify 826 bp fragment in the region outside the T-DNA borders, all amplicons were on the pIG121-Hm reporter plasmid. The PCR conditions were as follows: pre-denature at 95°C for 3 min, 35 cycles of denature at 95°C for 30 s, annealing at 52-55°C (depending on the primer melting temperature (Tm)) for 30 s and extension at 72°C for 1 min, and final extension at 72°C for 5 min. The PCR products for the same sample were then mixed and run on 0.8% agarose gel at the same time and stained with GelGreen Nucleic Acid Gel stain (Hayward, CA, USA) and viewed under UV light using LuminoGraph I gel viewer (ATTO, Tokyo, Japan).

4.3 Results and Discussion

4.3.1 Quantification of ethylene evolved from explants

Watermelon explants were inoculated with *Agrobacterium* EHA105 containing a binary vector pIG121-Hm, and effect of different ethylene effectors on the ethylene evolution from the inoculated explants was compared. At 3 days after inoculation (DAI), ethylene concentration in the culture vial containing *Agrobacterium*-inoculated explants with no effector was significantly higher than the un-inoculated control explants (Fig. 4.4). Supplementation of silver nitrate or AVG, or co-transformation of ACC deaminase gene-containing pBBRacds effectively reduced the ethylene accumulation to the un-inoculated control level. Co-transformation of pBBRcont, a vector control in which ACC deaminase gene was digested out of the pBBRacds, resulted in the similar level of ethylene accumulation as no ethylene effector control, suggesting that the ethylene suppression effect in pBBRacds can be attributed to the presence of ACC deaminase gene.

The accumulation of ethylene gas in the headspace of the gas vials was not significantly different for samples treated with AVG, $AgNO_3$ and pBBRacds at 3 days after inoculation, while significant differences were observed at 5 DAI, with pBBRacds recording the lowest volume of ethylene accumulated in the headspace, explants cultivated in medium treated with AVG had the second lowest accumulated gas but showed no significant difference as compared to the un-inoculated samples, while $AgNO_3$ treated samples showed no significant differences as compare to the no effector samples and pBBRcont samples. At 7 DAI, ethylene evolved from the explants showed varying gradual increase for each treatment. The no effector samples recorded the highest average of accumulated gas which was not significantly different when compared to $AgNO_3$, AVG and pBBRcont samples, but was relatively different when compared to the un-inoculated and pBBRacds samples. The pBBRacds samples recorded lowest averages of gas even though it was significantly not different when compared to $AgNO_3$ and AVG treated samples. Thus it could be said that pBBRacds plasmid has a higher potential in regulating the ethylene synthesis in wild watermelon explants under *Agrobacterium*-mediated gene transfer as compared to the chemical inhibitors during the early stages of co-cultivation. Other studies (Ezura et al. 2000) has shown that the use of AVG was effective in inhibiting ethylene evolution in contrary to the effect of the ACC application that promoted ethylene evolution. Thus

in this study it can be said that the plasmid harboring the ACC deaminase gene is more effective in inhibiting ethylene evolution.

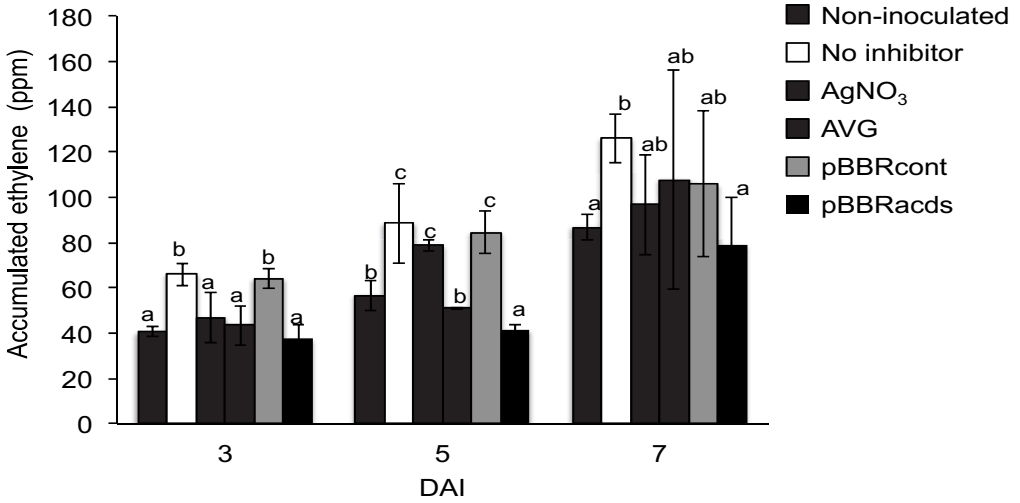

Figure 4.4. Effects of different ethylene inhibitors on the ethylene evolution from cotyledon explants inoculated with an *Agrobacterium* strain EHA105 harboring a binary vector pIG121-Hm. Accumulation of ethylene gas in the headspace of culture vials after varying days after inoculation (DAI) was measured using a gas chromatography. Non-inoculated, explants were not inoculated with *Agrobacterium*; No inhibitor, no ethylene inhibitors was used for transformation, $AgNO_3$, silver nitrate was included in the media; AVG, aminoethoxyvinlyglycine was included in the media; pBBRcont, pBBR control vector was co-integrated in the *Agrobacterium*; pBBRacds, pBBRacds vector that contained ACC deaminase gene was co-integrated in the *Agrobacterium*. Data are the averages and SD of three vials for each treatment, in which three explants were incubated in each vial. Letters on top of the bars indicate statistical significance at the 95% confidence level based on Duncan's mean comparison.

4.3.2 Histochemical assay of the GUS gene in explants

To evaluate more on the different ethylene effectors on the *Agrobacterium*-mediated gene transfer into watermelon explants, the *uidA* reporter gene was used in histochemical GUS assay (Fig 4.5). The GUS-expressing leaf area was viewed under the microscope and a photo captured to be used for analysis. Subsequently an image analyzer tool ImageJ was used to quantify the stained area and expressed as the percentage area over the total area of the explants (Fig. 4.6). The explants incubated with no effector showed the lowest percentages of stained areas as compared to those supplemented with ethylene effectors AVG and $AgNO_3$ chemical inhibitors. The effect of AVG in the present study in wild watermelon was consistent with previous

observations in melon (Ezura et al. 2000), where ACC synthase inhibitor AVG significantly enhanced transgene expression in *Agrobacterium*-mediated transformants.

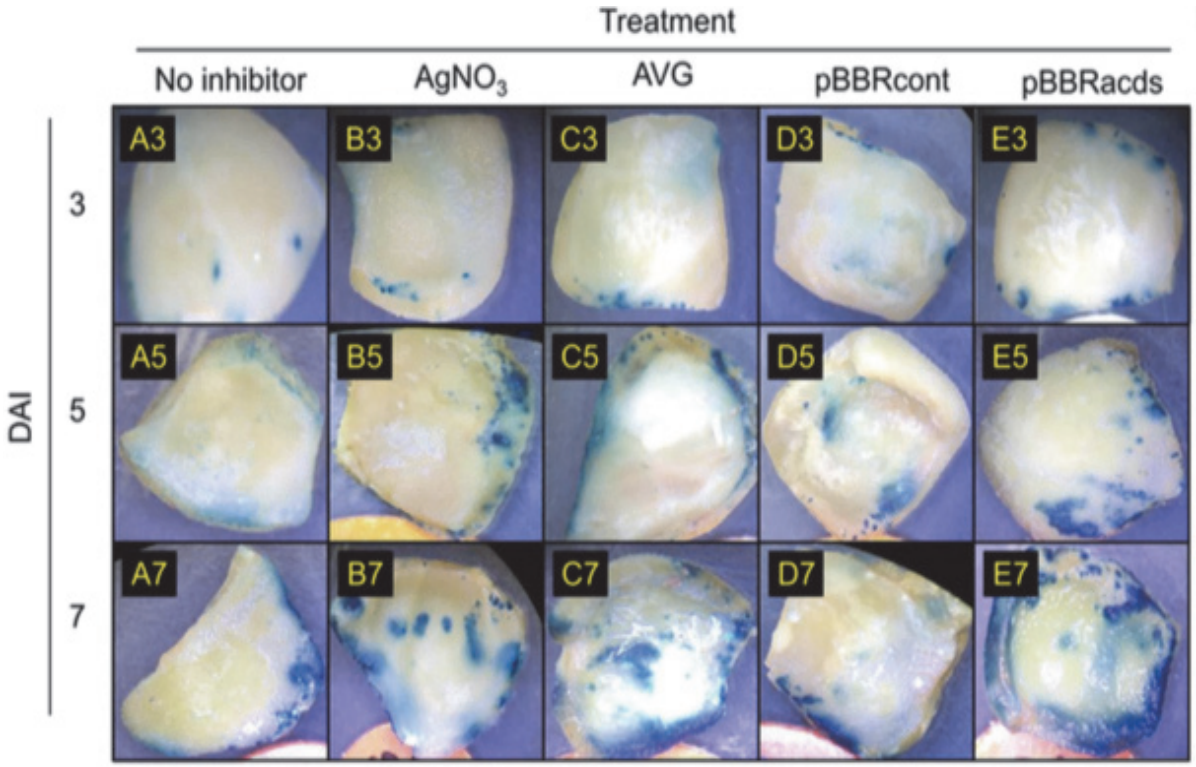

Figure 4.5. Histochemical GUS staining of watermelon cotyledon explants inoculated with an *Agrobacterium* strain EHA105 harboring pIG121-Hm binary vector. The horizontal axis represents different ethylene inhibitors as in the legend of Figure 2. Representative images of explants after varying DAI were shown.

Notably, explants co-transformed with pBBRacds achieved highest transformation efficiency, as the stained area occupied 45.48 ± 3.96% of the total surface area of the explant at 7 DAI (Figs. 4.5, 4.6). The higher percent of stained area gave an indication that there was higher gene transfer efficiency on the explants. This suggests that inhibiting ethylene evolution by the use of the pBBRacds greatly improved the *Agrobacterium*-mediated transformation. These observations also suggested that the chemical ethylene inhibitors enhanced the rate of gene transfer, but not as much as compared to the ACC deaminase gene-harbouring plasmid.

On the use of $AgNO_3$ to perturb the binding site of ethylene (a major obstacle to *Agrobacterium*-mediated gene transfer), Kumar et al. 2009 highlighted that addition of $AgNO_3$ in the co-culture medium had led to stimulation and regeneration of shoots from cotyledonary explants, this further testifies the effectiveness of

chemical regulators in overcoming the ethylene factors to aid plant transformation. Therefore the chemical inhibitors do play an important role in *Agrobacterium* mediated gene transfer. One challenge to the chemical inhibitors is that their long term effects on crop growth has not being widely evaluated, with some reports showing that increased use of $AgNO_3$ and AVG have been found out to reduce fruit size and weight in *Cucumis sp* (Custers and Nijs 1985) and highly reduce the reduce seed yield (Nejatzadeh-Barandozi et al. 2014) when used during the hybridization experiments in some crops.

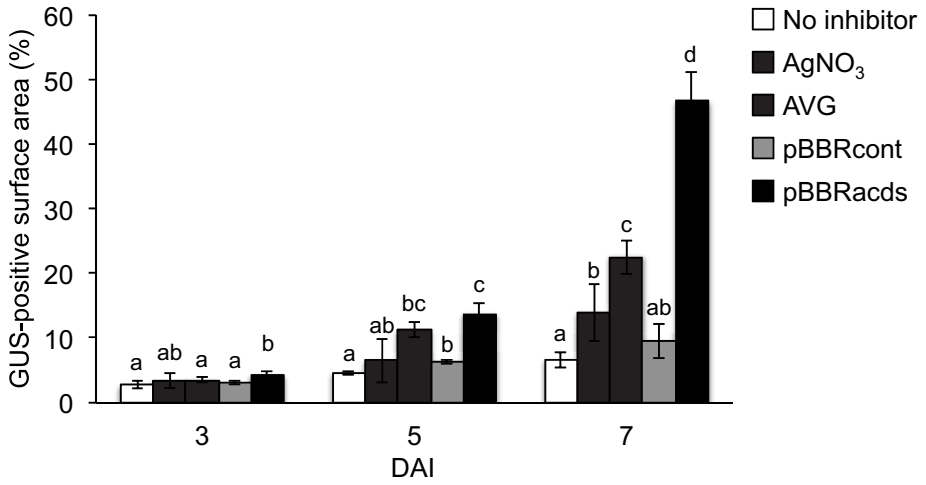

Figure 4.6. Quantification of leaf surface areas that showed GUS transgene expression on the cotyledonary explants of wild watermelon in the presence of different ethylene inhibitors. Values at varying DAI are shown. The ImageJ software was used to quantify the areas of blue stains on the explants. Nomenclature of the different ethylene inhibitors is the same as in Figure 2. Data are the average ± SD of 30 explants. Letters on top of the bars indicate statistical significance at the 95% confidence level based on Duncan's mean comparison.

The gene expression on explants inoculated with pBBRcont was almost equivalent to that of the no-effector treatment. This indicates that control plasmid used as a backbone for making pBBRacds, has little or no effect in inhibiting ethylene thus does not enhance gene transfer. Similar results showing the effectiveness of pBBRacds in increasing the efficiency of gene transfer when compared with the chemical inhiboitors like AVG has been noted previously. Nonaka et al. 2008 observed that inoculation with *A. tumefaciens* C58C1Rif^R (pBBRacds, pIG 121 Hm) yielded about six times higher than levels of gus activity than that inoculated with C58C1Rif^R (pIG 121 Hm).

The results on the change of the accumulated ethylene gas during co-cultivation (Fig. 4.2) and the efficiency of gene transfer judging from the GUS-positive surface area (Fig. 4.4) could suggest important stage in the co-cultivation period. The optimum co-cultivation has been suggested to be between 48-72 h (Pandey et al. 2013), thus it is important to minimize the evolved ethylene from the explants during this period to improve the efficiency of gene transfer from *Agrobacterium* to the explants cells. The lower ethylene concentration between 3-5 DAI in explants transformed with pBBRacds could have significantly contributed to the increase in gene transfer event. Knowing the critical point of gene transfer during co-cultivation will then come in handy when incorporating other factors that aid the efficiency of transformation.

4.3.3 Quantification of the enzymatic activity

To further quantify the effects of various ethylene effectors on the gene transfer efficiency, the spectrophotometric assay of the GUS enzymatic activity was performed to quantify the GUS enzyme activity on the explants as another method to quantify the gene transfer. The enzymatic activity was performed after the explants were co-cultivated with the treatments for a period of 7 days. The result shows that activity was highest in explants co-inoculated pBBRacds (8.68 nmole min^{-1} gFW^{-1}) (Fig. 4.7), which was almost 3-fold higher in explants than the no effector treatment (2.72 nmole min^{-1} gFW^{-1}). The activity was also significantly higher when compared to the explants co-cultivated in medium supplemented with chemical inhibitors $AgNO_3$ (4.54 nmole min^{-1} gFW^{-1}) and AVG (5.31 nmole min^{-1} gFW^{-1}). The results were consistent with GUS histochemical assay, demonstrating that pBBRacds was superior in improving the efficiency of *Agrobacterium*-mediated gene transfer.

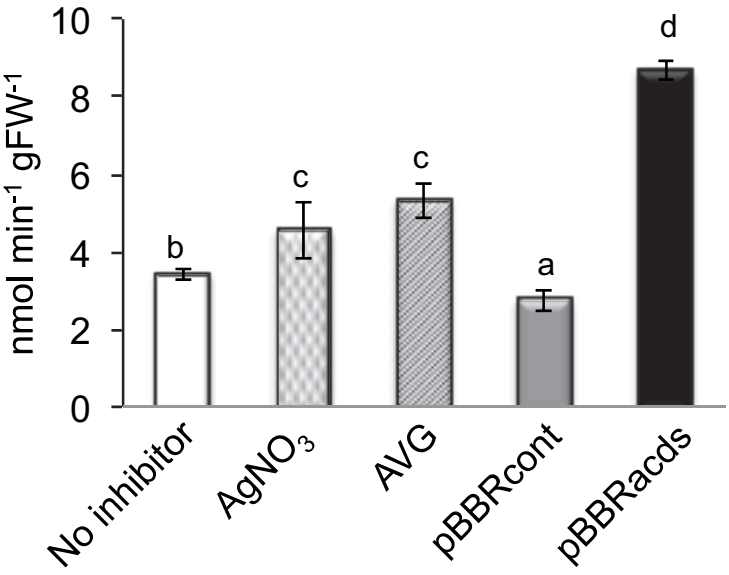

Figure 4.7. Spectrophotometric GUS enzyme assay using the total protein extracts from watermelon explants inoculated with *Agrobacterium* containing pIG121-Hm that were treated with different ethylene inhibitors. A total of 10 explants per treatment were harvested at 7 DAI, then protein extracts were independently prepared from individual explants and used for the enzyme assay. Nomenclature of the different ethylene inhibitors is the same as Figure 2. The 4-nitrophenyl β-D-glucuronide was used as a substrate. Enzyme activities were expressed as nmol of nitrophenyl produced per min per gram fresh weight of the explants. Data are average ± SD of ten explants. Letters on top of the bars indicate statistical significance at the 95% confidence level based on Duncan's mean comparison.

4.3.4 Shoot regeneration and quantification

The explants were further grown in the shoot inducing-media, and the number of explants that generated shoots were counted and compared among the treatments (Table 4.1). Consequently, the percentage of explants with shoots was not significantly different at 95% level among the treatment. However, the number of shoots per explant had a significant difference, with no effector and pBBRcont treatments recording the lower number of shoots, whereas AVG and pBBRacds recorded the higher number of shoots per explant. The GUS histochemical staining showed that the percentage of transformed explants was higher than 60% in the ethylene inhibition treatments ($AgNO_3$, AVG and pBBRacds), suggesting that less than 40% of the generated explants were escapes, in the control treatments the number of excapes shoots was higher with number of GUS positive shoots recorded at 15% for no inhibitor and at 26.67% for the pBBrcont treatment. A lower number of escapes were also noted when bottle gourds explants were co-cultivated in medium

supplemented with ethylene inhibitor (Han et al. 2005), in the same breath higher number of transformed explants in *Citrullus* species has been reported in Ntui et al. 2010 with the aid of ACC deaminase during *Agrobacterium* infection. The current results showed that the ethylene inhibitors have a positive effect on both the gene transfer on the explants that is carried over to the generated transgenic shoots.

Table 4.1. Effects of different ethylene inhibitors on transgenic shoot formation in wild watermelon.

Treatment	Explants with shoots (%)	No. of shoots per explant	GUS+ shoots per explant[1]	Transformation efficiency (%)[2]
No inhibitor	37.37a	0.7a	0.1a	15a
$AgNO_3$	37.61a	1.3ab	0.9b	69.23b
AVG	48.57a	2.6b	1.9c	74.51b
pBBRcont	40.74a	0.5a	0.1a	26.67a
pBBRacds	37.52a	2.9b	2.1c	74.12c

Data are the mean of 90 samples per treatment, one treatment was had ten explants, and replicated 3 time and further the experiment was repeated three times.

Means were separated with Duncan's mean separation test, and significant differences at >95% level were shown by the letters next to the numbers.

[1]Number of GUS-positive shoots per explant.

[2]Transformation efficiency is expressed as the percent of GUS-positive shoots per total number of shoots.

The results also suggested that ethylene inhibition does not only increase efficiency of gene transfer but also improves the regeneration of shoots from explants. The control treatments recorded the lowest number of shoots as compared to the treatments with ethylene inhibitors. AVG and pBBRacds, which were more effective in reducing evolved ethylene, recorded significantly higher number of shoots. The importance of ethylene inhibitors in plant regeneration has been elaborated by Eapen and George (1997).

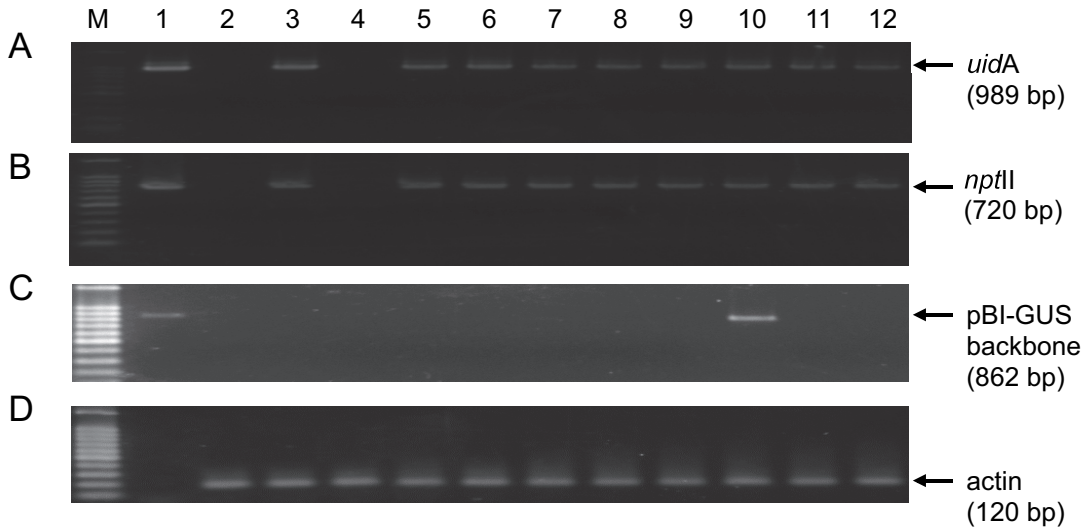

Figure 4.8. PCR amplification of the transgene fragments from transformed shoots of watermelon under different ethylene inhibitors. Genome DNAs were extracted from the randomly selected shoots and used as templates for amplifying fragments of (A) *uid*A 989 bp, (B) the *npt*II 720 bp transgenes, (C) a 862 bp region of pIG121-Hm backbone outside of T-DNA borders, and (D) endogenous wild watermelon actin as reference gene to check the intactness of the DNA. The amplified fragments (A, B, C) are segments in the pIG121-Hm reporter plasmid used in the experiment for monitoring the gene transfer. Lane M, DNA size marker; 1, pIG121-Hm plasmid DNA as positive control template; 2, non-transformed wild watermelon leaf disk; 3-12, genomic DNAs extracted from regenerated shoots treated with different inhibitors (3-4, no effector; 5-6, $AgNO_3$; 7-8, AVG; 9-10, pBBRcont; 11-12, pBBRacds).

4.3.5 Molecular confirmations of the GUS gene transfer on explants and shoots

PCR amplification of the genomic DNA from randomly selected transgenic shoots exhibited the expected size bands of 989 bp for the GUS gene, and 620 bp for the *npt*II gene for most of the selected shoots in all treatments (Fig 4.8 a and b). One sample in the "no effector" treatment did not give the expected band, suggesting that this shoot may represent one of the 'escapes', as it has been documented that selection under kanamycin usually gives a considerable number of escapes during *Agrobacterium* transformation (Kuvshinov et al. 1999; Yevtushenko and Misra 2010).

All other treatments i.e. $AgNO_3$, AVG and pBBRacds exhibited the GUS and nptII gene bands, thus suggesting that the transgene has been transferred into the selected shoots. The process of genetic transformation of plant cells by *Agrobacterium* or binary vectors involves the transfer and integration of the T-DNA regions (region between the left and right border) to the plant genome (Tzfira and Citovsky 2006), thus the regions of the binary vectors are not transferred or integrated into the plant cells. After a series of washing the explants and the shoots it is therefore

expected that the transformed shoots will not posses any genomic material from the regions of the binary vector other than the T-DNA. The genomic DNA from the shoots amplified with border primers (Fig 4.8c) did not show any 826 bp bands except for one sample in the pBBRcont treatment suggesting *Agrobacterium* contamination in this sample. In the other samples the results shows that there was no *Agrobacterium* contamination, therefore the transgenes has been successfully being transfer and integrated in the other samples.

In conclusion, we report that the effects of two chemical inhibitors for ethylene action ($AgNO_3$), ethylene biosynthesis (AVG), and a methodology for eliminating ethylene precursor ACC using *acdS*-harboring *Agrobacterium*, on the *Agrobacterium*-mediated transformation of drought-tolerant wild watermelon were comparatively analyzed. Consequently, *acdS*-harboring *Agrobacterium* was most effective compared to the other commonly used chemical inhibitors, in the suppression of ethylene accumulation during the co-cultivation period, transient expression of GUS transgene in the infected explants, and generation of transgenic shoot formation in wild watermelon. The present results, therefore, showed the potential of the non-chemical approach using ACC deaminase in controlling ethylene from explants and improving the efficiency of *Agrobacterium*-mediated transformation.

Chapter 5

Development of the CRISPR/Cas9-driven site-specific mutagenesis in wild watermelon (*Citrullus lanatus*)

5.1 Introduction

The study of genes and its protein function they encode has become a relevant need in the modern plant breeding. These functional studies help to understand the relationship between genotype and phenotype of organisms (Yang 2012). Although it sounds complex, one way to find the role of a gene is by overexpressing or suppressing/disrupting genes through interfering with coding sequence (Lee et al. 2015; Woo et al. 2015). This has been made easier by the availability of the complete genome sequences of various organisms (Ranz and Parsch 2012).

Novel technologies developed over the past decades have made it easier to study biological functions of genes (Bunnik and Roch 2013). One of the technology that have shown to be easy and rapid to study gene functions is the genome editing (Kamburova et al. 2017). The technology uses sequence specific nucleases, and this enables this technology to perform targeted genome modifications (Yin et al. 2017). The genome editing technology has also shown potential to revolutionize crop improvement, making it possible to create new varieties in a fast, efficient and technically simple way (Zhang et al. 2017). There are various tools available to use for the targeted genome modification like the zinc finger nucleases (ZFNs), transcription activator-like effector nucleases (TALENs) and the most recent clustered regularly interspaced short palindromic repeats/ CRISPR-associated protein 9 (CRISPR/Cas9 (Zhang et al. 2017).

The CRISPR/Cas9 has several advantages as compared to the other tools. It has shown to be highly efficient, easy to use and less error prone as compared to other tools used in genome editing (Zhang et al. 2016). The mostly used application of the CRISPR/Cas9 is the knockout of genes and introducing indels in the coding region leading to mutations that results in loss of function (Woo et al. 2015). The most important factor is that these mutations are stable and heritable in future generations (Curtin et al. 2017).

Studying the genes of the wild watermelon will lead to a better understanding the mechanisms responsible for the drought tolerance in the wild watermelon. This will come handy in breeding for improved drought tolerance in cultivated watermelon and other crops that are susceptible to drought.

In this research we aimed at constructing the CRISPR/Cas9 vectors to target an important gene member in the citrulline pathway, *N*-acetylglutamate kinase

(NAGK) to elucidate its function. Accumulation of citrulline has been found to be one of the tolerance mechanisms in the wild watermelon under drought, as citrulline has been found to have ROS scavenging abilities (Akashi et al. 2001).

5.2 Materials and methods

5.2.1 Chemicals

All reagents used here were purchased from Wako Chemicals, Osaka, Japan, or otherwise described elsewhere.

5.2.2 Plant materials and growth

Wild watermelon (*Citrullus lanatus* acc. No. 101117-1) (Kawasaki et al. 2000) from the Kalahari Desert in Botswana, that has been self-pollinated for at least three times were used in this study. For protoplast experiments, seedlings were prepared as described previously (Akashi et al. 2005) with following minor modifications. A scalpel and forceps were carefully used to de-coat and peel the seeds with minimum damage to the cotyledons. The de-coated seeds were sterilized in a solution containing 5% sodium hypochlorite and 0.005% Tween20 for 10 min and then rinsed five times with sterile water. The sterilized de-coated seeds were soaked in sterile water and kept in the dark overnight at 30°C. The next day the seeds were placed on basal medium containing Murashige and Skoog (1962) salts, 10 mg l^{-1} thiamine, 100 mg l^{-1} myo-inositol, 30 g l^{-1} sucrose and 0.8% agar in the dark at 30°C for 4 days for germination. The germinated seedlings were moved to a growth chamber under fluorescent lights with light intensity of 200-300 μmol photons m^{-2} s^{-1} and 16 h photoperiod at 25°C for 14 days.

For agroinfiltration experiments, the seeds were soaked overnight in water at 30°C in the dark, then in the next morning the seeds were planted in pots filled with a horticulture soil. The germinated seedlings were grown in a growth chamber under fluorescent lights of a light intensity of 300-350 μmol photons m^{-2} s^{-1} and 14 h photoperiod at 25°C until their fourth true leaves were fully expanded.

5.2.3 Selection of a target sequence

Candidates for the target sequence of CRISPR/Cas9-based genome editing was searched by the CRISPR-P 2.0 bioinformatics tool (http://crispr.hzau.edu.cn/CRISPR2/) (Liu et al. 2017), using the Cla022273 gene for *N*-acetylglutamate kinase as the target locus, and *Citrullus lanatus* cv 97103 (v1.0) (Guo et al. 2013) as the target genome. In this target search, parameter for the PAM motif was NGG, and the guide sequence length was 20 nucleotides. From the selected

131 target sequence candidates, restriction enzyme site in the upstream vicinity of the PAM motifs presence was used as a final selection criterion. Among the selected sequences, one sequence matched this selection criterion, and was selected for use in this study. The sequence of CCGATCTTAGTCCATGGCGG*TGG* (*Sty*I restriction site is underlined, with PAM motif in italic), designated as the chr8+22159587 locus, was selected as the target sequence in this study. Two potential off-target sites, CCGATCCGATTCAATGGCGGCGG and CCCAACATAATCCATGGCGGAGG, were deduced by the CRISPR-P tool as the highest off-scores, and designated as chr5+26996803 and chr-5934126 loci, respectively. Genomic sequences of the target in wild watermelon (*Citrullus lanatus* acc. No. 101117-1) were examined by direct sequencing of the PCR product using their flanking primers: CLAGK-210F and CLAGK-909R (Table 5.1) for the chr8+22159587 locus. For potential off-target loci, the primers AGK_off_1F and AGK_off_1R for the chr5+26996803 locus, AGK_off_2F and AGK_off_2R for the chr5-5934126 locus were used to amplify off-targets.

Table 5.1. Oligonucleotide primers used in this study

Usage	Primer name	Primer sequence
NAGK-sgRNA cassette construction		
	AtU-F	CTCCGTTTTACCTGTGGAATCG
	AtU3_R	CCACCGCCATGGACTAAGATCGTGACCAATGTTGCTCC
	AtU6_R	CCACCGCCATGGACTAAGATCGCAATCACTACTTCGTCT
	sgRNA-U3_F	ACGATCTTAGTCCATGGCGGTGGTTTTAGAGCTAGAAAT
	sgRNA-U6_F	GCGATCTTAGTCCATGGCGGTGGTTTTAGAGCTAGAAAT
	sgRNA-R	CGGAGGAAAATTCCATCCAC
	AtU_ApaI_F	ACGGGCCCAGCAGCAAAGGATTTACTTTAA
	sgRNA_KpnI_R	CGTGGTACCGGAGGAAAATTCCATCCA
NAGK target locus amplification		
	CLAGK-210F	ATGGGCCCGAGTTGATGTTCTCTCGGAA
	CLAGK-909R	ATGGGCCCTCCGCCGATTCTTCCTTC
Potential off-target loci amplification		
	AGK_Off_1Fr	TTCATGTTCAGAATCCTTATCGCC
	AGK_Off_1Rr	CTTATCGATTATGCCCTCACAAGG
	AGK_Off_2Fr	GAATATCGGAACCAAGATCATCGC
	AGK_Off_2Rr	CAGTCATGTCCAGTGCAAGAGC
Sequencing		
	M13-F	GTAAAACGACGGCCAG
	M13-R	CAGGAAACAGCTATGAC

5.2.4 Construction of the Cas9/sgRNA vectors

The sgRNA expression cassette was constructed using plasmids for genome editing in plants (Fig. 5.1), with a three-step PCR amplification process as per Ma et al. 2015 with some modifications (Fig. 5.2). The promoter and the sgRNA sequences were initially amplified from pYLsgRNA-AtU6-1 (Addgene no 66202) and pYLsgRNA-AtU3b (Addgene no 66198) vectors (Fig 5.1 a and b). The vectors were used as template to amplify AtU6 and AtU3 promoter insert with AtU6_F, AtU6_R, AtU3_F and AtU3_R primers, the sgRNA insert was amplified using primer sgU6_F, sgU6_R, sgU3_F and sgU3_R.

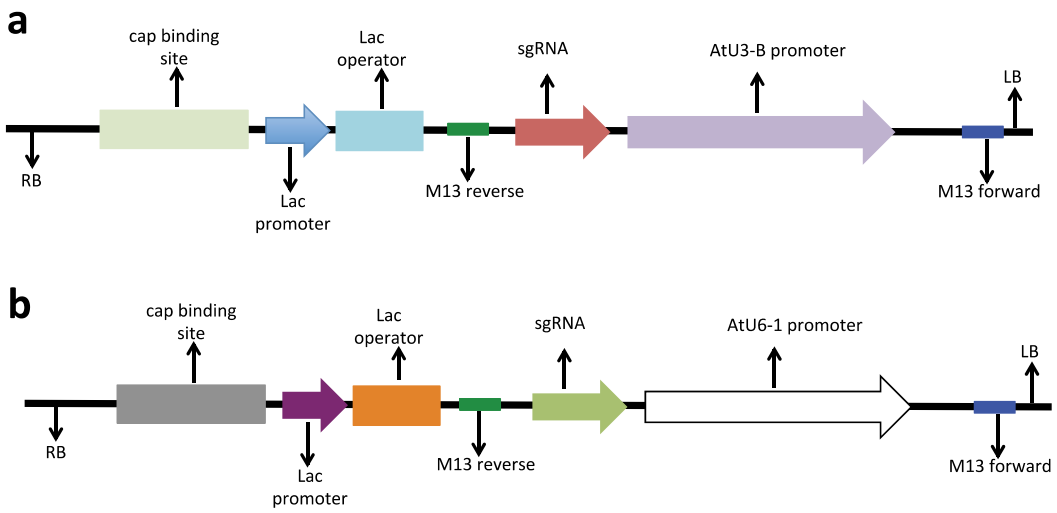

Fig 5.1. The schematic diagrams of the guide RNA vectors

The guide RNA vectors used in this study to amplify the promoter and the sgRNA used to design the gRNA expression cassettes. (a) pYLsgRNA-AtU6-1 (Addgene no 66202) and (b) pYLsgRNA-AtU3b (Addgene no 66198).

The promoter reverse and sgRNA forward primers were designed to have matching overlapping sequences of the selected gRNA for the targeted AGK gene. The overlapping extensions were used as the primers for the secondary PCR. The promoter insert and sgRNA insert were allowed to self anneal without any primers to have an U3-AGK-sgRNA and U6-AGK-sgRNA expression cassettes (Fig. 5.2).

The sgRNA expression cassettes were then amplified with AtU_ApaI_F and sgRNA_KpnI_R primers, to add the *Apa*I and *Kpn*I restriction sequence extension for the cloning purposes. The final expression cassettes were then purified and digested

with *Sty*I to confirm the restriction site and the gRNA. After confirmation the sgRNA cassettes were then digested with the respective (*Apa*I and *Kpn*I) enzymes (NIPPON GENE, Toyama, Japan) and cloned to the pK7WGF2::hcas9 vector (Fig 5.3a) using Ligation High ver.2 (TOYOBO, Osaka, Japan) to have a final expression vector pK7WGF2::hCas9 (Addgene 46965) to have a final vectors pK7WGF2-U3-AGK-sgRNA and pK7WGF2-U6-AGK-sgRNA respectively (Fig 5.3 b and c).

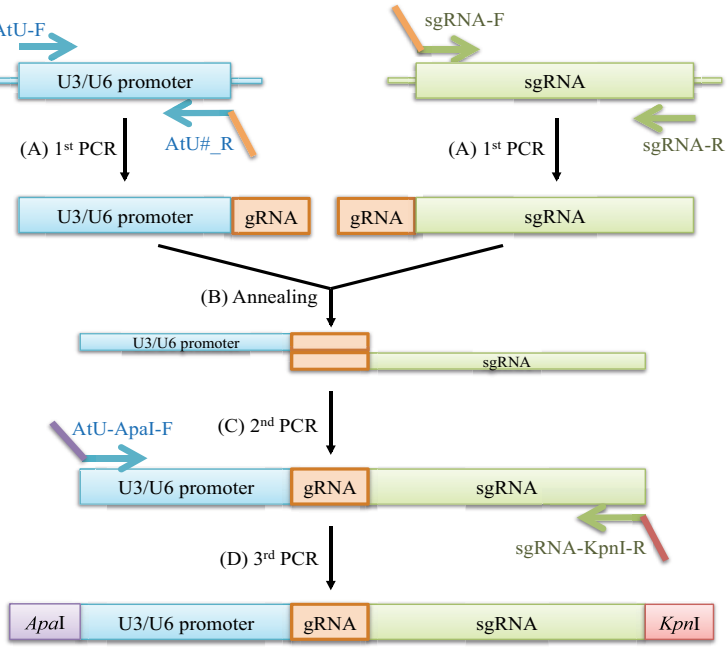

Figure 5.2. Construction strategy of the sgRNA expression cassette

A three-step PCR process of generating the sgRNA expression cassette is shown. Oligonucleotide primers used for the PCRs are shown in colored arrows. (A) Fragments for AtU3 and AtU6 promoters (light blue box), and sgRNA backbone (light green box) were generated by 1st PCR, using primers with NAGK-gRNA overhang sequence, which is shown in orange line. (B) The PCR products were mixed and annealed via complementary sequence of the gRNA. (C) 2nd PCR was performed using the overlapped DNA as a template. (D) 3rd PCR was done using primers with *Apa*I and *Kpn*I overhangs, which are shown in purple and pink lines, respectively. All the nucleotide primers used for the construction are shown in Table 5.1.

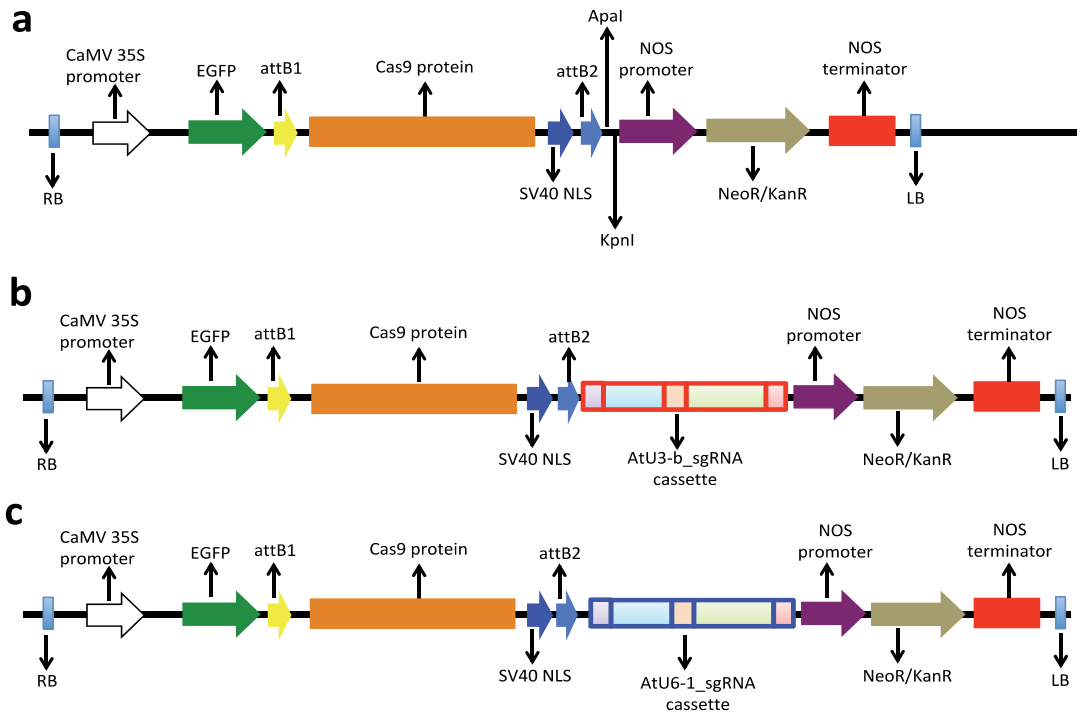

Figure 5.3. The schematic diagrams of the CRISPR/Cas 9 vectors

The diagrams showing the T-DNA of the (a) original CRISPR/Cas9 vector coupled with EGFP but without the gRNA expression cassette, (b) the CRISPR/Cas9 with the cloned AtU3-b-gRNA expression cassette, and (c) the CRISPR/Cas9 with the cloned AtU6-1-gRNA expression cassette.

5.2.5 Protoplast extraction and transfection

Protoplast isolation was performed following the Yoo et al. 2007 and Zhai et al. 2009 with minor modifications. About 3g of the fully expanded cotyledons was harvested, and cut into small dices of about 1 mm with a sterile scalpel inside the clean bench. The cut dices were then quickly transferred into a 50 mL falcon tube with 10 mL of an enzymatic solution (20 mM MES (pH 5.7), 1.5% (wt/vol) cellulase R10 (Yakult Pharmaceutical, Tokyo, Japan), 0.4% (wt/vol) macerozyme R10 (Yakult Pharmaceutical, Tokyo, Japan), 0.4 M mannitol and 20 mM KCl). The solution was warmed at 55 °C for 10 min to have all reagents dissolve and to inactivate DNAse and proteases and enhance enzyme solubility, then cooled to room temperature before being sterilized by running through a 0.45 µm syringe-driven filter. The shredded cotyledons were then mixed with the enzymatic solution and incubated in the dark for 5 h with shaking at 40 rpm at 25°C.

After 5 h, the mixture was then diluted with 10 mL of the W5 solution (2 mM MES (pH 5.7) containing 154 mM NaCl, 125 mM $CaCl_2$ and 5 mM KCl) then sieved

through a sterile nylon mesh to collect only the protoplast mixture and discard the remaining bigger discs. The protoplasts were then pelleted at 100x*g* for 2 min, and then the supernatant solution was carefully pipetted out. The protoplast was then re-suspended in 10 mL of W5 solution and kept in ice for 30 mins to have the protoplasts settled at the bottom, and then the W5 solution was pippeted out as much as possible.

Next the protoplasts were suspended in the MMG solution (4 mM MES (pH 5.7) containing 0.4 M Mannitol and 15 mM $MgCl_2$). The suspended protoplasts was the aliquoted in 200 µL into 2 mL eppendorf tubes to prepare for transfection, then 20 µL of vector DNA was added to each tube and gentle mixed. About the same volume of PEG solution (40% (wt/vol) PEG4000 in ddH_2O containing 0.2 M Mannitol and 100 mM $CaCl_2$) was added to the protoplast/vector DNA mixture and mixed by gentle tapping and flicking the tube upside down. The transfection mixture was kept in room temperature for 20mins before the transfection was stopped by adding 700 µL of the W5 solution and gentle flicking the tubes. The transfected protoplasts where then collected at 100x*g* for 2 min and then supernatant pipetted out as much as possible. The transfected protoplast pellet was then suspended in to 1 ml of W1 solution (4 mM MES (pH 5.7) containing 0.5 M mannitol and 20 mM KCl) then culture overnight in the dark at 25°C in a tissue culture plate.

The next day the transfected protoplasts were then collected at 100x*g* for 3mins and the W1 solution pipetted out. Protoplast DNA was extracted using the DNAeasy PLANT MINI KIT (Qiagen, CA USA) as per manufactures protocol.

5.2.6 Transient expression

Transient expression was performed using the EHA105 strain of *Agrobacterium tumefaciens*. The constructed vectors were electroporated into the EHA105 competent cells, and then incubated in solid agar plates overnight. The following day single colonies were picked to confirm then cultured in liquid LB medium until OD600 of 0.4-0.5 was reached. The culture was then infiltrated into the leaf using a 1 mL syringe. The plants were then managed for 2 days and leaf samples collected for fluorescence visualization and DNA extraction. The DNA was extracted using the DNAeasy PLANT MINI KIT (Qiagen, CA USA) as per manufactures protocol.

5.2.7 Analysis of mutations

Amplification of target site was performed on a T100 Thermal cycler (Bio-Rad Laboratories, Watford, UK) with using KOD FX NEO high-fidelity proofreading enzyme (Toyobo) using primers CLAGK-210F and CLAGK-909R. The expected was of 699 bp size, designed to overlap the targeted mutagenesis site. The PCR fragments were then subjected to restriction digestion using the *Sty*I enzymes to pre-analyze any mutation on the samples. The PCR products were separated in an agarose gel electrophoresis, and the uncut amplicons were then subjected to purification using MinElute Gel Extraction kit (Qiagen, CA USA), and then sub-cloned into an Invitrogen TOPO-BLUNT vector (Life Technologies, Carlsbad, CA, USA). Sequence reactions were performed by BigDye terminator v3.1 Cycle Sequencing Kit (Life Technology) using the M13_F and M13_R primers, and ABI3100 sequencer in the Research Center for Bioscience and Technology, Tottori University, was used to analyse the sequences.

5.2.8 Preparation of EcArgC coupling enzyme

The EcArgC coupling enzyme was prepared as per Takahara et al. 2007. An expression vector pET15b-AGPR (EcArgC) was transformed into competent cells of *E. coli* BL21 (DE3) strain by heat shock method, and then cultured in LB agar medium containing 50 mg l^{-1} ampicillin and cultured overnight at 37°C. The single colonies were picked and cultured in liquid LB medium at 37°C with shaking at 220 rpm until an OD600 of 0.5 was reached. Protein expression was induced by addition of 1 mM isopropyl-β-D-thiogalactose (IPTG) and cells were further cultured for another 3h, and then harvested by centrifugation at 10,000x*g* for 10 min and the supernatant removed completely.

Purification of the recombinant proteins was done by re-suspending the pellet in the equilibration buffer (100 mM Potassium Phosphate buffer (pH 7.5), 600 mM potassium chloride (KCl), 10 mM imidazole). The mixture was then homogenized with a UR-20P handy sonic (Tomy Seiko, Tokyo, Japan) at 30 sec intervals 10 times. The homogenized mixture was then centrifuged at maximum speed for 10 min at 4°C and the supernatant collected into new tubes. The supernatant was finally subjected to Ni-NTA agarose purification following manufactures instructions with minor modifications. The wash buffer was prepared as follows; 100 mM Potassium

phosphate buffer, 600 mM KCl, 20 mM imidazole and elution buffer as follows; 100 mM Potassium phosphate buffer, 600 mM KCl, 250 mM imidazole. The purity of the protein samples were confirmed by polyacrylamide gel electrophoresis, snap frozen in liquid nitrogen and stored at -30°C until use in assaying.

5.2.9 Preparation of samples for quantification of NAGK activity

To quantify the NAGK activity, three different treatments were prepared i.e. mock infection (only H_2O), Cas9 vector control infection (the CRISPR/Cas9 vector without the NAGK_sgRNA cassette) and the NAGK_sgRNA infection (CRISPR/Cas9 vector with NAGK_sgRNA cassette). The wild watermelon was grown in the growth chamber under the same condition described in methods section. The plants were maintained until they have four fully developed true leaves. The *Agrobacterium* strain with the above vectors were cultured in liquid LB medium until the OD600 of 0.4-0.5, and was used to agroinfiltrate the leaves using a sterile 1 ml syringe. The plants were then incubated for 3 days under the same growth conditions. The leaf samples were collected after 3 days of incubation and quickly snap frozen in liquid nitrogen and stored under -80°C until use in the enzymatic activity.

Protein was extracted by homogenizing the 50 mg of samples using the pestle and mortar with a 1 ml homogenization buffer (50 mM HEPES pH 7.6, 1 mM EDTA pH 8.0, 5%(w/v) polyvinylpolypyrrolidone (PVPP), 1 mM DTT and 1 mM phenylmethane sulfonylfluoride (PMSF). The homogenized samples were then centrifuged at 12,000x*g* for 30 min at 4°C. Then the supernatant was then mixed with the additional 1 mL of plant enzyme buffer (50 mM HEPES pH 7.6, 1 mM EDTA, 1 mM DTT). Then, the solution was desalted by draining through a PD MiniTrap G-25 column (GE healthcare, Buckinghamshire, UK) by use of gravity. The protein concentration was quantified by the Bradford assay with Protein Assay CBB Solution (Nacalai, Kyoto, Japan) and 0.1% Bovine Serum Albumin (BSA) at absorbance at 620 nm using the Multiscan FC (Thermo Fisher Scientific, Massachusetts, USA).

5.2.10 Quantification of the NAGK activity in agro-infiltrated leaves

The *NAGK* activity assay was performed as described previously (Takahara et al. 2007), by monitoring the depletion of the β-nicotinamide-adenine dinucleotide phosphate (β-NADPH) in the reaction under the EcArgC coupling enzyme. The assay

was carried out in a 50 mM potassium phosphate buffer, pH7.0, 20 mM $MgCl_2$, 10 mM adenosine 5'-triphosphate (ATP) (Oriental Yeast, Tokyo, Japan), 0.4 mM β-nicotinamide-adenine dinucleotide phosphate (β-NADPH) (Oriental Yeast, Tokyo, Japan), 10 μg/ml EcArgC and plant protein sample. The assay was initiated by addition of 15 mM of *N*-acetylglutamate (Tokyo Chemical Industries, Tokyo, Japan) as substrate. A reference sample was set up without the substrate. The activity was continuously monitored at 340 nm on UH5300 spectrophotometer (Hitachi LTD, Tokyo, Japan), and estimation was based on the Beer-Lambert law (Swinehart 1962);

$A=\varepsilon \times l \times c$,

where A is the absorbance at 340nm

ε is extinction coefficient of NADPH

l is the length of passage in the cuvette (1cm)

C is concentration of NADPH

The molar coefficient of the NADPH was determined at 6,220 M^1 cm^1 (Fluscione et al. 2008) while the path length of the cuvette was 1 cm. Enzyme activity was calculated as described previously (Takahara et al. 2007)

5.3. Results and Discussion

5.3.1 Setup for the protoplast and agroinfiltration systems

The *in vitro* system using the protoplast and *in vivo* system using the agroinfiltrated leaves were set up to evaluate the mutagenesis caused by the designed vectors. The *in vitro* protoplast system had an advantage for the rapidness, while the *in vivo* agroinfiltration system had an advantage for observing the mutagenesis on the fully-grown leaves and also analyzing any morphological and physiological effects caused by mutagenesis.

5.3.2 Detection of mutation

To do preliminary screening of mutants, the genomic DNA was extracted from the both transfected protoplasts and agro-infiltrated leaves, then PCR were done to amplify the target *NAGK* gene using the specific primers. The PCR products were then subjected to *Sty*I restriction digestion to identify any loss of the *Sty*I site on the locus. Undigested PCR product showed 699 bp band, whereas if digested by StyI, the amplicon was split and generated two bands of 170 and 529 bp (Fig. 5.4). The results showed that the both agroinfiltrated and protoplast samples treated with CRISPR/Cas9-NAGK construct contained a mixture of *Sty*I-mutated and non-mutated amplicons. The heterozygosis nature of the amplified DNA could be attributed to the fact that the editing efficiency was not 100%.

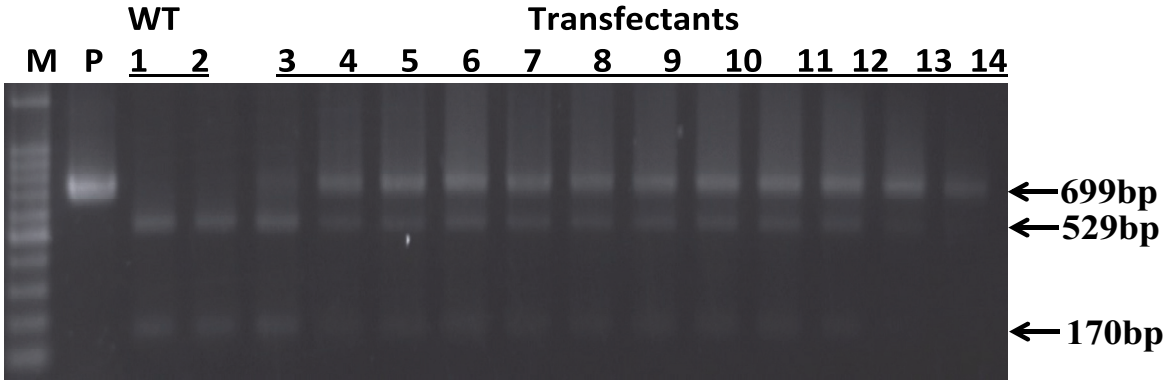

Figure 5.4. Analysis of the target *NAGK* locus by *Sty*I cleavage of the PCR products amplified from DNA extracts protoplasts samples after transfection with pK7WGF2-U6-AGK-sgRNA expression vectors. The two arrows at 170 and 529 bp indicates the expected DNA fragments resulting from the *Sty*I cleavage of the 699 bp PCR product. Top arrow indicates the expected 699 bp size of PCR products from *NAGK* genes. Lane M, 100 bp DNA size marker; P, Undigested PCR product from untreated leaves; 1-2, digested PCR products from untreated (unedited) sample; 3-14 digested PCR products from transfected DNA.

5.3.3 Confirmation of directed mutagenesis by sequencing independent mutants

To determine the nature of mutations on the target gene, the *Sty*I-uncleavable PCR bands from the transfectants were purified from the agarose gel. The purified products were then subcloned to the TOPO blunt vector. The independent clones obtained from the TOPO blunt cloning were subjected to the sequencing. The DNA sequences demonstrated the presence of various mutations in the targeted gene (Fig 5.5 and 5.6). Interestingly, the frequency of nucleotide substitutions was very high among the sequences. These replacements were observed mostly around the *Sty*I site which were situated upstream of the PAM sequence. The substitutions varied in positions on the targeted sequence, and they also varied in number ranging from one to three replacements per sequence (Fig. 5.5 and 5.7). Most importantly, these nucleotide substitutions only appeared on the target sequence but not found in other regions of the target gene, indicating that target sequence was specifically edited in this experiment.

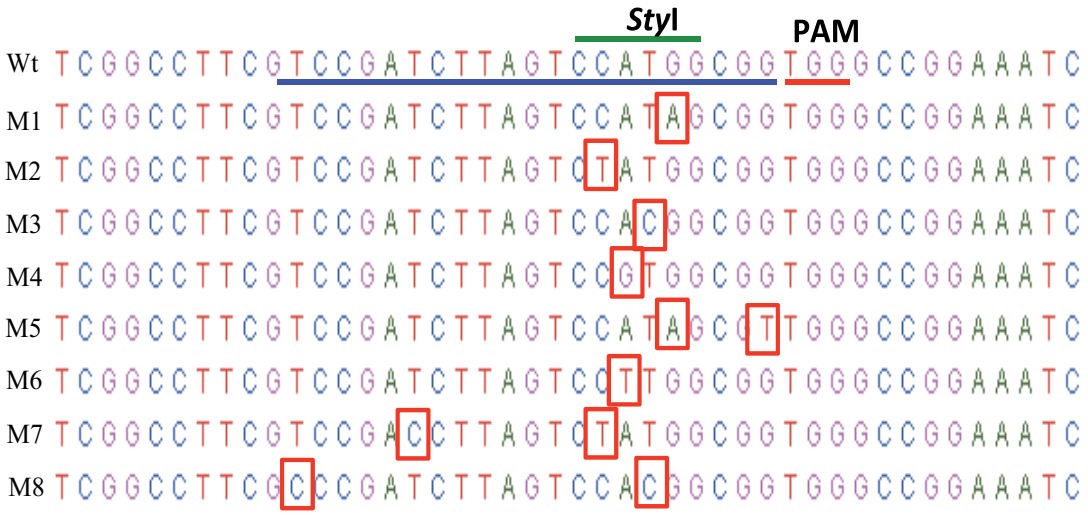

Figure 5.5 Sequence alignments of the sequence mutants. The target sequence on the wild type is underlined in blue color and the PAM sequence is underlined with the red color. Representative sequences of some of the substitution mutations identified on the samples. The *Sty*I site is shown by the green bar over the sequence. The mutations are highlighted in orange boxes.

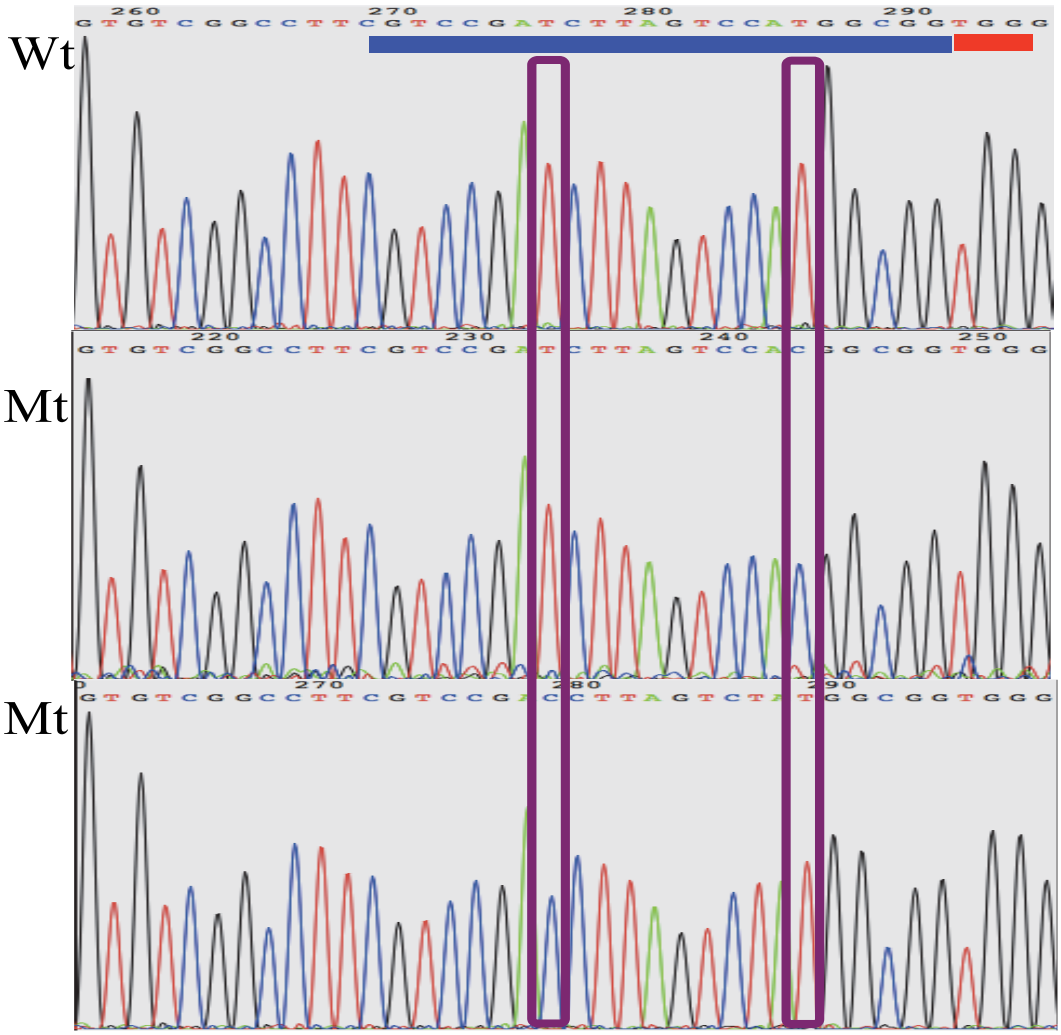

Fig 5.6. The Sanger sequence chromatograms of the wild type (Wt) and the two mutant sequences (Mt). The target sequence on the wild type is underlined in blue color and the PAM sequence is underlined with the red color.

Analysis of the *NAGK* sequence showed that substitutions were only localized on the gRNA and near the PAM motif only (Fig 5.7), as no other substitution were observed on the sequence stretch that flanks the gRNA site on the *NAGK* sequence. This then suggests that the substitutions were effected by transfection with *NAGK*:sgRNA:Cas9 vector, thus suggesting some editing events as the other samples from treatments without the expression cassettes did not show any substitutions on the similar region.

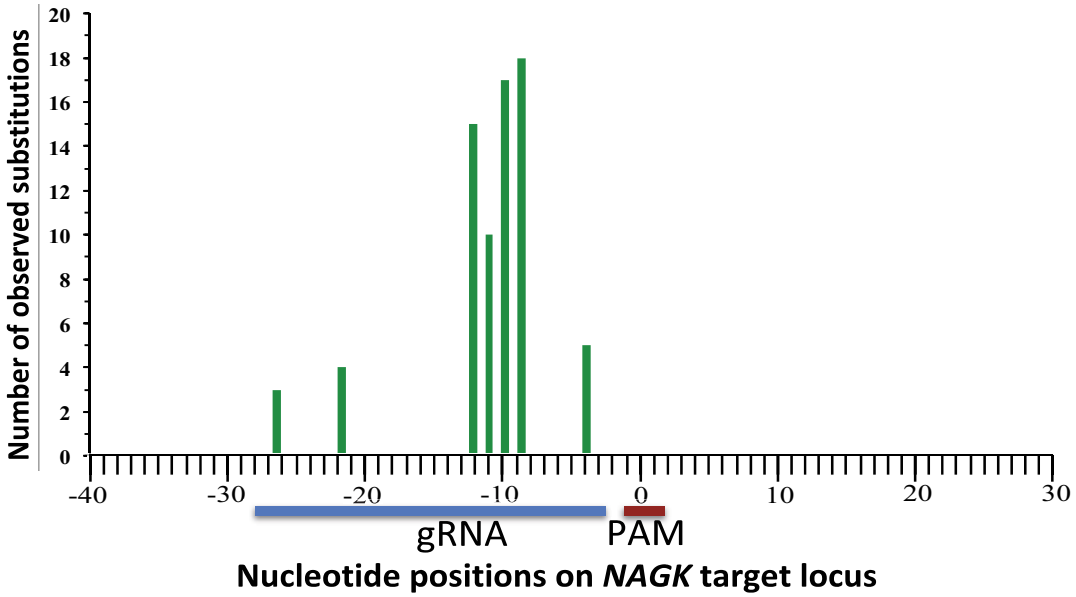

Figure 5.7. A graphical presentation showing the distribution of nucleotides substitution on the flanking sites of the PAM motif of the target *NAGK* sequence of the wild watermelon. The X-axis represent the position of NAGK sequence in which the center of PAM motif was set as zero, while the Y-axis represents the number of observed substitutions at a particular position of the genome.

A total of 124 clones were analyzed and the number of clones that showed at least one substitution per clones was very high (Table 5.2). The number of substitutes per clone varied from 1 to 3 nucleotides. The frequency of a single nucleotide substitution was very high as compared double or triple nt substitutes. The positions of these substitutes varied greatly on the target site as shown in figure 5.7. These substitutions have shown to be highly localized near the PAM motif upstream on the target gRNA.

Table 5.2 Frequency and positions of the nucleotide substitutions

Promoter for gRNA	Total clones	Clones with substitutions	Frequency of substitutions per clone		
			1nt	2nt	3nt
AtU3-1	64	40	27	11	2
AtU6-b	64	32	26	5	1

A closer observation on the trend of these substitutions has shown a higher frequency of inter-conversion between thymine (T) and cytosine (C). The substitution of these two bases showed a higher frequency in either direction. The interaction of these

bases during genome editing has been reported in other studies with varying degree of results. Abdullah et al. 2016 stated that a single T↔C nucleotide change in a codon could have a different result depending on the position of the substituted base. The conversion of thymine to cytosine produced activated the un-active mGFP expression gene (Li et al. 2018).

Table 5.3 Trend of nucleotide substitution in on-target sequence

Substituted nucleotide	Original nucleotide: A	T	G	C
A	-	0	13	0
T	6	-	7	13
G	7	0	-	0
C	0	26	0	-

Whether these nucleotide substitutions were responsible for the observed reduction in the *NAGK* enzyme activity and morphological changes on the leaves cannot be concretely proved at present. But it is possible that substitutions were highly effective in altering the *NAGK* gene function, as has been observed in loss-of-function of mutated genes in both plants and animals (May 2017; Li et al. 2017). Further careful analysis has to be done in the future to confirm if indeed it is a case of base editing. It has been shown that a difference in just one nucleotide on the sequence can result in altering the gene function (Sun et al. 2016; Kim et al. 2017; Lu and Zhu 2016; Harmsen et al. 2018).

5.3.4. Analysis of off-target editing

The main concern in targeted genome editing technique is the unplanned mutagenesis on genes that have closely similar sequences with the gRNA sequence for the target gene. Therefore it is important to analyze any chances of mutagenesis on the potential off-targets loci. The online CRISPR-P tool that I used to design the target gRNA sequence also provided a list of the potential off-target loci in watermelon genome. The two off-target candidates were selected on the basis of having an almost perfect base pairing within the last 6 bp at the 5' of the PAM as

compared to the target *NAGK* sequence. It has been suggested that the Cas9 system have low tolerance to variation in sequences proximal to PAM sequence, resulting in minimal or no editing at all if there is any difference in perfect base pairing on the 3' of the gRNA, whereas distal (close to the 5' of gRNA) mismatches can be tolerated thus resulting in off-target editing (Hsu et al. 2014; Cong et al. 2013).

Therefore, these two off-targets candidates with four nucleotides mismatch to the target site of our NAGK_sRNA were selected for off-target analysis, and primers AGK_offtarget_1 and AGK_offtarget_2 (Table 5.1) were designed to amplify 660 and 680 bp respectively of the off target genes, and the PCR amplicons were cloned and sequenced. The results show that no mutagenesis was observed on the off-target gene sequences in ten independent clones (Fig. 5.8). This observation suggested that genetic sequence alteration appears specific to the target locus.

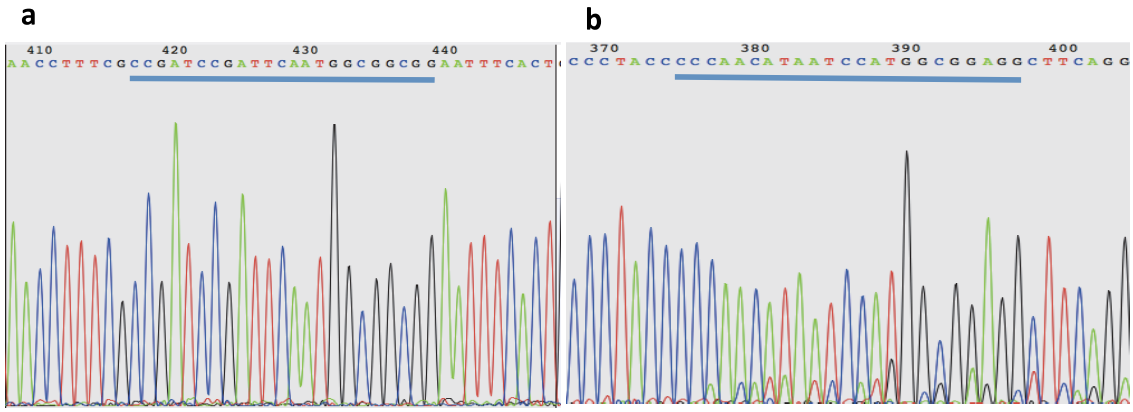

Figure 5.8. The sequencing chromatography of the off-target analysis showing that no specific mutagenesis occurred on the untargeted genes. (a) off-target 1 and (b) off-target 2. The putative off target sequences are underlined in blue for both the selected off target analysed

5.3.5 Morphological and physiological effects on the leaves

N-acetylglutamate kinase (*NAGK*) has been shown to have a mutual and highly important interaction with the plastid P-II proteins (Burillo et al. 2004; Maheswaran et al. 2004; Feria-Bourrellier et al. 2009). This protein is suggested to be involved in the sensing and signal transduction of carbon/nitrogen balance. Therefore, any disturbance of the *NAGK* level will result not only in the disruption of the citrulline biosynthesis but also may disturb the sensing of the carbon/nitrogen balance. This may result in unmonitored energy status, and this can be fatal to plant cells.

Monitoring plant morphology is one of the first and easiest methods to determine if the plant growth and development systems are not functioning properly.

In this study, the leaves were infiltrated with the three different treatments (Fig. 5.9), which were either of; (1) mock, whereby only distilled water was to monitor the damage on the leaves caused by physical pressure of the syringe during infiltration. The leaves infiltrated with only water showed minimal damaged on them giving an impression that the physical damage was not the much (Fig. 5.9a). Even though damage might vary from one leaf to another but in general it was within the same range. To monitor the effect of the *Agrobacterium* and the CRISPR vector on the leaves, treatment 2 was designed to contain the EHA105 *Agrobacterium* harboring the CRISP/Cas9 vector. The CRISPR vector used in here did not contain any gRNA expression cassettes. The damage caused by treatment 2 (Fig. 5.9b) was within the same range with water-mock treatment, as only little damaged was visible on all the leaves infiltrated with EHA/Cas9. This suggested that the both the *Agrobacterium* and untransformed CRISPR vector have little or no effect on leaves.

The infiltration of the wild watermelon leaves with *NAGK*:sgRNA:Cas9 vector was performed as the main treatment to see any physiological changes on the leaf. The observation showed that the leaf infiltrated with *NAGK*:sgRNA:Cas9 vector had highly visible damage around the infiltration area (Fig. 5.9c). This suggested that the *NAGK* gene might have been disrupted and rendered malfunctional through the CRISPR/Cas9-driven genome editing.

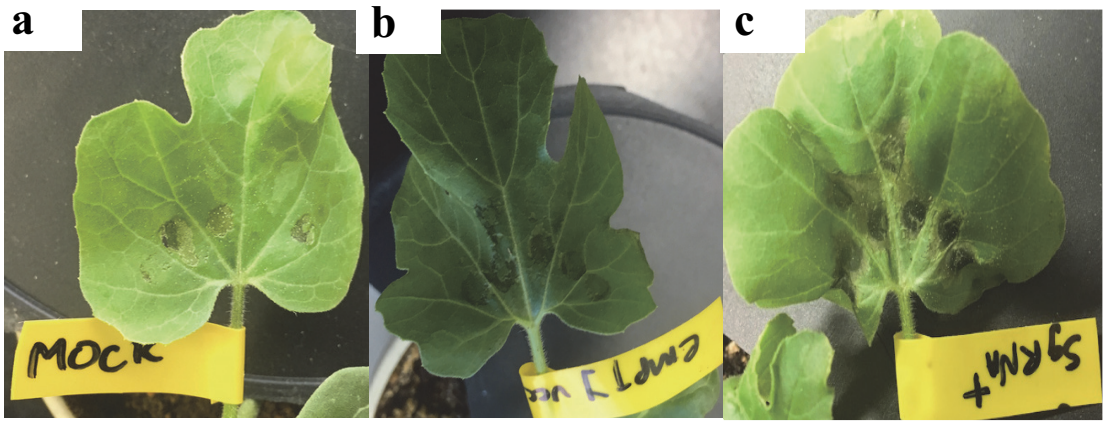

Figure 5.9. Morphological appearance of infiltrated leaf samples after three-day incubation
The wild watermelon were agroinfiltrated using a 1 mL syringe with EHA105 strain incubated overnight until OD500 was reached, the three different treatments used were (a) only distilled water was used as a treatment to infiltrate the leaves, (b) the CRISPR/Cas9 (pK7WGF2::hCas9) without the gRNA expression cassette insert, and (c) the CRISPR/Cas9 vector coupled with the *NAGK*:sgRNA:Cas9 vector.

To analyze biochemical changes that may have happened on the citrulline pathway, a spectrophotometric assay of the *NAGK* enzyme activity was performed. In the citrulline biosynthesis pathway, *NAGK* enzyme converts *N*-acetylglutamate and ATP to produce *N*-acetyglutamate 5-phosphate plus ADP. Then the resultant *N*-acetyglutamate 5-phosphate with another substrate NADPH was converted under the enzymatic process of NAGPR and produces *N*-acetyglutamate 5-semialdehyde, inorganic phosphate and $NADP^+$. Therefore, the activity of NAGK can be monitored through the rate of NADPH consumption in the reaction, by using a spectrophotometer at absorbance of 340 nm (Wu et al. 1986; Heinrich et al. 2004; Takahara et al. 2007; Winter et al. 2015).

In this study, the same idea was used to quantify the activity of *NAGK* in the agroinfiltrated leaves. The rate of NADPH consumption on the two control samples (mock-H_2O and the Cas9 vector without gRNA) showed similar tendencies, as they recorded higher extinction rate of 203.93 and 220.62 μmole μg $protein^{-1}$ min^{-1} respectively (Fig. 5.10). The *NAGK*:sgRNA:Cas9 vector agroinfiltrated samples showed a significantly reduced rate of oxidation at 120.46 μmole μg $protein^{-1}$ min^{-1}.

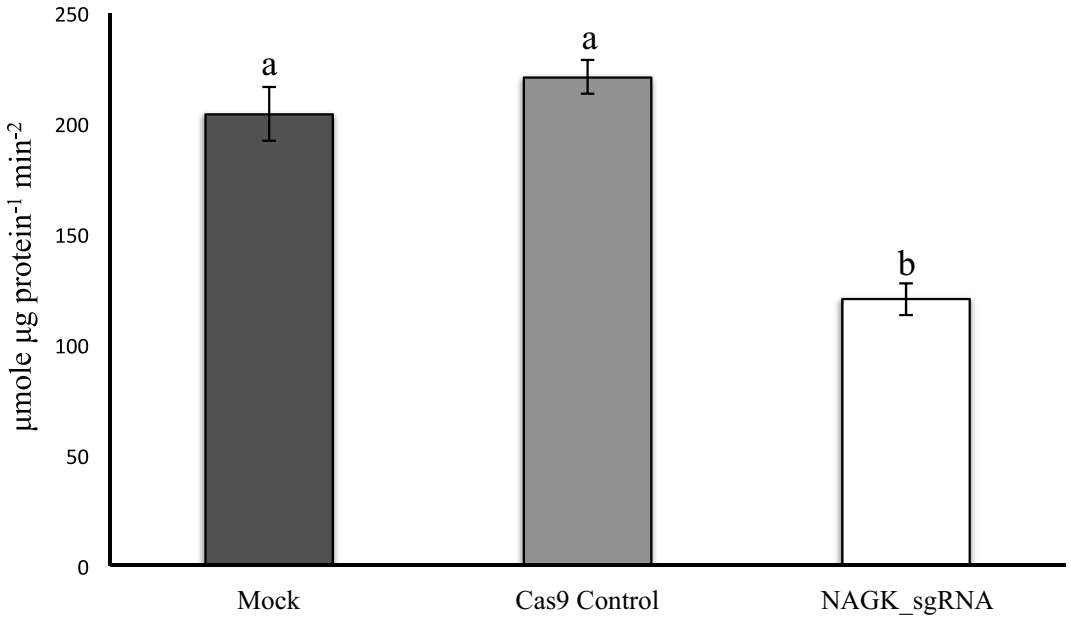

Figure 5.10. Enzymatic activity assay of *NAGK* in the watermelon leaves which were treated by agroinfiltration. The *NAGK* activity is expressed as nmol of NADPH used per min per protein in the sample. Letters on top of the bars indicate statistical significance at the 95% confidence level based on Duncan's mean comparison.

The results showed that foliar *NAGK* activity was suppressed by the action of *NAGK*:sgRNA:Cas9 vector, suggesting that loss-of-function of *NAGK* by the genome editing might result in the decreased protein abundance in this transient assay.

In this study, a site-specific genome editing tool driven by the CRISPR/Cas9 system was developed to target specific gene on the wild watermelon. Although the results are still inconclusive and further analysis should be done, the high frequency of nucleotide substitution gave an idea that some mutations occurred in the target locus. Morphological defects on the leaves and the reduction of the *NAGK* enzymes activity observed in the agroinfiltrated leaves of wild watermelon were consistent with the occurrence of nucleotide alteration. Improving these tools to maximize the efficiency, especially to induce various mutations like indels on the target sites, will be anticipated in the future analysis. Genetic manipulation of wild watermelon, for the functional genomics, is important for elucidating the molecular mechanisms of drought tolerance, and exploitation of genetic resource in this plant.

Chapter 6

Conclusions

The conclusions brought forward for the thesis study are;

(i) Variations exist on the data collected from natural and controlled environment growing conditions in watermelon

The physiological analysis of the two watermelon species in the natural (open field) and controlled environment (growth chamber) was done to observe any variation. Consequently, similar trend in the physiological changes were observed under moisture deficit stress, such as suppression of stomatal conductance, photosynthetic CO_2 assimilation and photochemical processes, and up-regulation of non-photochemical quenching for dissipating excess light energy. However, variations were observed between the two environmental condition; one was the rapidness in response to moisture deficit for both watermelon, where physiological responses to the stress was more rapid in natural condition in comparison to that in controlled environmental condition. The other variation was the intensity of drought response, in that the magnitude of physiological alteration was larger in the natural condition, as exemplified in the larger buildup of non-photochemical quenching in the natural condition under moisture stress.

(ii) Transcriptional up-regulation contributes to the fortification of chloroplast APX activity in the leaves of drought-stressed wild watermelon

Ascorbate peroxidase (APX) plays an important role in detoxifying reactive oxygen species under environmental stress. Although previous work in drought-tolerant wild watermelon has shown an increase in chloroplast APX enzyme activity under drought, molecular entities of APX have remained uncharacterized. In this study, structure and transcriptional regulation of the APX gene family in watermelon were characterized. Five APX genes, designated as CLAPX1 to CLAPX5, were identified from watermelon genome. The mRNA alternative splicing was suggested for CLAPX5, which generated two distinct deduced amino acid sequences at their C-terminus, in resemblance to a reported alternative splicing of chloroplast APXs in pumpkin. This observation suggests that two isoenzymes for stromal and thylakoid-bound APXs may be generated from the CLAPX5 gene. Phylogenetic analysis classified CLAPX isoenzymes into three clades, i.e., chloroplast, microbody, and cytosolic. Physiological analyses of wild watermelon under drought showed a decline in

stomatal conductance and CO2 assimilation rate, and a significant increase in the enzyme activities of both chloroplast and cytosolic APXs. Profiles of mRNA abundance during drought were markedly different among CLAPX genes, suggesting distinct transcriptional regulation for the APX isoenzymes. Up-regulation of CLAPX5-I and CLAPX5-II was observed at the early phase of drought stress, which was temporally correlated with the observed increase in chloroplast APX enzyme activity, suggesting that transcriptional up-regulation of the CLAPX5 gene may contribute to the fortification of chloroplast APX activity under drought. Our study has provided an insight into the functional significance of the CLAPX gene family in the drought tolerance mechanism in this plant.

(iii) The importance of inhibiting ethylene during *Agrobacterium* transformation in wild watermelon

Ethylene (C_2H_4), a phytohormone that is produced in response to both abiotic and biotic stresses, is an important factor influencing the efficiency of *Agrobacterium*-mediated transformation. In this study, effects of various ethylene inhibitors on the efficiency of *Agrobacterium*-mediated genetic transformation in drought-tolerant wild watermelon was comparatively examined. Consequently, in comparison to the application of chemical inhibitors such as $AgNO_3$ and aminoethoxyvinylglycine (AVG), lower ethylene level was observed when the infecting *Agrobacterium* contained a gene for 1-aminocyclopropane-carboxylic acid (ACC) deaminase (*acdS*), which cleaves ethylene precursor ACC into α-ketobutyrate and ammonia. GUS histochemical and spectrophotometric enzyme assays showed that *acdS* was more effective in enhancing gene transfer than the chemical ethylene inhibitors. Efficiency of transgenic shoots formation was higher in *acdS*- and AVG-treated explants. These observations demonstrated that controlling the ethylene level during co-cultivation and shoot formation, particularly using the *acdS*-harboring *Agrobacterium*, is advantageous for enhancing the transformation efficiency in this plant.

(iv) Site directed mutagenesis in wild watermelon

Genome editing technologies, such as the CRISPR/Cas9 system, has been an important technology used in functional studies. In this study, therefore, the focus was to develop the CRISPR/Cas9 genome editing system in wild watermelon, as a tool for

studying gene functions. The *N*-acetylglutamate kinase (NAGK) gene, a plausible committing step in citrulline biosynthesis in wild watermelon was selected as the target for genome editing. Agroinfiltration of an *Agrobacterium* containing a binary vector encoding a CRISPR/Cas9-NAGK cassette showed necrotic defects on the leaves of the infected wild watermelon plants, in contrast to the control infection. Biochemical analysis showed a reduction of the NAGK enzyme activity in the protein extract from the infected leaves. Analysis of the genome sequence extracted from the agroinfiltrated leaves and the cassette-introduced protoplasts displayed high frequency of various nucleotide substitutions on the targeted locus, but not on the other region of the NAGK gene. Deletion-type mutations, which have been commonly observed in genome editing in other plants, were not observed in the present analysis. Analysis of the potential off-targets sequences did not show any sequence alteration. Although further research and development will be needed to achieve maximum efficiency for the gene knockout study, the present observations indicated that target locus was specifically edited at a higher frequency in wild watermelon, suggesting that the genome editing technique can be an powerful tool for studying drought-tolerant wild plant resources in the future analyses.

References

Adams DO and Yang SF (1979) Ethylene biosynthesis: Identification of 1-aminocyclopropane-1-carboxylic acid as an intermediate in the conversion of methionine to ethylene. Proc Natl Acad Sci USA 76:170-174

Agrotis A and Ketteler R (2015) A new age of functional genomics using CRISPR/Cas9 in arrayed library screening. Front Genet 6: 300

Akama K, Shiraishi H, Ohta S, Nakamura K, Okada K and Shimura Y (1992) Efficient transformation of *Arabidopsis thaliana*; comparison of the efficiencies with various organs, plant ecotypes and *Agrobacterium* strains. Plant Cell Rep 12: 7-11

Akashi K, Miyake C and Yokota A (2001) Citrulline, a novel compatible solute in drought-tolerant wild watermelon leaves, is an efficient hydroxyl radical scavenger. FEBS Lett 508: 438-442

Akashi K, Nishimura N, Ishida Y and Yokota A (2004) Potent hydroxyl radical-scavenging activity of drought-induced type-2 metallothionein in wild watermelon Biochem Biophys Res Commun 323: 72–78

Akashi K, Morikawa K and Yokota A (2005) *Agrobacterium*-mediated transformation system for the drought and excess light stress-tolerant wild watermelon (*Citrullus lanatus*). Plant Biotechnol 22: 13-18

Akashi K, Yoshida K, Kuwano M, Kajikawa M, Yoshimura K, Hoshiyasu S, Inagaki N and Yokota A (2011) Dynamic changes in the leaf proteome of a C3 xerophyte, *Citrullus lanatus* (wild watermelon), in response to water deficit. Planta 233: 947-960

Akashi K, Yoshimura K, Kajikawa M, Hanada K, Kosaka R, Kato A, Katoh A, Nanasato Y, Tsujimoto H and Yokota A (2016) Potential involvement of drought-induced Ran GTPase *CLRan1* in root growth enhancement in a xerophyte wild watermelon. Biosci Biotechnol Biochem 80: 1907-1916

Alberts B, Johnson A, Lewis J, Morgan D, Raff M, Roberts K and Walter P (2014) Molecular Biology of the Cells. 6th ed. Garland Science: New York and Abingdon, UK

Amako K, Chen GX and Asada K (1994) Separate assays specific for ascorbate peroxidase and guaiacol peroxidase and for the chloroplastic and cytosolic isozymes of ascorbate peroxidase in plants. Plant Cell Physiol 35: 497-504

Armenteros JJA, Sønderby CK, Sønderby SK, Nielsen H and Winther O (2017) DeepLoc: prediction of protein subcellular localization using deep learning. BMC Bioinformatics 33: 3387–3395

Ashraf M and Harris PJC (2013) Photosynthesis under stressful environments: An overview. Photosynthetica 51: 163-190

Athar H and Ashraf M (2005) Photosynthesis under drought stress. in: (ed.) Pessarakli M. Photosynthesis 2nd Ed. CRC Press, New York. Pp. 795-810

Bassi PK and Spencer MS (1985) Comparative evaluation of photoionization and flame ionization detectors for ethylene analysis. Plant Cell Environ 8: 161–165

Beyer EM (1976) A potent inhibitor of ethylene action in plants. Plant Physiol 58:268–271

Belide S, Hac L, Singh SP, Green AG and Wood CC (2011) *Agrobacterium*-mediated transformation of safflower and the efficient recovery of transgenic plants via grafting. Plant Methods 7: 12

Blum A (2014) Genomics for drought resistance – getting down to earth. Funct Plant Biol 41: 1191–1198

de Block M, de Brouwer D and Tenning P (1989) Transformation of *Brassica napus* and *Brassica oleracea* using *Agrobacterium tumefaciens* and the expression of the *bar* and *neo* genes in the transgenic plants. Plant Physiol 91: 694-701

Boller T and Kende H (1980) Regulations of wound ethylene synthesis in plants. Nature 286: 259-260

Bolwell GP and Woztaszek P (1997) Mechanisms for the generation of reactive oxygen species in plant defense - a broad perspective. Physiol Mol Plant Pathol 51: 347-366

Bowler C, Montagu MV and Inze D (1992). Superoxide dismutase and stress tolerance. Annu Rev Plant Phys 43: 83-116.

Bradford MM (1976) A rapid and sensitive method for the quantitation of microgram quantities of protein utilizing the principle of protein-dye binding. Anal Biochem 72: 248-254

Bray EA (1997) Plant responses to water deficit. Trends Plant Sci. 2:48-54

Brunner I, Herzog C, Dawes M, Arend M, and Sprisen C (2015) How tree roots respond to drought. Front Plant Sci 6: 547

Bunnik EM and le Roch KG (2013) An introduction to functional genomics and system biology. Adv Wound Care 9: 490-498

Burillo S, Luque I, Fuentes I and Contreras A (2004) Interactions between the nitrogen signal transduction protein PII and *N*-acetylglutamate kinase in organisms that perform oxygenic photosynthesis. J Bacteriol 186, 3346-3354

Buttler WL (1966) Fluorescence yield in photosynthetic systems and its relation to electron transport. Curr Top Bioenerg 1: 49-73

Carvallo CHS, Zehr AB, Gunaratna N, Anderson J, Kononowicz HH, Hodges TK and Axtell JD (2004) *Agrobacterium*-mediated transformation of sorghum: factors that affect transformation efficiency. Genet Mol Biol 27: 259-269

Caverzan A, Passaia G, Rosa SB, Ribeiro CW, Lazzarotto F and Margis-Pinheiro M (2012) Plant responses to stresses: role of ascorbate peroxidase in the antioxidant protection. Genet Mol Biol 35: 1011-1019

Centritto M, Lauretti M, Monteverdi MC and Serraj R (2009) Leaf gas exchange, carbon isotope discrimination, and grain yield in contrasting rice genotypes subjected to water deficits during the reproductive stage. J Exp Bot 60: 2325-2339

Cermak T, Doyle EL, Christian M, Wang L, Zhang Y, Schmidt C, Baller JA, Somia NV, Bogdanove AJ and Voytas DF (2011) Efficient design and assembly of custom TALEN and other TAL effector-based constructs for DNA targeting. Nucleic Acids Res 39:e82

Chaves MM (1990) Effects of water deficits on carbon assimilation. J Exp Bot 42: 1-16

Chen YM, Ferrar TS, Lohmeier-Vogel E, Morrice N, Mizuno Y, Berenger B, Ng KK, Muench DG and Moorhead GB (2006) The PII signal transduction protein of *Arabidopsis thaliana* forms an arginine-regulated complex with plastid N-acetyl glutamate kinase J Biol Chem 281: 5726-5733

Chen l, Dodd IC, Theobald JC, Belimov AA and Davies WJ (2013) The *Rhizobacterium Variovorax paradoxus* 5C-2, containing ACC deaminase, promotes growth and development of *Arabidopsis thaliana* via ethylene-

dependent pathway. J Exp Bot 64: 1565-1573
Chew O, Whelan J and Millar AH (2003) Molecular definition of the ascorbate-glutathione cycle in Arabidopsis mitochondria reveals dual targeting of antioxidant defenses in plants. J Biol Chem 278: 46869–46877.
Chira S, Gulei D, Hajitou A, Zimta A-A Cordelier P and Berindan-Neagoe I (2017) CRISPR/Cas9: Transcending the reality of genome editing. Nucleic Acids Res 7: 211-222
Choi PS, Soh WY, Kim YS, Yoo OJ and Liu JR (1994) Genetic transformation and plant regeneration of watermelon using *Agrobacterium tumefaciens*. Plant Cell Rep 13: 344-348
Cong L, Ran FA, Cox D, Lin S, Barretto R, Habib N, Hsu PD, Wu X, Jiang W, Marraffini LA and Zhang F (2013) Multiplex genome engineering using CRISPR/Cas9 systems. Science 339:819-823
Curtin SJ, Xiong Yer, Michno J-M, Campbell BW, Stec AO, Cerm T, Starker C, Voytas DF, Eamen AL and Stupar RM (2017) CRISPR/Cas9 and TALENs generate heritable mutations for genes involved in small RNA processing of *Glycine max* and *Medicago truncatula*. Plant Biotechnol J 16: 1125-1137
Custers JBM and den Nijs APM (1986) Effects of aminoethoxyvinylglycine (AVG), environment, and genotype in overcoming hybridization barriers between *Cucumis* species. Euphytica 35: 639-647
Dehairs J, Talebi A, Cherifi Y and Swinnen JV (2016) CRISP-ID: decoding CRISPR mediated indels by Sanger sequencing. Sci Rep 6:28973
Demmig-Adams B and Adams WW (1996) The role of xanthophyll cycle carotenoids in the protection of photosynthesis. Trends Plants Sci 1: 1
Demmig-Adams B and Adams WW (2006) Photoprotection in an ecological context: the remarkable complexity of thermal energy dissipation. New Phytol 172, 11-21.
Desclaux D and Roumet P (1996) Impact of drought stress on the phenology of two soybean (*Glycine max* L. *Merr*) cultivars. Field Crops Res 46: 61-70
Durai S, Mani M, Kandavelou K, Wu J, Porteus MH and Chandrasegaran S (2005) Zinc finger nucleases: custom-designed molecular scissors for genome engineering of plant and mammalian cells. Nucleic Acids Res 33: 5978-5990
Eapen S and George L (1997) Plant regeneration from peduncle segments of oil seed Brassica species: influence of silver nitrate and silver thiosulfate. Plant Cell Tiss Organ Cult 51: 229-232.
Eisenhut M, Brautigam A, Timm S, Florian A, Tohge T, Fernie AR, Bauwe H and Weber APM (2017) Photorespiration is crucial for dynamic response of photosynthetic metabolism and stomatal movement to altered CO_2 availability. Molecular Plant 10: 47-61
Ezura H, Yuhashi KI, Yasuta T and Minamisawa K (2000) Effect of ethylene on *Agrobacterium tumefaciens*-mediated transfer to melon. Plant Breeding 119: 75-79
Falciatore A, Formiggini F and Bowler C (2002) Reporter genes and in vivo imaging. In: (eds.) Gilmartin PM, Bowler C. Molecular Plant Biology. Vol 2, Oxford University Press, New York. pp. 265-282
Faraloni CI, Cutino R, Petruccelli AR, Leva S, Lazzeri G and Torzillo G (2011) Chlorophyll fluorescence techniques as a rapid tool for *in vitro* screening of olive cultivars (*Olea europaea* L.) tolerant to drought stress. Environ Exp Bot 73: 49-56.
Farooq M, Wahid A, Kobayashi N, Fujita D, and Basra SMA (2009) Plant drought stress: effects, mechanisms and management. Agron Sustai Dev 29: 185-212

Farooq M, Hussain M, Wahid A and Siddique KHM (2012) Drought stress in plants: An overview; in, Plant responses to drought from morphological to molecular features ed. Aroca R. Springer-Verlag Berlin Heidelberg

Feria-Bourrellier AB, Ferrario-Méry S, Vidal J and Hodges M (2009). Metabolite regulation of the interaction between Arabidopsis thaliana PII and *N*-acetyl-l-glutamate kinase. Biochem Biophys Res Commun 387: 700-704.

Fernandez-Murga ML, Gil-Ortiz F, Llacer JL and Rubio V (2004) Arginine biosynthesis in Thermotoga maritime: characterization of the arginine- sensitive *N*-acetyl-L-glutamate kinase. J Bacteriol 186: 6142-6149

Flexas J and Medrano H (2002) drought inhibition of photosynthesis in C3 plants: Stomatal and non-stomatal limitations revisited. Ann Bot 89:183-189

Flexas J, Bota J, Loreto F, Cornic G and Sharkey TD (2004) Diffusive and metabolic limitations to photosynthesis under drought and salinity in C_3 plants. Plant Biology 6: 269-279.

Flower DJ and Ludlow MM (1986) Contribution of osmotic adjustments to dehydration tolerance of water stressed pigeonpea (*Cajanus cajan* (L) Millsp) leaves. Plant Cell Environ 9: 33-40

Gaj T, Gersbach CA and Barbas III CF (2013) ZFN, TALEN, and CRISPR/Cas-based methods for genome engineering. Trends Biotechnol 31: 397-405

Gelvin SB (2003) *Agrobacterium*-mediated plant transformation: the biology behind the "gene-ockeying" tool. Microbiol Mol Biol Rev 67: 16-37

Genty B, Briantais J-M and Baker NR (1989) The relationship between the quantum yield of photosynthetic electron transport and quenching of chlorophyll fluorescence. Biochim Biophys Acta 990: 87-92

Gill SS and Tuteja N (2010) Reactive oxygen species and antioxidant machinery in abiotic stress tolerance in crop plants. Plant Physiol Biochem 48: 909-930

Gitelson AA, Gritz Y and Merzlyak MN (2003) Relationships between leaf chlorophyll content and spectral reflectance and algorithms for non-destructive chlorophyll assessment in higher plants. J Plant Physiol 160: 271-282

Glick BR, Penrose DM and Li J (1998) A model for the lowering of plant ethylene concentrations by plant growth-promoting bacteria. J Theor Biol 190: 68-68

Glick BR (2005) Modulation of plant ethylene levels by the bacterial enzyme ACC deaminase. FEMS Microbiol Lett 251: 1-7

Good AG and Zaplachinski ST (1994) The effects of drought stress on free amino acid accumulation and protein synthesis in *Brassica napus*. Physiol Plant 90: 9-14

Grewal KS, Buchan GD and Tonkin PJ (1990) Estimation of field capacity and wilting point of some New Zealand soils from their saturation percentages. New Zeal J Crop Hort Sci 18: 241-246

Guo S, Zhang J, Sun H, et al. (2013) The draft genome of watermelon (*Citrullus lanatus*) and resequencing of 20 diverse accessions. Nature Genet 45: 51-58

Han J-S, Kim CK, Park SH, Hirschi KD and Mok I (2005) *Agrobacterium*-mediated transformation of bottle gourd (*Lagenaria siceraria* Standl.). Plant Cell Rep 23:692-698

Harmsen T, Klaasen S, van de Vrugt H, and te Riele H (2018) DNA mismatch repair and oligonucleotide end protection promote base-pair substitution distal from the CRISPR/Cas9-induced DNA break. Nucleic Acid Res 46: 2945-2955

Harvey RB (1922) Growth of plants in artificial light. Botanical Gazette 74: 447-451

Hayatu M, Muhammad SY and Habibu UA (2014) Effect of water stress on the leaf relative water content and yield of some cowpea (*Vigna Unguiculata* (L) Walp.) Genotype. IJSTR 3: 7

Heinrich A, Maheswaran M, Ruppert U and Forchhammer K (2004) The *Synechococcus elongatus* PII signal transduction protein controls arginine synthesis by complex formation with *N*-acetyl-L-glutamate kinase. Mol Microbiol 52: 1303-1314

Herppich WB and Peckman K (2000) Infuence of drought on mitochondrial activity, photosynthesis, nocturnal acid accumulation and water relations in the CAM plants *Prenia sladeniana* (ME-type) and *Crassula lycopodioides* (PEPCK-type). Ann Bot 86: 611-620

Herrera-Estrella L, Simpson J and Martínez-Trujillo M (2005) Transgenic Plants: An Historical Perspective. in: (ed.) Peña L. Transgenic Plants: Methods and Protocols. Methods in Molecular Biology, vol 286. Humana Press

Heywood V, Casas A, Ford-Lloyd B, Kell S and Maxted N (2007) Conservation and sustainable use of crop wild relatives. Agric Ecosyst Environ 121: 245-255

Hiner ANP, Rodriguez-Lopez JN, Arnao MB, Raven EL, Novas FG and Acousta M (2000) Kinetic study of the inactivation of ascorbate peroxidase by hydrogen peroxide. Biochem J 348: 321-328

Honma M and Shimomura T (1978) Metabolism of 1-aminocyclopropane-1-carboxylic acid. Agric Biol Chem 42: 1825-1831

Hood EE, Gelvin SB, Melchers LS and Hoekama A (1993) New *Agrobacterium* helper plasmids for gene transfer to plants. Transgenic Res. 2:208-218.

Hopkins J and Maxted N (2011) Crop wild relatives: Plants conservation for food security. Crop Wild Relatives: Plant conservation for food security. Natural England Research Reports, Number 037. Natural England, Sheffield

Horsch R B, Klee HJ, Stachel S, Winans SC, Nester EW, Rogers SG and Fraley RT (1986) Analysis of *Agrobacterium tumefaciens* virulence mutants in leaf disks. Proc Natl Acad Sci USA 83:2571-2575

Hsu PD, Lander ES and Zhang F (2014) Development and application of CRISPR-Cas9 for genome engineering. Cell 157

Hu B, Jin J, Guo A, Zhang H, Luo J and Gao G (2015) GSDS 2.0: an upgraded gene feature visualization server. Bioinformatics 31:1296-1297

Hunt AG (2012) RNA regulatory elements and polyadenylation in plants. Front Plant Sci 2: 109

Hunt AG, Xing D and Li Q (2012) Plant polyadenylation factors: conservation and variety in the polyadenylation complex in plants. BMC Genomics 13: 641

Ishida Y, Saito H, Hiei Y and Komari T (2003) Improved protocol for transformation of maize (*Zea mays* L.) mediated by *Agrobacterium tumefaciens*. Plant Biotechnol 20: 57-66

Ishikawa T, Yoshimura K, Sakai K, Tamoi M and Takeda T (1998) Molecular characterization and physiological role of a glyoxysome-bound ascorbate peroxidase from spinach. Plant Cell Physiol 39: 23-34

Ishikawa T and Shigeoka S (2008) Recent advances in ascorbate biosynthesis and the physiological significance of ascorbate peroxidase in photosynthesizing organisms. Biosci Biotechnol Biochem 72: 1143-1154

Janga MR, Campbell LM and Rathore KS (2017) CRISPR/Cas9-mediated targeted mutagenesis in upland cotton (*Gossypium hirsutum* L.). Plant Mol Biol 94:349-360

Janiak A, Kwaśniewski M and Szarejko I (2016) Gene expression regulation in roots under drought. J Exp Bot 67: 1003-1014

Jefferson RA (1987) Assaying chimeric genes in plants: The GUS gene fusion system. Plant Mol Biol Rep 5: 387-405

Jensen MH and Collins WL (1985) Hydroponic vegetable production. Hort Review 7: 483-558.

Jespersen, Kjærsgaird Ivh, Østergaard L and Welinder KG (1997) From sequence analysis of three novel ascorbate peroxidases from *Arabidopsis thaliana* to structure, function and evolution of seven types of ascorbate peroxidase. Biochem J 326: 305-310

Kakkar A and Verma VK (2011) *Agrobacterium*-mediated biotransformation. J Appl Pharm Sci 1: 29-35.

Kala RG, Abraham V, Sobha S, Jayasree PK, Suni AM and Thulaseedharan A (2012) *Agrobacterium*-mediated genetic transformation and somatic embryogenesis from leaf callus of *Hevea brasiliensis*: Effect of silver nitrate. In: (eds.) Sabu A and Augustine A. Prospects in Bioscience: Addressing the Issues. Springer, New Delhi, India. pp 303-315

Kamburova VS, Nikitina EV, Shermatov SE, Buriev ZT, Kumpatla SP, Emani C and Abdurakhmonov IY (2017) Genome editing in plants: An overview of tools and applications. Int J Agron 7315351

Kanesisa K and Goto S (2000) KEGG: Kyoto encyclopedia of genes and genomes. Nucleic Acid Res 28: 27-30.

Kanehisa K, Goto S, Kawashima S and Nakaya A (2002) The KEGG database at genomeNet. Nucleic Acid Res 30: 42-46

Kautsky H, Appel W and Amann H (1960) Chlorophyll fluorescence and carbon assimilation. Biochemische Zeitschrift 322: 277-292.

Kawasaki S, Miyake C, Kohchi T, Fujii S, Uchida M and Yokota A (2000) Response of wild watermelon to drought stress: Accumulation of an ArgE homologue and citrulline in leaves during water deficits. Plant Cell Physiol 41: 864-873.

Kim J, Chang C and Tucker ML (2015) To grow old: regulatory role of ethylene and jasmonic acid in senescence. Front Plant Sci 6: 20

Kim K, Ryu S-M, Kim S-T, Baek G, Kim D, Lim K, Chung E, Kim S and Kim J-S (2017) Highly efficient RNA-guide base editing in mouse embryos. Nature Biotechnol 35: 435-437

Kitajima S, Tomizawa K, Shigeoka S and Yokoya A (2006) An inserted loop region of stromal ascorbate peroxidase is involved in its hydrogen peroxide-mediated inactivation. FEBS J. 273: 2704-10

Kitajima S (2008) Hydrogen peroxide-mediated inactivation of two chloroplastic peroxidases, ascorbate peroxidase and 2-Cys peroxiredoxin. Photochem Photobiol 84: 1404-1409

Koetle MJ, Finnie JF, Balázs E and van Staden J (2015) A review on factors affecting the *Agrobacterium*-mediated genetic transformation in ornamental monocotyledonous geophytes. S Afr J Bot 98: 37-44

Kohler RE (2002) Landscapes and labscapes: exploring the lab-field border in biology. Chicago, IL, USA: University of Chicago Press.

Kong L and Yeung EC (1994) Effects of ethylene and ethylene inhibitors on white spruce somatic embryo maturation. Plant Sci 104: 71-80

Krall JP and Edward GE (1992) Relationship between photosystem II activity and CO2 fixation in leaves. Physiol Plantarum 86: 180-187

Krause GH and Weis F (1991) Chlorophyll fluorescence and photosynthesis: the basic. Ann Rev Plant Physiol Plant Mol. Biol 42: 313-349

Kumar V, Parvatam G and Ravishankar GA (2009) $AgNO_3$ – a potential regulator of ethylene activity and plant growth modulator. Electron J Biotechnol. 12: 1-15.

Kuvshinov V, Koivu K, Kanerva A and Pehu E (1999) *Agrobacterium tumefaciens*-mediated transformation of green house-grown *Brassica rapa* ssp. oleifera. Plant Cell Rep 18: 773-777

Lee G-J, Kim D-G, Kwon SJ, Choi H and Kim DS (2015) Identification of mutagenesis in plant populations, in. eds. Koh H-J, Kwon S-Y, and Thompson M. Current technologies in plant molecular breeding: A guidebook to plant molecular breeding for researchers. Springer, Dordrecht, Netherlands. Pp 205-240.

Li Q and Hunt AG (1997) The polyadenylation of RNA in plants. Plant Physiol 115: 321-325

Li RH, Guo P-P, Michael B, Stefania G and Salvatore C (2006) Evaluation of chlorophyll content and fluorescence parameters as indicators of drought tolerance in Barley. Agric Sci China 5: 751-757

Li J, Tang Y, Qin Y, Li X and Li H (2012) *Agrobacterium*-mediated transformation of watermelon (*Citrullus lanatus*). Afr J Biotechnol 11: 6450-6456

Li J, Sun Y, Du J, Zhao Y and Xia L (2017) Generation of targeted point mutations in rice by a modified CRISPR/Cas9 system. Mol Plant 10: 526-529

Limpens J, Granath G, Aerts R, Heijmans MM, Sheppard LJ, Bragazza L, Williams BL, Rydin H, Bubier J, Moore T et al. 2012. Glasshouse vs field experiments: do they yield ecologically similar results for assessing N impacts on peat mosses? New Phytologist 195: 408-418

Liu YJ, Yuan Y, Liu YY, Liu Y, Fu JJ, Zheng J and Wang GY (2012) Gene families of maize glutathione-ascorbate redox cycle respond differently to abiotic stresses. J Plant Physiol 169: 183-192

Liu H, Ding Y, Zhou Y, Jin W, Xie K and Chen L-L. (2017) CRISPR-P 2.0: An improved CRISPR-Cas9 tool for genome editing in plants. Mol Plant 10: 530-532.

Loke JC, Stahlberg EA, Strenski DG, Haas BJ, Wood PC and Li QQ (2005). Compilation of mRNA polyadenylation signals in Arabidopsis revealed a new signal element and potential secondary structures. Plant Physiol 138: 1457-1468

Lowder LG, Zhang D, Baltes NJ, Paul JW, Tang X, Zheng X, et al. 2015. A CRISPR/Cas9 toolbox for multiplexed plant genome editing and transcriptional regulation. Plant Physiol 169:971-985

Lu Y and Zhu J-K (2017) Precise editing of the targeted base in the Rice genome using a modified CRISPR/Cas9 system. Mol Plant 10: 523-525

Ma X, Zhang Q, Zhu Q, Liu W, Chen Y, et al. (2015) A robust CRISPR/Cas9 system for convenient, high-efficiency multiplex genome editing in monocot and dicot plants. Mol Plant 8: 1274-1284.

Mano S, Yamaguchi K, Hayashi M and Nishimura M (1997) Stromal and thylakoid-bound ascorbate peroxidases are produced by alternative splicing in pumpkin. FEBS Lett 413: 21-26

Manter DK and Kerrigan J (2004) A/Ci curve analysis across a range of woody plant species: influence of regression analysis parameters and mesophyll conductance J Exp Bot 55: 2581-2588

Manter DK, Bond BJ, Kavanagh KL, Rosso PH and Filip GM (2000) Pseudothecia of Swiss needle cast fungus, *Phaeocryptopus gaeumannii*, physically block stomata of douglas-fir, reducing CO2 assimilation. New Phytol 148: 481-491

Marsh, LS and Albright LD (1991) Economically optimum day temperatures for greenhouse hydroponic lettuce production part I: A computer model. Trans ASAE 34: 550-556

Martínez-Carrasco R, Sánchez-Rodriquez J and Pérez P (2002) Changes in chlorophyll fluorescence during the course of photoperiod and in response to drought in *Casuarina equisetifolia* forst. and forst. Photosynthetica 40: 363-368

Marutani-Hert M, Bowman KD, McCollum GT, Mirkov TE, Evens TJ and Niedz RP (2012) A dark incubation period is important for *Agrobacterium*-mediated transformation of mature internode explants of sweet orange, grapefruit, Citron, and a Citrange rootstock. PLoS ONE 7: e47426.

Masahiro M, Hirosji K, Tatsuya T and Kintake S (2016) Relationship Between Photochemical quenching and non-photochemical quenching in six species of cyanobacteria reveals species difference in redox state and species commonality in energy dissipation. Plant Cell Physiol 57: 1510-1517

Mathobo R, Marais D and Steyn MJ (2017) The effect of drought stress on yield, leaf gaseous exchange and chlorophyll fluorescence of dry beans (*Phaseolus vulgaris L.*) Agric Water Manag 180: 118-125

Maxwell K and Johnson GN (2000) Chlorophyll fluorescence—a practical guide. J Exp Bot 51: 659-668

May A (2017) Base editing on the rise. Nat Biotechnol 35: 5

McDonnell L, Plett JM, Andersson-Gunneras S, Kozela C, Dugardeyn J, Van Der Straeten D, Glick BR, Sundberg B and Regan S (2009) Ethylene levels are regulated by a plant encoded 1-aminocyclopropane-1-carboxylic acid deaminase. Physiol Plant 136: 94-109

Minami R, Uchiyama K, Murakami T, Kawai J, Mikami K and Yamada T (1998) Properties, sequence, and synthesis in *Escherichia coli* of 1-aminocyclopropane-1-carboxylate deaminase from *Hansenula saturnus.* J Biochem 123: 1112-1118

Mir G, Domenech J, Huguet G, Guo WJ, Goldsbrough P, Atrian S and Molinas MA (2004) Plant type 2 metallothionein (MT) from cork tissue responds to oxidative stress. J Exp Bot 55: 2483-2493

Mittler R (2002) Oxidative stress, antioxidants and stress tolerance. Trends Plant Sci 7: 405-410

Mittler R, Vanderauwera S, Gollery M and van Breusegem F (2004) Reactive oxygen gene network of plants. Trends Plant Sci 9:490-498

Miyake C and Yokota A (2000) Determination of the rate of photoreduction of O_2 in the water-water cycle in wild watermelon leaves and enhancement of rate of limitation of photosynthesis. Plant Cell Physiol 40: 335-343

Mohsen S, Foad M and Majid A (2017) Impact of drought stress on yield, photosynthesis rate, and sugar alcohols contents in wheat after anthesis in semiarid region of Iran. Arid Land Res Manag 31: 204-218

Muller P, Li X-P and Niyogi K (2001) Non-photochemical quenching. A response to excess light energy. Plant Physiol125: 1558-1566

Murchie EH and Lawson T (2013) Chlorophyll fluorescence analysis: a guide to good practice and understanding some new applications. J Exp Bot 64: 3983-3998

Murashige T and Skoog F (1962) A revised medium for rapid growth and bio assays with tobacco tissue cultures. Physiol Plant 15: 473-497

Nakai K and Horton P (1999) PSORT: a program for detecting the sorting signals of proteins and predicting their subcellular localization. Trends Biochem Sci 24:34-35

Nakano Y and Asada K (1981) Hydrogen peroxide is scavenged by ascorbate-specific peroxidase in spinach chloroplasts. Plant Cell Physiol 22: 867-880.

Nanasato Y, Miyake C, Takahara K, Kohzuma K, Munekage YN, Yokota A and Akashi K (2010) Mechanisms of drought and high light stress tolerance studied in a xerophyte, *Citrullus lanatus* (wild watermelon). in: Rebeiz CA, et al. (eds.), The Chloroplast. Advances in Photosynthesis and Respiration. Vol 31. Basics and Applications. Springer, Dordrecht, Netherlands. Pp. 363-377

Nejatzadeh-Barandozi F, Darvishzadeh F and Aminkhani A, (2014) Effect of nano silver and silver nitrate on seed yield of *Ocimum basilicum* L. Bioorganic Med Chem Lett 4: 1-6

Nester EW, Gordon MP, Amasino RM and Yanofsky MF (1984) Crown gall: a molecular and physiological analysis. Annu Rev Plant Physiol 35: 387-413.

Newell CA (2000) Plant transformation technology, developments and applications. Mol Biotechnol 16: 53-65

Niinements U, Diaz-Espejo A, Flexas J, Galmes J and Warren CR (2009) Role of mesophyll diffusion in constraining potential photosynthetic productivity in the field. J Exp Bot 60: 2249-2270

Noctor G and Foyer CH (1998) Ascorbate and glutathione: Keeping active oxygen under control. Annu Rev Plant Physiol Plant Mol Biol 49: 249-279

Nonaka S, Yuhashi K-I, Takada K, Sugaware M and Ezura H (2008) Ethylene production in plants during transformation suppresses vir gene expression in *Agrobacterium tumefaciens*. New Phytol 178: 647-656

Nonaka S and Ezura H (2014) Plant-*Agrobacterium* interaction mediated by ethylene and super-*Agrobacterium* conferring efficient gene transfer. Front Plant Sci 5:1–7.

Noodén LD, Guiamét JJ and John I (1997) Senescence mechanisms. Physiol plant101: 746-753

Ntui VO, Khan RS, Chin DP, Nakamura I and Mii M (2010) An efficient *Agrobacterium tumefaciens*-mediated genetic transformation of "Egusi" melon (*Colocynthis citrullus* L.). Plant Cell Tiss Organ Cult 103: 15-22

Ohya T, Morimura Y, Saji H, Mihara T and Ikawa T (1997) Purification and characterization of ascorbate peroxidase in roots of Japanese radish. Plant Sci 125: 137-145

Osakabe Y, Osakabe K, Shinozaki K and Tran LSP (2014) Response of plants to water stress. Front Plant Sci 5:86.

Panchuk II, Volkov RA and Schoffl F (2002) Heat stress and heat shock transcription factor-dependent expression and activity of ascorbate peroxidase in Arabidopsis. Plant Physiol 129: 838-853

Pandey S, Mishra A, Patel MK and Jha B (2013) An efficient method for *Agrobacterium*-mediated gebetic transformation and plant regeneration in Cumin (*Cuminum cyminum* L.). Appl Biochem Biotechnol 171: 1-9

Pandey S, Fartyal D, Agarwal A, Shukla T, James D, Kaul T, Negi YK, Arora S and Reddy MK (2017) Abiotic stress tolerance in plants: Myriad roles of ascorbate peroxidase. Front Plant Sci 8: 581

Park SM, Lee JS, Jegal S, Jeon BY, Jung M, Park YS, Han SL Shin YS, Her NH, Lee JH, Lee MY, Ryu KH, Yang SG and Ham CH (2005) Transgenic watermelon rootstock resistant to CGMMV (cucumber green mottle mosaic virus) infection. Plant Cell Rep 24: 350-356

Parrot DL, Anderson AJ and Carman JG (2002) *Agrobacterium* induces plant cell death in wheat (*Triticum estivum* L.). Physiol Mol Plant Pathol 60: 59-69

Pickersgill B (2007) Domestication of Plants in the Americas: Insights from Mendelian and molecular genetics. Ann Bot 100: 925-940

Pinheiro C and Chaves MM (2011) Photosynthesis and drought: can we make metabolic connections from available data? J Exp Bot 62:869-882

Pirzad A, Shakiba MR, Zehtab-Salmasi S, Mohammadi SA, Darvishzadeh R and Samadi A (2011) Effect of water stress on leaf relative water content, chlorophyll, proline and soluble carbohydrates in *Matricaria chamomilla* L. J Med Plant Res 5:2483-2488

Plucknett D, Smith N, Williams J and Murthi-Anishetty N (1987) Gene Banks and the World's Food. Princeton University Press, Princeton, USA

van de Poel B and van der Straeten D (2014) 1-aminocyclopropane-1-carboxylic acid (ACC) in plants: more than just the precursor of ethylene! Front Plant Sci 5: 640

Poorter H, Fiorani F, Pieruschka R, Wojciechowski T, van der Putten WH, Kleyer M, Schurr U and Postma J (2016) Pampered inside, pestered outside? Differences and similarities between plants growing in controlled conditions and in the field. New Phytol 212: 838-855

Prasch CM and Sonnewald U (2015) Signaling events in plants: Stress factors in combination change the picture. Environ Exper Bot 114: 4-14

Pua EC and Chi GK (1993) The regulatory role of ethylene on cell differentiation and growth of Mustard plants *in vitro.* in. (eds.) You C, Chen Z and Ding Y in: Biotechnology in Agriculture: proceeding of the first Asia-pacific conference on Agricultural Biotechnology. Beijing, China. Pp 344-347

Qiao D, Mao P, Ma X and Yang H (2011) The effects of mannitol and $AgNO_3$ for perennial ryegrass transformation mediated by *Agrobacterium tumefaciens*. Acta Physica Sinica: 20: 102-110

Raffeiner B, Serek M and Winkelmann (2009) *Agrobacterium tumefaciens*-mediated transformation of Oncidium and Odontoglossum orchid species with the ethylene receptor mutant gene etr1-1. Plant Cell Tiss Organ Cult 98: 125-134

Rahman AM (1973) Effect of moisture stress on plants. Phyton 15 67-86

Ranz JM and Parsch J (2012) Newly evolved genes: Moving from comparative genomics to functional studies in model systems. Bioessays 34: 477-483

Reynolds SG (1970) The gravimetric methods of soil moisture determination: Part 1: A study of equipment, and methodological problems. J Hydrol 11: 258-273.

Riccardi F, Gazeau P, de Vienne D and Zivy M (1998) Protein changes in response to progressive water deficit in maize, quantitative variation and polypeptide identification. J Plant Physiol 117: 1253-1263.

Riva GA, González-Cabrera J, Vázquez-Padrón R and Ayra-Pardo C (1998) *Agrobacterium tumefaciens*: a natural tool for plant transformation. Electron J Biotechnol 1:3

Roy R, Agrawal V and Gupta SC (2009) Comparison of drought-induced polypeptides and ion leakage in three tomato cultivars. Biologia Plant 53: 685-690

Sanda S, Yoshida K, Kuwano M, Kawamura T, Nakajima M, Akashi K and Yokota A (2011) Responses of the photosynthetic electron transport system to excess light energy caused by water defecit in wild watermelon. Physiol Plant 142: 247-264

Saxena SC, Joshi P, Grimm B and Arora S (2011) Alleviation of ultraviolet- C induced oxidative through overexpression of cytosolic ascorbate peroxidase. Biologia 66: 1052-1059

Schachtman DP and Goodger JQ (2008) Chemical root to shoot signaling under drought. Trends Plant Sci 13: 281-287.

Schreiber U, Bilger W, Hormann H and Neubauer C (2000) Chlorophyll fluorescence as a diagnostic tool: basics and some aspects of practical relevance. in: (ed.) Raghavendra AS. Photosynthesis: a comprehensive treatise. Cambridge, UK: Cambridge Univesity Press; 320-33

Schneider CA, Rasband WS and Eliceiri KW (2012) NIH Image to ImageJ: 25 years of image analysis. Nat Methods 9: 671-675

Sheffield J and Wood EF (2007) Characteristics of global and regional drought, 1950–2000: Analysis of soil moisture data from off-line simulation of the terrestrial hydrologic cycle. J Geophys Res 112: D17115

Shen Y, Ji G, Haas BL, Wu X, Zheng J, Reese GJ and Li QQ (2008) Genome level analysis of rice mRNA 3'-end processing signals and alternative polyadenylation. Nucleic Acids Res 36: 3150-3161

Shigeoka S, Ishikawa T, Tamoi M, Miyagawa Y, Takeda T, Yabuta Y and Yoshimura K (2002) Regulation and function of ascorbate peroxidase isoenzymes. J Exp Bot 53: 1305-1319

Singh RP, Shelke GM, Kumar A and Jha PN (2015) Biochemistry and genetics of ACC deaminase: a weapon to "stress ethylene" produced in plants. Front Microbiol 6: 937

Sivanandhan G, Arunachalam C, Vasudevan V, Kapiledev G, Sulaimain AA, Selvara N, Ganapathi N and Lim YP (2016) Factors affecting *Agrobacterium*-mediated transformationin *Hybanthus enneaspermus* (L.) F. Muell. Plant Biotechnol Rep 10:49-60

Skirycz A and Inze D (2010) More from less: plant growth under limited water. Curr Opin Biotechnol 21: 197-203

Swinehart DF (1962) The Beer-Lambert Law. Journal of chemical education 39; 7

Smart RE (1974) Rapid estimation of relative water content. Plant Physiol 53: 258-260

Sofo A, Scopa A, Nuzzaci M and Vitti A (2015) Ascorbate peroxidase and catalase activities and their genetic regulation in plants subjected to drought and salinity stresses. Int J Mol Sci 16: 13561-13578

Sorek R, Lawrence C and Wieden-Heft B (2013) CRISPR-mediated adaptive immune systems in bacteria and archaea. Annu Rev Biochem 82: 237-266

Strasser RJ, Srivastava A and Tsimilli-Michael M (2000) The fluorescence transient as a tool to characterize and screen photosynthetic samples. in: (eds.) Yunus M, Pathre U, Mohanty P. Probing Photosynthesis: Mechanisms, Regulation and Adaptation. Taylor and Francis, London. pp. 445-483

Sun Y, Zhang X, Wu C, He Y, Ma Y, Hou H, Guo X, Du W, Zhao Y and Xia L (2016) Engineering herbicide-resistant rice plants through CRISPR/Cas9 homologous recombination of acetolactate synthase. Mol Plant 9: 628-631

Suratman F, Huyop F, Wagiran A, Rahmat Z, Ghazali H and Parveez GKA (2010) Cotyledon with hypocotyl segment as an explant for the production of transgenic

Citrullus vulgaris Schrad (Watermelon) Mediated by *Agrobacterium tumefaciens*. Biotechnology 9: 106-118

Sytykiewicz H (2016) Expression patterns of genes involved in ascorbate-glutathione cycle in aphid-infested maize (*Zea mays* L.) Seedlings. Int J Mol Sci 17: 268

Tabei Y, Yamanaka H and Kanno T (1993) Adventitious shoot induction and plant regeneration from cotyledons of mature seed in watermelon (Citrullus lanatus L.). Plant Tiss Cult Lett 10: 235-241

Taiz L and Zeiger E (2010) Plant Physiology. 6th Edition, Sinauer Associates, Sunderland

Takahara K, Akashi K and Yokota A (2007) Purification and characterization of glutamate *N*-acetyltranferase involved in citrulline accumulation in wild watermelon. FEBS J 272: 5353-5364

Takasaki T, Hatakeyama K and Hinata K (2004) Effect of silver nitrate on shoot regeneration and agrobacterium mediated transformation of turnip (Brassica rapa L. var. rapifera). Plant Biotechnol 21:225-228

Tao C, Jin X, Zhu L, Xie Q, Wang X and Li H (2017) Genome-wide investigation and expression profiling of APX gene family in *Gossypium hirsutum* provide new insights in redox homeostasis maintenance during different fiber development stages. Mol Genet Genomics (online)

Teixeira FK, Menezes-Benavente L, Margis R and Margis-Pinheiro M (2004) Analysis of the molecular evolutionary history of the ascorbate peroxidase gene family: inferences from the rice genome. J Mol Evol 59: 761-770

Tsitsimpelis I, Wolfenden I and Taylor CJ (2016) Development of a grow-cell test facility for research into sustainable controlled-environment agriculture. Biosyst Eng 150: 40-53

Tzfira T and Citovsky V (2006) *Agrobacterium*-mediated genetic transformation of plants: biology and biotechnology. Curr Opin Biotechnol 17: 147-154

Uddling J, Gelang-Alfredsson J, Piikki K and Pleijel H (2007) Evaluating the relationship between leaf chlorophyll concentration and SPAD-502 chlorophyll meter readings. Photosynth Res 91: 37-46

Urnov FD, Rebar EJ, Holmes MC, Zhang HS and Gregory PD (2010) Genome editing with engineered zinc finger nucleases. Nat Rev Genet 11, 636–646

Untergasser A, Cutcutache I, Koressaar T, Ye J, Faircloth BC, Remm M and Rozen SG (2012) Primer3-new capabilities and interfaces. Nucleic Acids Res 40: e115

Veena, Jiang H, Doerge RW and Gelvin SB (2003) Transfer of T-DNA and vir proteins to plant cells by *Agrobacterium tumefaciens* induces expression of host genes involved in mediating transformation and suppresses host defense gene expression. Plant J 35: 219-226

Wahlroos T, Susi P, Tylkina L, Malyshenko S, Zvereva S and Korpela T (2003) *Agrobacterium*-mediated transformation and stable expression of the green fluorescent protein in *Brassica rapa*. Plant Physiol Biochem 41: 773-778

Wang X, Xu Y, Han Y, Bao S, Du J, Yuan M, Xu Z and Chong K (2006) Overexpression of RAN1 in rice and Arabidopsis alters primordial meristem, mitotic progress, and sensitivity to auxin. Plant Physiol 140: 91-101

Wang K, L-C, Li H and Ecker JR (2002) Ethylene biosynthesis and signaling networks. Plant Cell S131-S151

Winter G, Todd CD, Trovato M, Forlani G and Funck D (2015) Physiological implications of arginine metabolism in plants. Front Plant Sci 6:534

Wittwer SH and Castilla N (1995) Protected cultivation of horticultural crops worldwide. Hort Technology 5: 6-23

Woo M-O, Markkandan K, Paek N-C, Jeong S-C, Choi S-B, and Seo HS (2015) Isolation and functional studies in genes, in. eds. Koh H-J, Kwon S-Y, and Thompson M. Current technologies in plant molecular breeding: A guidebook to plant molecular breeding for researchers. Springer, Dordrecht, Netherlands. Pp. 241-296

Wu JT, Wu LH and Knight JA (1986) Stability of NADPH; Effect of various factors on the kinetics of degradation. Clinical Chem 32: 314-319

Wu X, Liu M, Downie B, Liang C, Ji G, Li QQ and Hunt AG (2011) Genome-wide landscape of polyadenylation in Arabidopsis provides evidence for extensive alternative polyadenylation. Proc Natl Acad Sci USA 108: 12533-12538

Xiong D, Chen J, Yu T, Gao W, Ling X, Li Y, Peng S and Huang J (2015) SPAD-based leaf nitrogen estimation is impacted by environmental factors and crop leaf characteristics. Sci Rep 5: 13389

Yang X (2012) Use of functional genomics to identify candidate genes underlying human genetic association studies of vascular diseases. Arterioscler Thromb Vasc Biol 32: 216-222

Yevtushenko DP and Misra S (2010) Efficient *Agrobacterium*-mediated transformation of commercial hybrid poplar *Populus nigra* L. x *P. maximowiczii* A. Henry. Plant Cell Rep 29: 211-221

Yin G, Xin X, Song C, Chen X, Zhang J, Wu S, Li R, Liu X and Lu X (2014) Activity levels and expression of antioxidant enzymes in the ascorbate-glutathione cycle in artificially aged rice seed. Plant Physiol Biochem 80: 1-9

Yin K, Gao C and Qiu J-L (2017) Progress and prospects in genome editing. Nat Plants 3: 17107

Yoo SD, Cho YH and Sheen J (2007) Arabidopsis mesophyll protoplasts: a versatile cell system for transient gene expression analysis. Nat Protoc 2: 1565-72

Yoshimura K, Ishikawa T, Nakamura Y, Tamoi M, Takeda T, Tada T, Nishimura K and Shigeoka S (1998) Comparative study on recombinant chloroplastic and cytosolic ascorbate peroxidase isozymes of spinach. Arch Biochem Biophys 353: 55-63

Yoshimura K, Yabuta Y, Tamoi M, Ishikawa T and Shigeoka S (1999) Alternative spliced mRNA variants of chloroplasts ascorbate peroxidase isoenzymes in spinach leaves. Biochem J 338: 41-48

Yoshimura K, Yabuta Y, Ishikawa T and Shigeoka S (2000). Expression of spinach ascorbate peroxidase isoenzymes in response to oxidative stresses. Plant Physiol 123: 223-234

Yoshimura K, Masuda A, Kuwano M, Yokota A and Akashi K (2008) Programmed proteome response for drought avoidance/tolerance in the root of a C_3 xerophyte (wild watermelon) under water deficits. Plant Cell Physiol 49: 226-241

You J and Chan Z (2015) ROS regulation during abiotic stress responses in crop plants. Front Plant Sci 6: 1092

Zahir ZA, Munir A, Asghar HN, Shaharoona B and Arshard M (2008) Effectiveness of rhizobacteria containing ACC deaminase for growth promotion of peas (*Pisum sativum*) under drought conditions. J Microbiol Biotechnol 18: 958-963.

Zakhidov E, Nematov S and Kuvondikov V (2016). Monitoring of the Drought Tolerance of Various Cotton Genotypes Using Chlorophyll Fluorescence, in. ed. Najafpour MM. Applied Photosynthesis - New Progress. InTech, Rijeka, Crotia

Zhai Z, Jung H and Vatamaniuk OK (2009). Isolation of Protoplasts from Tissues of 14-day-old Seedlings of Arabidopsis thaliana. JoVE. 30.

Ziemienowicz A (2014) *Agrobacterium*-mediated plant transformation: Factors, applications and recent advances. Biocatal Agric Biotechnol 3: 95-102

Zivcak M, Kalaji HM, Shao H-B, Olsovska K and Brestic (2014) Photosynthetic proton and electron transport in wheat leaves under prolonged moderate drought stress. J Photochem Photobiol 137: 107-115

Zhang Y (2014) Genome editing with ZFN, TALEN and CRISPR/Cas Systems: The applications and future prospects. Adv Genet Eng 3:1

Zhang Y, Liang Z, Zong Y, Wang Y, Liu J, Chen K, Qiu J-L and Gao C (2016) Efficient and transgene-free genome editing in wheat through transient expression of CRISPR/Cas9 DNA or RNA. Nat Commun 7:12617

Zhao D, Yuan S, Xiong B, Sun H, Ye L, Li J, et al. (2016) Development of a fast and easy method for *Escherichia coli* genome editing with CRISPR/Cas9. Microb Cell Fact 15:205

Zhang H, Zhanga J, Langa Z, Botella JS and Zhu J-K (2017) Genome editing-principles and applications for functional genomics research and crop improvement. Crit Rev Plant Sci 36: 291-309

Summary (English)

Drought has been documented as the major threat to food security worldwide. It is therefore important to study plants that have shown to be drought tolerant. Wild watermelon grows in the harsh desert conditions of the Kalahari Desert in Botswana. Previous studies have shown that various proteins and compounds are induced and accumulated in this plant when exposed to drought stress, which are believed to contribute to drought stress tolerance. It is therefore attractive to study this plant and unravel the drought tolerance mechanisms it possesses. The information acquired in studying this plant can be useful for future plant breeding programs.

Various studies have been performed on wild watermelon to understand the drought tolerance mechanisms, but these studies have always been performed in artificial environment. The extent of similarity or dissimilarity of the experimental results obtained between in artificial environments and in the natural environment has never been addressed. In this part of study, drought physiological responses of wild (*Citrullus lanatus* Acc. 101117-1) and a cultivar (*Citrullus lanatus* L. cv Matsuribayashi-777) watermelons were evaluated in both natural and artificial environments. For the natural environment, the plants were planted in a field in Botswana during the summer of 2017, while for the artificial environment the plants were grown in the growth chamber. The weather data in the natural conditions showed daily variations in factors like temperature, solar radiance, humidity and wild speed, while minimal rainfall was recorded. These variations have been thought to cause additional stress to the plant. Observation on the plants showed different kinds of variations on plant physiology. Under the natural environment, response to water deficit was very rapid. Down-regulation in the photosynthetic assimilation and stomatal closure was more rapid in the natural conditions under drought stress. Effects on the fluorescence parameters showed that the photochemical quenching reduced rapidly in the early days of the drought stress in the natural environment, as compared to the artificial condition. Drought-induced heat dissipation of the absorbed energy through the non-photochemical quenching mechanisms was higher in natural conditions for both plants. Interestingly, even though the results were different in terms of intensity, the trend of physiological response was similar between the two

environments. These observations shows that artificial condition can be used to study effects of environmental stress of plants, but care must be taken when interpreting the results.

Ascorbate peroxidase (APX) plays an important role in detoxifying reactive oxygen species under environmental stress. Although previous work in wild watermelon has shown an increase in chloroplast APX enzyme activity under drought, molecular entities of APX have remained uncharacterized. In this study, structure and transcriptional regulation of the APX gene family in watermelon were characterized. Five APX genes, designated as *CLAPX1* to *CLAPX5*, were identified from watermelon genome. The mRNA alternative splicing was suggested for *CLAPX5,* which generated two distinct deduced amino acid sequences at their C-terminus, in resemblance to a reported alternative splicing of chloroplast APXs in pumpkin. This observation suggests that two isoenzymes for stromal and thylakoid-bound APXs may be generated from the *CLAPX5* gene. Phylogenetic analysis classified *CLAPX* isoenzymes into three clades, *i.e.*, chloroplast, microbody, and cytosolic. Physiological analyses of wild watermelon under drought showed a decline in stomatal conductance and CO_2 assimilation rate, and a significant increase in the enzyme activities of both chloroplast and cytosolic APXs. Profiles of mRNA abundance during drought were markedly different among *CLAPX* genes, suggesting distinct transcriptional regulation for the APX isoenzymes. Up-regulation of *CLAPX5-I* and *CLAPX5-II* was observed at the early phase of drought stress, which was temporally correlated with the observed increase in chloroplast APX enzyme activity, suggesting that transcriptional up-regulation of the *CLAPX5* gene may contribute to the fortification of chloroplast APX activity under drought. Our study has provided an insight into the functional significance of the *CLAPX* gene family in the drought tolerance mechanism in this plant.

Ethylene (C_2H_4), a phytohormone that is produced in response to both abiotic and biotic stresses, is an important factor influencing the efficiency of *Agrobacterium*-mediated transformation. In this study, effects of various ethylene inhibitors on the efficiency of *Agrobacterium*-mediated genetic transformation in wild watermelon was comparatively examined. Consequently, in comparison to the application of chemical inhibitors such as $AgNO_3$ and aminoethoxyvinylglycine (AVG), lower ethylene level was observed when the infecting *Agrobacterium* contained a gene for 1-

aminocyclopropane-carboxylic acid (ACC) deaminase (acdS), which cleaves ethylene precursor ACC into α-ketobutyrate and ammonia. GUS histochemical and spectrophotometric enzyme assays showed that acdS was more effective in enhancing gene transfer than the chemical ethylene inhibitors. Efficiency of transgenic sh oots formation was higher in acdS- and AVG-treated explants. These observations demonstrated that controlling the ethylene level during co-cultivation and shoot formation, particularly using the acdS-harboring *Agrobacterium*, is advantageous for enhancing the transformation efficiency in this plant.

Wild watermelon has shown to accumulate various compounds such as citrulline under drought. These metabolic alterations have been suggested to contribute to the drought tolerance mechanism of the plant. Therefore, it is important to study the entities of the mechanisms at molecular level. Loss of function has been widely used as a method of choice for functional studies of genes in plants. Genome editing technologies, such as the CRISPR/Cas9 system, has been an important technology used in functional studies. In this study, therefore, the focus was to develop the CRISPR/Cas9 genome editing system in wild watermelon, as a tool for studying gene functions. The *N*-acetylglutamate kinase (NAGK) gene, a plausible committing step in citrulline biosynthesis in wild watermelon was selected as the target for genome editing. Agroinfiltration of an *Agrobacterium* containing a binary vector encoding a CRISPR/Cas9-NAGK cassette showed necrotic defects on the leaves of the infected wild watermelon plants, in contrast to the control infection. Biochemical analysis showed a reduction of the NAGK enzyme activity in the protein extract from the infected leaves. Analysis of the genome sequence extracted from the agroinfiltrated leaves and the cassette-introduced protoplasts displayed high frequency of various nucleotide substitutions on the targeted locus, but not on the other region of the NAGK gene. Deletion-type mutations, which have been commonly observed in genome editing in other plants, were not observed in the present analysis. Analysis of the potential off-targets sequences did not show any sequence alteration. Although further research and development will be needed to achieve maximum efficiency for the gene knockout study, present observations indicated that target locus was specifically edited at a higher frequency in wild watermelon, suggesting that the genome editing technique can be an powerful tool for studying drought-tolerant wild plant resources in the future analyses.

Summary (Japanese)

乾燥ストレスは、世界の食料供給を脅かす律速要因の一つであり、乾燥耐性を有する植物の研究はその克服のために重要と考えられる。野生種スイカはアフリカ・ボツワナ共和国のカラハリ砂漠に自生する乾燥耐性植物である。これまでの研究で、乾燥に暴露された野生種スイカにおいて様々なタンパク質や化合物が誘導されて蓄積し、これらの応答が乾燥ストレスへの防御に関与していることが示唆されており、この植物の乾燥耐性機構に興味が持たれる。

野生種スイカの乾燥ストレス耐性の分子生理機構に関する従来の研究報告は、全て人工的な気象環境の下で実験されたものであった。しかし野生種スイカの生理および分子応答が、人工気象環境と自然環境においてどの程度近似しており、またはどの程度の相違が見られるのかについては、全く知見が得られていなかった。そこで本研究では、野生種スイカ(*Citrullus lanatus* Acc. 101117-1)および栽培種スイカ(*Citrullus lanatus* L. cv. Matsuribayashi-777)の乾燥ストレスに対する生理応答について、自然環境および人工環境での比較を行った。自然環境の実験では、2017 年の夏にボツワナの圃場で栽培した植物を用い、人工環境の実験では、人工気象機を用いた。自然環境では、実験期間内において、降雨はほとんど観測されず、また気温、日照、湿度、風量などに大きな日較差が観測され、これらの変が植物へのストレス要因になったと考えられる。また、これら 2 種類の環境条件においてスイカの生理応答に相違が見られた。自然環境下では、乾燥ストレスに対する応答は迅速であり、光合成の二酸化炭素固定の抑制や気孔閉鎖などが迅速に行われた。クロロフィル蛍光解析においても、乾燥ストレスの初期段階における光化学的消光の抑制が、自然環境下においてより迅速に起こることが観測された。これらのことから、吸収光エネルギーの熱散逸は、自然環境下の乾燥ストレスにおいてより強く誘導されていることが示唆された。興味深いことに、生理応答の振幅の大きさには違いが観察されるものの、両環境条件において野生種スイカは類似の生理応答を示すことが見いだされた。これらの観察結果は、実験

結果の解釈に留意する必要はあるが、野生種スイカの環境ストレス応答を解析するにあたり、人工気象条件での実験が有効であることを示している。

アスコルビン酸ペルオキシダーゼ(APX)は、環境ストレス下において活性酸素種の消去に重要な役割を果たす。過去の報告で、乾燥ストレス下の野生種スイカにおいて葉緑体型 APX の酵素活性が上昇することが示唆されているが、その分子的実体については不明であった。そこで本研究では、スイカにおける APX 遺伝子ファミリーの構造と転写応答について解析した。スイカゲノムより見いだされた、*CLAPX1* から *CLAPX5* までの 5 遺伝子のうち、*CLAPX5* については、alternative splicing により C 末端アミノ酸配列の異なる CLAPX5-I と CLAPX5-II の 2 種のタンパク質が生じることが示唆された。このことから、カボチャの葉緑体型 APX と同様に、ストロマ型とチラコイド型の 2 種の APX タンパク質が 1 遺伝子の mRNA alternative splicing により生じることが予測された。系統樹解析により CLAPX タンパク質群は、葉緑体型、ミクロソーム型および細胞質型の 3 種のクレードに属することが示唆された。野生種スイカを乾燥ストレスに暴露したところ、気孔伝導度や二酸化炭素固定速度の低下に伴い、葉緑体型および細胞質型 APX の酵素活性が有意に上昇していた。乾燥下における *CLAPX* 発現は遺伝子毎に大きく異なっており、各遺伝子が独自の転写制御を受けていることが示唆された。乾燥ストレス初期において *CLAPX5-I* と *CLAPX5-II* の発現上昇がみられ、この上昇時期は葉緑体型 APX の酵素活性変化の様相に近似していたことから、転写制御が葉緑体型 APX の酵素活性の強化に貢献することが示唆された。これらの結果は、*CLAPX5* 遺伝子が野生種スイカの乾燥耐性に関与することを示唆するものと思われる。

各種のストレスに応答して誘導される植物ホルモンのエチレンは、アグロバクテリウム法による形質転換の効率に影響を及ぼすことが知られる。本研究では、野生種スイカをアグロバクテリウム法により形質転換する際に、様々なエチレン阻害剤がその効率に及ぼす影響を解析した。その結果、エチレン前駆体の 1-aminocyclopropane-carboxylic acid (ACC)をケトブチル酸とアンモニアに分解する ACC デアミナーゼ遺伝子(*acdS*)を有するアグロバクテリウ

ムを用いた際に、硝酸銀や aminoethoxyvinylglycine (AVG)などの化学阻害剤に比べ、エチレン蓄積が抑制されることが示された。また、GUS 組織染色解析および 酵素活性解析により、*acdS* 遺伝子は化学阻害剤に比べ遺伝子導入促進効果が高いことが示された。さらに、形質転換シュートの形成効率は、*acdS* 遺伝子導入区または AVG 処理区において高かった。これらの実験結果は、野生種スイカにおいて、*acdS* 遺伝子等を利用してエチレン産生を抑制することが形質転換体作出に有効であることを示している。

野生種スイカは乾燥に応答して、代謝制御を変化させ、シトルリンなどの化合物を蓄積して乾燥に適応することが報告されている。これら代謝制御の生理的意義を解析するにあたり、代謝関連遺伝子群を遺伝子工学的に操作して分子レベルで遺伝子機能解析を行うことは有効と考えられる。そこで本研究では、近年開発された CRISPR/Cas9 ゲノム編集技術を野生種スイカに適用することを試みた。標的遺伝子として、シトルリン生合成の律速酵素と推定される *N*-acetylglutamate kinase (NAGK)を選び、アグロインフィルトレーションにより野生種スイカの葉組織に CRISPR/Cas9-NAGK カセットを含むアグロバクテリウムを接種したところ、接種された組織の抽出液において NAGK 酵素活性の有意な低下と、NAGK 標的配列に依存した壊死が観察された。接種葉のゲノム DNA を解析したところ、標的配列内において塩基欠失変異は見いだされなかったが、高頻度で塩基置換変異が検出された。野生種スイカにおける CRISPR/Cas9 法の確立のためには更なる検討が必要であるが、これらの結果は、CRISPR/Cas9 法によるゲノム編集が野生種スイカにおいても実施可能であることを示しており、将来的に野生種スイカが持つ乾燥耐性の分子機構を解明する上で有用なツールとして期待される。

List of publications

Chapter 3

Malambane, G., Tsujimoto, H. and Akashi, K. (2018)

The cDNA structures and expression profile of the ascorbate peroxidase gene family during drought stress in wild watermelon. Journal of Agricultural Science 10: 56-71

Chapter 4

Malambane, G., Nonaka, S., Shiba, H., Ezura, H., Tsujimoto, H. and Akashi, K. (2018) Comparative effects of ethylene inhibitors on *Agrobacterium*-mediated transformation of drought tolerant wild watermelon. Bioscience, Biotechnology, and Biochemistry 82: 433-441